

Enclosure 3

Replacement Steam Generator

Divider Plate Weld Joint Separation

Root Cause Evaluation

Non-Proprietary Version

San Onofre Nuclear Generating Station, Units 2 & 3 REPLACEMENT STEAM GENERATORS

Divider Plate Weld Joint Separation Root Cause Evaluation Report

Non-proprietary Version

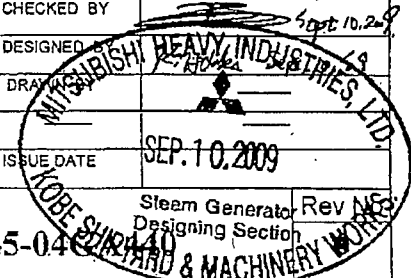
Supplier Status Stamp

VPL No:	SO23-617-1-M1415, Rev. 0	QC	n/a
<input type="checkbox"/> DESIGN DOCUMENT	ECP NO.	n/a	
<input checked="" type="checkbox"/> REFERENCE DOCUMENT - INFORMATION ONLY	<input type="checkbox"/> VIRPIOM MANUAL		
MFG MAY PROCEED: <input checked="" type="checkbox"/> YES <input type="checkbox"/> NO <input type="checkbox"/> N/A	CDM @ RELEASE: <input checked="" type="checkbox"/> YES <input type="checkbox"/> NO		
A STATUS IS REQUIRED FOR DESIGN DOCUMENTS AND IS OPTIONAL FOR REFERENCE DOCUMENTS. DRAWINGS ARE REVIEWED AND APPROVED FOR ARRANGEMENTS AND CONFORMANCE TO SPECIFICATION ONLY. APPROVAL DOES NOT RELIEVE THE SUBMITTER FROM THE RESPONSIBILITY OF ADEQUACY AND SUITABILITY OF DESIGN, MATERIALS, AND/OR EQUIPMENT REPRESENTED.			
<input checked="" type="checkbox"/> 1. APPROVED			
<input type="checkbox"/> 2. APPROVED EXCEPT AS NOTED - MAKE CHANGES AND RESUBMIT.			
<input type="checkbox"/> 3. NOT APPROVED - CORRECT AND RESUBMIT FOR REVIEW. NOT FOR FIELD USE.			
APPROVALS: (SIGNATURE/DATE)	(PRINT) Last Name	POS-TITLE (if T/PE/T)	Verify by Initials
<i>[Signature]</i>	OLECH		<i>[Initials]</i>
R.S. <i>[Signature]</i>	Calhoun		<i>[Initials]</i>
Other:			

Poor Quality Document
Best Available Copy
Signed: D. Schafer *[Signature]* 9/10/09
Document Originator Date

SCEDE(123) 3 REV. 2 12/05

Purchase Order No. 4500024051
Specification No. SO23-617-01R3

CONTENT		REMARKS	PURCHASER	ORDER No.	DATE	Nuclear Component Designing Department Steam Generator Designing Section		
DESCRIPTION	PAGE			ITEM No.	REFERENCE			
FIGURE	SHEET			Edison (MNES)	2564001		Sep. 10, '09	APPROVED BY <i>[Signature]</i> Sept. 10, 2009
TOTAL	484 PAGE				G055/G056		<i>[Signature]</i>	CHECKED BY <i>[Signature]</i> Sept. 10, 2009
					DESIGNED BY <i>[Signature]</i>			
					DRAWING NO. <i>[Signature]</i>			
					ISSUE DATE SEP. 10, 2009			
Distribution	Edison			DWG. No.				
1		NSGS	1	1	1		2	
						Steam Generator Designing Section Rev. NSG		

MITSUBISHI HEAVY INDUSTRIES, LTD. KOBE SHIPYARD & MACHINERY WORKS



Revision History

Document No. L5-04GA440 (0)

No.	Revision	Date	Approved	Checked	Prepared
0	Initial issue -This document is non-proprietary version of L5-04GA436.	See cover sheet			



Executive Summary

Background

A crack in the weld between the divider plate and the channel head on the 3B RSG was reported on March 18, 2009 after completion of the ASME Section III secondary side hydrostatic pressure test.

The crack found on the 3B RSG led to an immediate PT and UT examinations of the 3A and 3B RSGs to determine the extent of condition. The examinations determined that the Alloy 152 butter, which is the equivalent material to Alloy 690 but in a weld filler form, underneath the divider plate had separated from the low alloy steel (LAS) channel head base metal, and that there were areas where the stainless steel clad had also separated from the channel head base metal. Although the 3A RSG exhibited similar butter/clad separation, it did not exhibit a similar large crack in the divider plate weld. However, nine small cracks were found on one side of this weld.

Shortly thereafter, PT and UT examinations were performed at the San Onofre site on the already delivered Unit-2 RSGs. The examinations resulted in no recordable indications, thus confirming the integrity of the divider plate-to-channel head weld and the bond between the butter/clad and the base metal. Even though the butter groove on the 2B RSG is narrower than on the 2A RSG, there is no difference in accessibility for UT between both RSGs, because the essential parameters of the groove geometry are the same on both RSGs.

This report describes the work performed to determine the root cause of butter/clad separation on the Unit-3 RSGs.

Root Cause Evaluation Summary

The evaluation concluded that the root cause of butter separation on the Unit-3 RSGs was the air carbon-arc gouging applied to remove the stainless steel clad from the channel head area where the structural butter was to be applied. The structural butter is required on the SONGS RSGs due to the fact that the divider plate is a structural attachment supporting the tubesheet.

Gouging was performed using a carbon electrode and left carbon deposits on the base metal. Gouging was followed by grinding which was designed to remove the heat affected zone and should, but it did not, remove the carbon deposits completely. The carbon deposits left behind resulted in the localized areas of high carbon and high base metal hardness (due to carburization).

The evaluation concluded that the root cause promoted a direct cause which led to butter separation initiation. This cause was a localized weak bond between the butter and the channel head base metal. Butter separation also caused limited area separation of the channel head clad.



It is also possible, but less probable, that the root cause promoted hydrogen induced cracking (HIC) in the high base metal hardness/high stress areas, most likely in the butter groove corner areas, due to hydrogen preferentially diffusing into these areas.

The evaluation concluded that the contributing causes which led to extensive butter separation were: 1) weld joint loading during thermal transients (IPWHT, PWHT) and 2) weld joint loading during primary side hydrostatic testing.

Also, the following causes could contribute to HIC that possibly could have occurred on the U3 RSGs, but did not occur on the U2 RSGs: (1) different (worse) butter groove corner geometry, (2) lower post-bake temperature and (3) shorter pre-heat time, as all of them could result in harmful hydrogen concentrations in the butter groove corner areas.

Extent of Condition

The evaluation concluded that the extent of condition was limited to the Unit-3 RSGs divider plate-to-channel head weld joint butter area for the following reasons:

- a) The clad was removed by gouging only on the Unit-3 RSGs; on the Unit-2 RSGs, it was removed by machining.
- b) For the Unit-3 RSGs, the pre-heat duration was only one third of that for the Unit-2 RSGs, and the post-baking temperature was lower than that for the Unit-2 RSGs. Both conditions would result in a higher hydrogen concentration in the finished weld (butter).
- c) The Unit-3 RSG butter groove has a smaller corner radius and a steeper side slope than the Unit-2 groove. These differences caused the residual stresses from shrinkage of the butter in the direction perpendicular to the fusion boundary in the Unit-3 RSGs to be nearly three times as high as in the Unit-2 RSGs.
- d) The Unit-2 RSGs passed the primary side hydrostatic pressure test without an incident.
- e) The UT examinations of the Unit-2 RSGs did not identify any separation of the butter or clad from the base metal.

It was further concluded that this condition did not apply to the Unit-2 RSGs or to any other dissimilar weld joint within the SONGS RSGs.



Table of Contents

1.0 EVENT DESCRIPTION..... 3

2.0 IMMEDIATE INVESTIGATIVE ACTIONS..... 3

 2.1 ACTIONS FOR THE UNIT-3 RSGs 3

 2.1.1 Visual Inspection and Dye Penetrant Examinations..... 3

 2.1.2 UT Examinations 3

 2.1.3 Unit-3 Divider Plate Flatness..... 3

 2.1.4 Unit-3 Divider Plate Weld Fillet Dimensions 3

 2.2 ACTIONS FOR THE UNIT-2 RSGs 3

 2.2.1 Visual Inspection and Dye Penetrant Examinations..... 3

 2.2.2 UT Examinations 3

 2.2.3 Unit-2 Divider Plate Flatness..... 3

 2.2.4 Unit-2 Divider Plate Weld Fillet Dimensions 3

3.0 LONG-TERM INVESTIGATIVE ACTIONS 3

 3.1 UNIT-3 AS-BUILT SAMPLE INVESTIGATION..... 3

 3.2 I-TYPE SAMPLE TESTS 3

 3.3 T-TYPE SAMPLE TESTS 3

 3.4 HYDROGEN INDUCED CRACKING INVESTIGATION 3

 3.4.1 Fracture Toughness Tests 3

 3.4.2 Buttering Mock Up Tests..... 3

 3.4.3 Tensile Restraint Cracking (TRC) Tests 3

 3.4.4 Residual Hydrogen Evaluation..... 3

 3.4.5 Carbon Deposition Effect Evaluation 3

 3.4.5.1 Carbon Effect on Fusion Boundary Hardness 3



3.4.5.2 Carbon Induced Cracking Tests.....	3
3.5 REHEAT CRACKING INVESTIGATION	3
3.6 ADDITIONAL INVESTIGATIONS.....	3
3.7 DESIGN COMPARISON	3
3.8 ANALYTICAL INVESTIGATIONS	3
3.8.1 Channel Head Butter	3
3.8.2 Divider Plate Fit Up.....	3
3.8.3 Channel Head-to-Tubesheet Weld.....	3
3.8.4 Channel Head-to-Tubesheet Weld PWHT.....	3
3.8.5 Hydrostatic Test.....	3
3.8.6 Hydrogen Diffusion	3
3.9 FABRICATION PROCESS INVESTIGATION	3
3.9.1 Channel Head Cladding	3
3.9.2 Clad Removal Prior to Buttering.....	3
3.9.3 Buttering	3
3.9.4 Welding of Divider Plate to Channel Head	3
3.9.5 Other Fabrication Steps	3
3.9.6 Hydrostatic Test Records.....	3
3.9.7 Flaw Detection Accuracy.....	3
3.10 MATERIALS.....	3
4.0 EVALUATION OF RESULTS	3
4.1 PRINCIPLES OF DISSIMILAR METAL WELDING.....	3
4.2 MECHANISM OF SEPARATION.....	3
4.2.1 Weak Bond	3
4.2.2 Hydrogen Induced Cracking (HIC).....	3



4.3 ROOT CAUSE DETERMINATION 3

5.0 EVALUATION SUMMARY 3

5.1 ROOT CAUSE 3

5.2 DIRECT CAUSES 3

5.3 CONTRIBUTING CAUSES 3

5.4 EXTENT OF CONDITION 3



- Attachment-A Unit 3 As-Built Sample Investigation
- Attachment-B I-Type Tensile Test
- Attachment-C I-Type Metallurgical Examination
- Attachment-D Additional I-Type Test
- Attachment-E T-Type Test
- Attachment-F Fracture Toughness Test
- Attachment-G Buttering Mock Up Test
- Attachment-H Tensile Restraint Cracking Test
- Attachment-I Measurement of Residual Hydrogen
- Attachment-J Carbon Residue Influence on Fusion Boundary Hardness
- Attachment-K Reheat Cracking Investigation
- Attachment-L Alloy 152 Butter Residual Stresses Analysis
- Attachment-M 2D Analysis to Evaluate the Effect of the Divider Plate Offset
- Attachment-N 3D Analysis to Evaluate the Channel Head-to-Tubesheet Weld Shrinkage
- Attachment-O 3D Analysis to Evaluate the Channel Head-to-Tubesheet Weld PWHT
- Attachment-P 3D Analysis Including the Actual Condition of 3B RSG
- Attachment-Q Hydrogen Diffusion Analysis
- Attachment-R Fabrication Process Comparison
- Attachment-S Additional Investigation of Boat Samples



List of Acronyms

The following list defines the acronyms used in this document.

2A and 2B	SONGS Unit-2 RSGs for trains A and B
3A and 3B	SONGS Unit-3 RSGs for trains A and B
CH	Channel Head
CMTR	Certified Material Test Report
DAC	Distance Amplitude Curve (an Ultrasonic Test parameter)
DP	Divider Plate
EPMA	Electron Probe Micro-Analyzer
ESW	Electro-Slag Welding
FEA	Finite Element Analysis
FEM	Finite Element Model
FPWHT	Final Post-Weld Heat Treatment
HAZ	Heat Affected Zone
IPWHT	Intermediate Post-Weld Heat Treatment
LAS	Low Alloy Steel (channel head & Tubesheet material)
MHI	Mitsubishi Heavy Industries, LTD
PT	Dye Penetrant Testing
PWHT	Post-Weld Heat Treatment
RSG	Replacement Steam Generator
SCE	Southern California Edison
SEM	Scanning Electron Microscope
SMAW	Submerged Arc Welding
SONGS	San Onofre Nuclear Generating Station
TS	Tubesheet
UT	Ultrasonic Testing
UTS	Ultimate Tensile Strength
VT	Visual Testing



1.0 EVENT DESCRIPTION

As a part of the fabrication process, the Replacement Steam Generators (RSGs) for SONGS Unit-2 underwent the shop hydrostatic pressure tests in mid-2008. Since then, they were delivered to the SONGS site and are currently in storage on site. The Unit-3 RSGs underwent the shop hydrostatic pressure tests in early 2009. Table 1-1 shows the dates of all hydrostatic tests.

Table 1-1 Hydrostatic Pressure Test Dates

SONGS RSG	Primary side hydrostatic pressure test completion date	Secondary side hydrostatic pressure test completion date
2A		
2B		
3A		
3B		

On the 3B RSG, a 120 mm (5-inch) long crack on the cold leg side of the divider plate-to-channel head weld was reported on March 18, 2009 during inspection after completion of the primary and secondary side hydrostatic pressure tests (see Figure 1-1).

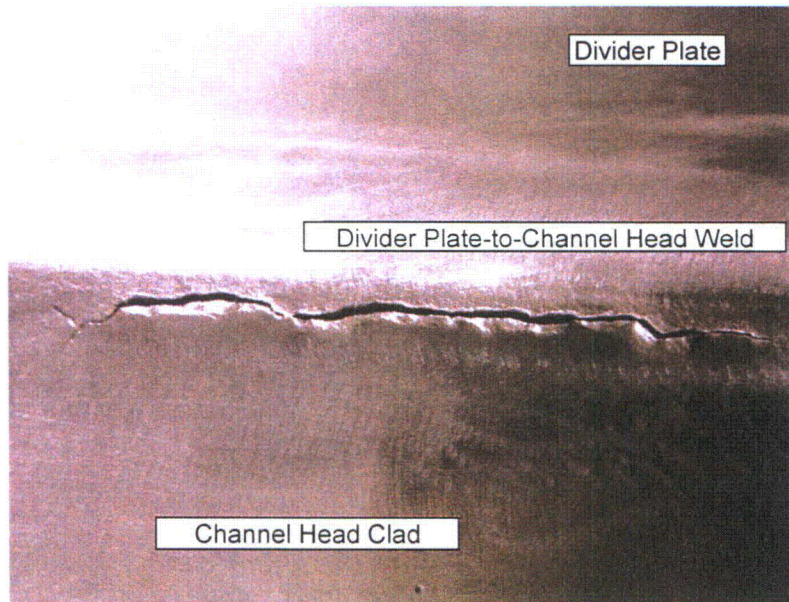


Figure 1-1 RSG 3B Crack in the Divider Plate-to-Channel Head Weld



The divider plate separates the hot leg side from the cold leg side of the channel head and is welded to the channel head and the tubesheet. Figure 1-2 is a photograph taken in the 2A RSG that shows the tubesheet, channel head and divider plate after the hydrostatic test and electropolishing.

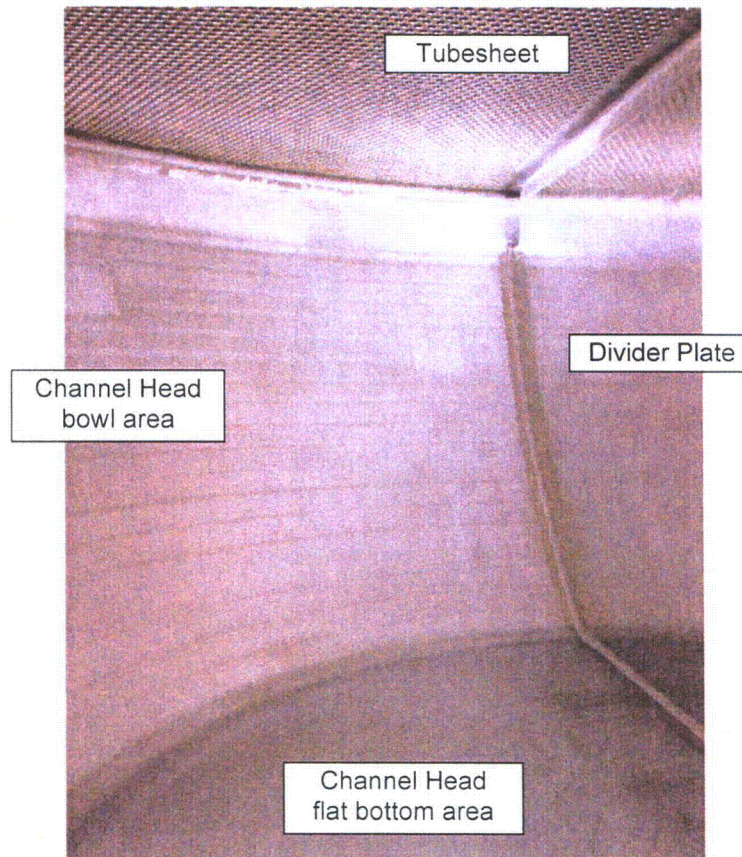


Figure 1-2 RSG 2A Channel Head after Hydrotest & Electropolishing

2.0 IMMEDIATE INVESTIGATIVE ACTIONS

The crack found on the 3B RSG weld led to immediate inspection of the 3A and 3B RSGs to determine the extent of condition. Both underwent VT inspection and PT and UT examinations, which confirmed butter/clad separation from the channel head base metal on both RSGs.

Immediately following these findings, at the SONGS site, Edison performed similar examinations on the Unit-2 RSGs. Those examinations found no indications of separation anywhere within the channel head. These positive results allowed for focusing the root



cause evaluation efforts on investigation of the design and fabrication differences between the Unit-2 and Unit-3 RSGs.

The root cause investigations are described in Section 3.

2.1 Actions for the Unit-3 RSGs

On both Unit-3 RSGs, VT inspection, and PT and UT examinations were performed by MHI in the shop.

2.1.1 Visual Inspection and Dye Penetrant Examinations

On the 3B RSG, PT examinations revealed no indications on either the divider plate-to-channel head or divider plate-to-tubesheet welds, not counting the crack on the cold side of the divider plate-to-channel head weld found during VT inspection after the hydrostatic test.

On the 3A RSG, nine small cracks were found on the hot side of the divider plate-to-channel head weld (Figure 2.1-1). The PT indications were in the center of the channel head flat bottom area, extending over a total distance of approximately 1200 mm (~47"). No indications were found on the cold side of the weld..

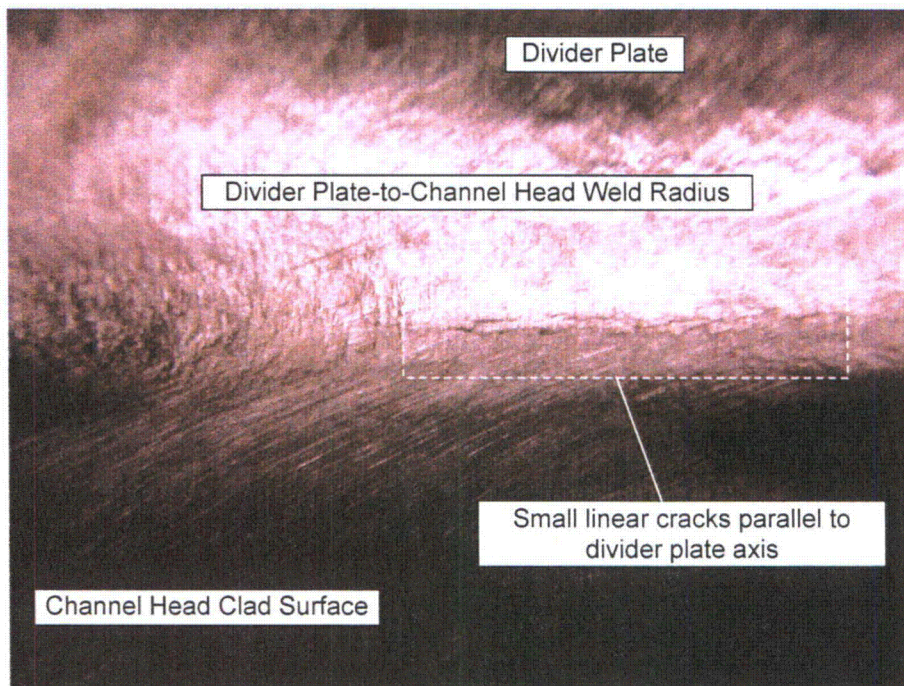


Figure 2.1-1 RSG 3A Hot-Side Divider Plate-to-Channel Head Weld PT Indications



No PT indications were found on the divider plate-to-tubesheet welds on the 3A or 3B RSGs.

2.1.2 UT Examinations

On both Unit-3 RSGs, straight beam UT examinations were performed from the outside of the channel head underneath the divider plate weld joint and from the inside of the channel head in the areas adjacent to the divider plate. Clad and butter separation was detected under and adjacent to the divider plate on both RSGs. Figures 2.1-2 and 2.1-3 show the areas where butter/clad separation was detected.



3#B-RSG: Result of Straight Beam UT (From inside)

Location of Indication

- X-distance
 - Hot side
 - Cold side
- Y-distance
 - Hot side
 - Cold side
- Beam Path Distance
 - Hot side
 - Cold side

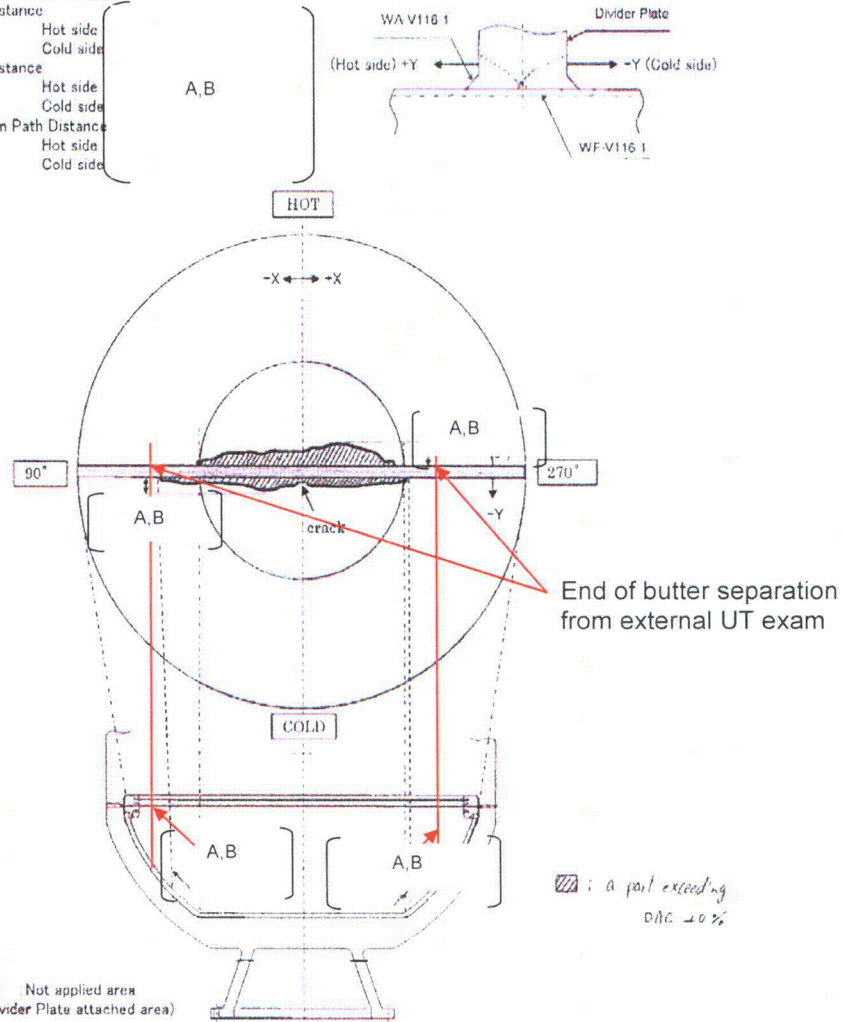


Figure 2.1-2 RSG 3B Butter/Clad Separation Map



3#A-RSG: Result of Straight Beam UT (From inside)

Location of Indication

- X-distance
 - Hot side
 - Cold side
- Y-distance
 - Hot side
 - Cold side
- Beam Path Distance
 - Hot side
 - Cold side

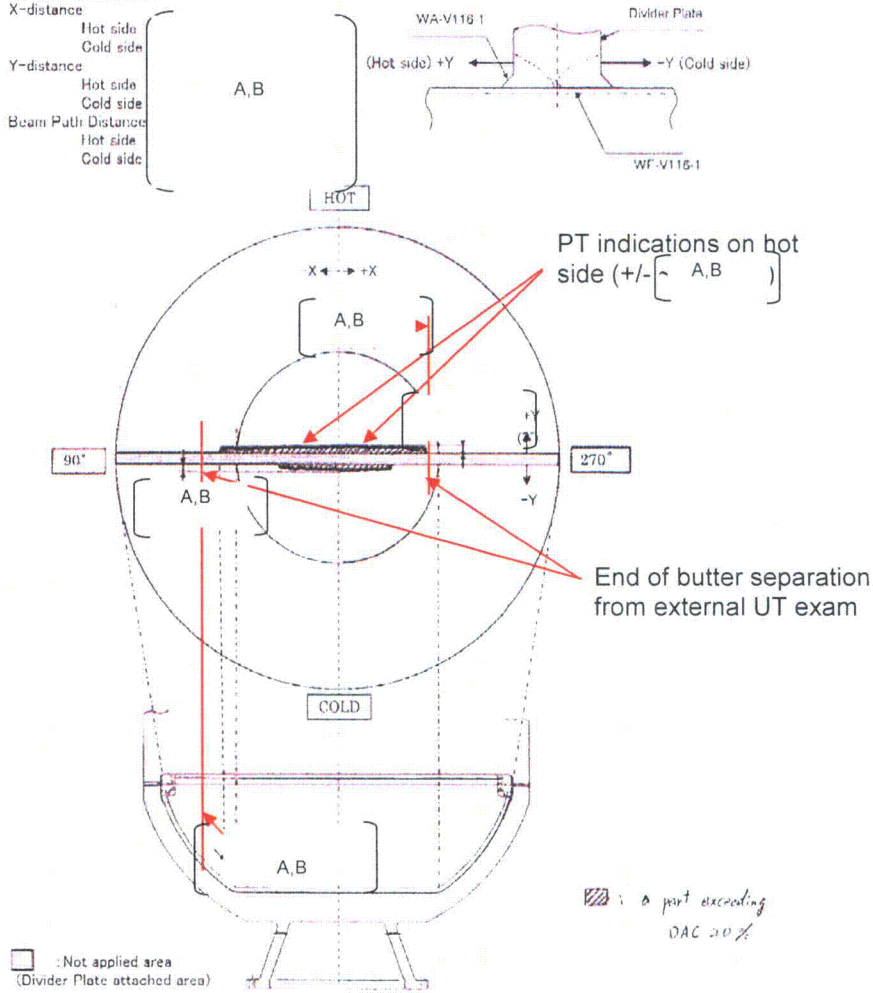


Figure 2.1-3 RSG 3A Butter/Clad Separation Map

The dimensions of the butter/clad separation area envelopes are summarized in Table 2.1-1.



Table 2.1-1 Butter/Clad Separation Area Envelopes

Distance from RSG centerline	RSG-3B, mm (inch)	RSG-3A mm (inch)
0° axis (hot side)		
90° axis (internal UT)		
90° axis (external UT – under DP)		
180° axis (cold side)		
270° axis (internal UT)		
270° axis (external UT – under DP)		

* Note: PT indications near the center

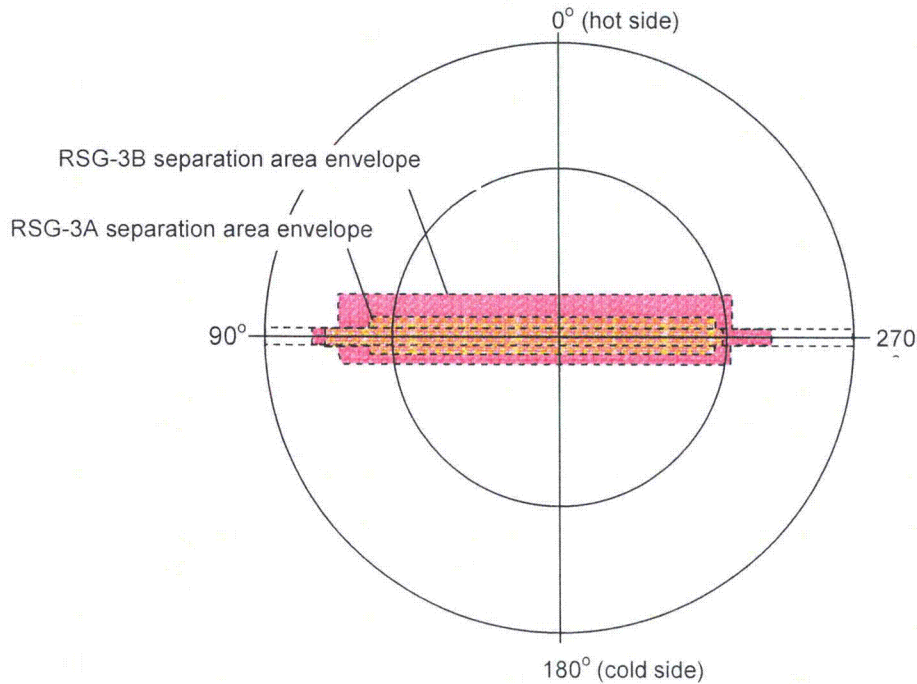


Figure 2.1-4 Unit-3 Butter/Clad Separation Area Envelopes



Note that the 3A RSG underwent two primary side and two secondary side hydrostatic pressure tests, while the 3B RSG underwent only one of each test. Even so, the size of the clad separation area on the 3B RSG is the larger of the two. This indicates that the number of pressure tests is not a contributing cause of the butter/clad separation.

2.1.3 Unit-3 Divider Plate Flatness

Divider plate flatness in the Unit-3 RSGs was measured by MHI in the shop. The measurement results showed that the flatness for the 3A RSG was within 1.5 mm (0.06") which was within the fabrication tolerance and that the flatness for the 3B RSG was within the accuracy of the measurement (0 mm). Perpendicularity of the divider plate could not be measured, but it was visually judged as meeting the design requirements (i.e. no offset).

2.1.4 Unit-3 Divider Plate Weld Fillet Dimensions

The divider plate-to-channel head welds have an outer fillet that is made by manual welding and grinding. The goal of the weld final geometry is to provide a smooth transition between the vertical and horizontal planes, free of notches or other stress risers. The fillet corner radius is larger than a minimum value of [A,B], and the legs of the fillet are longer than a minimum value of [A,B]. The divider plate-to-tubesheet weld fillets have similar dimensions.

From a structural viewpoint, the weld fillet toe area allows the tensile forces from the divider plate to distribute into the channel head over a wider area, thus reducing the average stress in the butter area. Therefore, a wider weld fillet is good, so is the larger corner radius.

The results of the weld fillet measurements for the Unit-3 RSGs are listed in Table 2.1-2. All of the dimensions are greater than the minimum required values. The local elastically calculated stresses underneath the divider plate are, therefore, less than the Code allowables.

Table 2.1-2 Unit-3 RSG Divider Plate Weld Fillet As-Built Dimensions

Parameter, mm (inch)	Drawing	RSG-3A	RSG-3B
Minimum fillet-to-fillet width in flat bottom area			
Maximum fillet-to-fillet width, in flat bottom area			
Minimum fillet radii in flat bottom area			
Maximum fillet radii in flat bottom area			

2.2 Actions for the Unit-2 RSGs

On both Unit-2 RSGs, VT inspection, and PT and UT examinations were performed by Edison at the SONGS site with MHI attending.



2.2.1 Visual Inspection and Dye Penetrant Examinations

On the 2A RSG, one 9.5 mm (0.375") linear surface indication was found on the hot leg side, however, this indication was not characterized as a crack-like indication.

On the 2B RSG, PT examinations revealed no indications on either the divider plate-to-channel head or divider plate-to-tubesheet welds.

2.2.2 UT Examinations

On both 2A and 2B RSGs, straight beam UT examination was performed from the outside of the channel head underneath the divider plate weld joint and from the inside of the channel head in the areas adjacent to the divider plate. Clad and butter separation was not detected under or adjacent to the divider plate on either one of the RSGs. The UT calibration block utilized during the examinations was supplied by MHI and was the same as that used for the Unit-3 RSG examinations.

2.2.3 Unit-2 Divider Plate Flatness

Divider plate flatness in the Unit-2 RSGs was measured by MHI at SONGS site. The measurement results showed that the flatness for both RSGs was within 2 mm (0.8"), which was within the fabrication tolerance. Perpendicularity could not be measured but it was visually judged as meeting the design requirements (i.e. no offset).

2.2.4 Unit-2 Divider Plate Weld Fillet Dimensions

The divider plate-to-channel head welds have an outer fillet that is made by manual welding and grinding. The goal of the weld final geometry is to provide smooth transition between the vertical and horizontal planes, free of notches or other stress risers. The fillet corner radius is larger than a minimum value of $\left[\begin{matrix} A,B \\ \end{matrix} \right]$ and the legs of the fillet are longer than a minimum value of $\left[\begin{matrix} A,B \\ \end{matrix} \right]$. The divider plate-to-tubesheet weld fillets have similar dimensions.

From a structural viewpoint, the weld fillet toe area allows the tensile forces from the divider plate, to distribute into the channel head over a wider area, thus reducing the average stress in the butter area. Therefore, a wider weld fillet is good, so is the larger corner radius.

The results of the weld fillet measurements for the Unit-2 RSGs are listed in Table 2.2-1. All of the dimensions are greater than the minimum required values. The local elastic stresses underneath the divider plate are, therefore, less than the Code allowables.

All of the fillet dimensions for the Unit-2 RSGs are similar to those for the Unit-3 RSGs.

**Table 2.2-1 Unit-2 RSG Divider Plate Weld Fillet As-Built Dimensions**

Parameter, mm (inch)	Drawing	RSG-2A	RSG-2B
Minimum fillet-to-fillet width in flat bottom area			
Maximum fillet-to-fillet width, in flat bottom area			
Minimum fillet radii in flat bottom area			
Maximum fillet radii in flat bottom area			

A,B

3.0 LONG-TERM INVESTIGATIVE ACTIONS

A "Fault Tree Analysis and Investigation Plan" was developed based on the process steps used to fabricate the channel head assembly. The analysis identified causes and effects for each process step and prescribed specific investigations to evaluate its potential effect on the butter/clad separation phenomenon. A diagram showing the plan is included in Attachment-R. The investigations and analyses identified in the plan are summarized in the following sections.

3.1 Unit-3 As-built Sample Investigation

Three boat samples were collected from the 3B RSG (Samples A, B and C), two strip samples were collected from the 3A RSG (Samples D and E) and two additional boat samples were collected from the 3A RSG (Samples F and G), for the purpose of examining the bond between the butter/clad and the channel head base metal. Sample C was selected based on UT measurements that established the boundary of the clad separation area. The sample included an area of clad separation and an area with an intact clad bond.

Table 3.1-1 provides description of the samples, Figure 3.1-1 shows the locations where the samples were collected, and Table 3.1-2 describes the analyses performed on the samples.

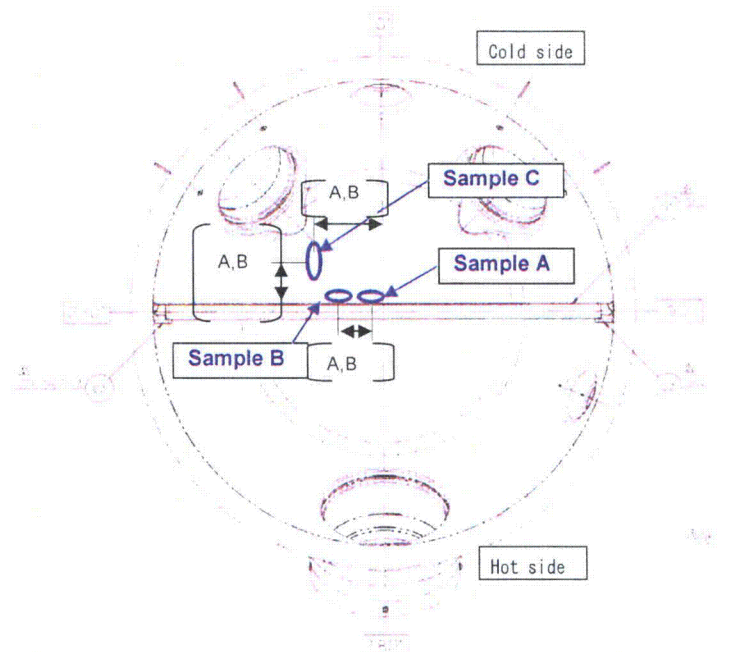


Table 3.1-1 Sample Collection Locations

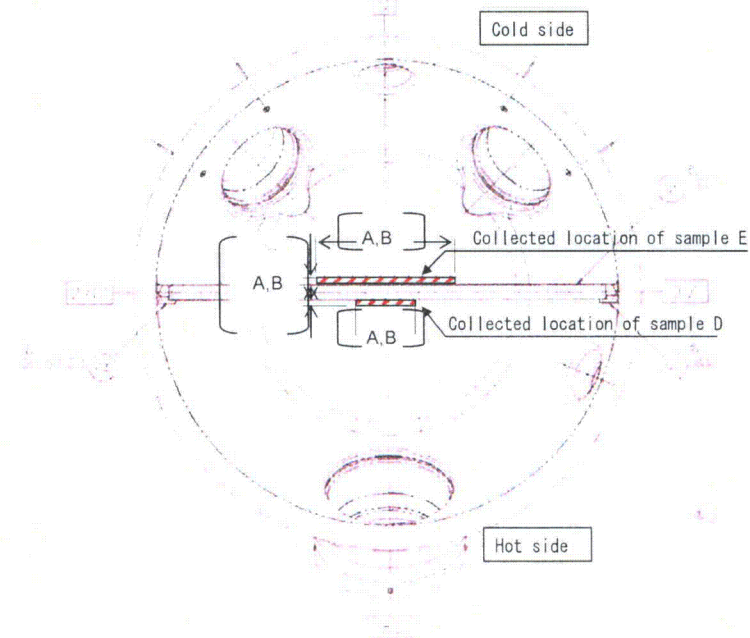
Sample No.	Location	Purpose
Sample A (from 3B)	Area with the divider plate weld crack, including weld fillet, transition zone and base metal	To investigate the nature of the crack and the Alloy 152 butter / clad separation from base metal
Sample B (from 3B)	Area with separated Alloy 152 butter, including butter, transition zone and base metal	To investigate the nature of the Alloy 152 butter separation from the base metal
Sample C (from 3B)	Area with stainless steel cladding near the separation area boundary (as identified by UT), including clad, transition zone and base metal	To investigate the nature of the clad separation from the base metal and to identify any differences from Samples A & B
Sample D (from 3A)	Large area of separated Alloy 152 butter and stainless steel clad only from the hot side	To investigate the nature of the Alloy 152 butter and the clad separation from the base metal
Sample E (from 3A)	Large area of separated Alloy 152 butter and stainless steel clad only from the cold side	To investigate the nature of the Alloy 152 butter and the clad separation from the base metal
Sample F (from 3A)	Area at the center of Sample E after Sample E removal, including base metal only	To investigate the nature of the Alloy 152 butter separation from the base metal
Sample G (from 3A)	Area of bonded Alloy 152 butter, including butter, transition zone and base metal, from the cold side	To identify any differences from the other samples

**Table 3.1-2 Sample Investigations**

Item	Method	Purpose
Sample appearance	Visual examination	Confirm that the sample has expected characteristics
Separation surface	Visual examination at low magnification	Evaluate the macro-structure of the separation/crack surface
Separation surface	SEM (Scanning Electron Microscope) examination at high magnification	Evaluate the micro-structure of the separation/crack surface
Macro-structure	Visual examination of the cross-section at low magnification after etching	Evaluate the macro-structure of the materials constituting the sample
Micro-structure	Visual examination of the cross-section at high magnification after etching	Evaluate the micro-structure of the materials constituting the sample, examine the existence of micro-cracking in LAS, and measure the grain size of HAZ
Hardness	Measure Vickers hardness	Evaluate the hardness distribution near the separation/crack surface
Chemical analysis	EPMA analysis	Evaluate chemical composition of the material near the separation/crack surface

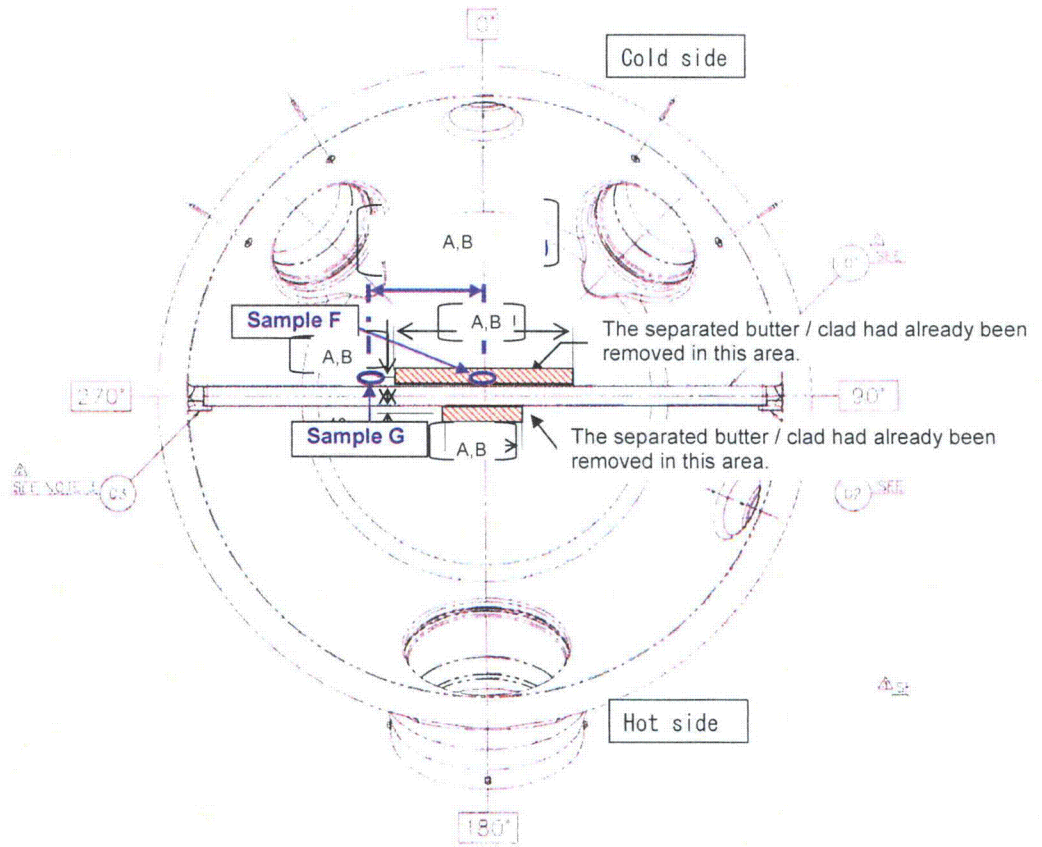


Boat Sample locations A, B and C



Strip Sample locations D and E

Figure 3.1-1 Sample Collection Locations (1/2)



Boat Sample locations F and G

Figure 3.1-1 Sample Collection Locations (2/2)



Examinations of the samples concluded that there were no significant differences between the seven samples removed from the 3A and 3B RSGs. The detailed conclusions were as follows:

- The crack observed on the surface of the divider plate-to-channel head weld fillet on the 3B RSG was a ductile fracture.
- Where the butter/clad separated from the base metal, the fracture surface characteristics were indicative of a brittle fracture. Figure 3.1-2 (left) shows quasi-cleavage and (right) shows Type II grain boundary-like pattern, both typical for brittle fractures.

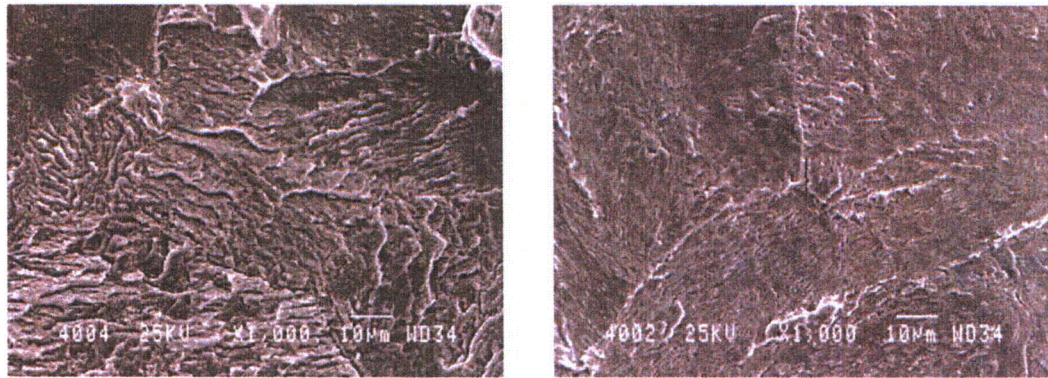


Figure 3.1-2 Fracture surfaces of the Unit-3 samples

- Butter/clad separation propagated along the butter/clad-to-base metal fusion boundary.
- The microstructures of the low alloy steel, Alloy 152 butter and stainless steel clad were as-expected (typical) with no reportable abnormalities.
- High hardness was observed in a "white zone" between the butter/clad and the base metal adjacent to the fusion boundary. (The white zone is a hardened layer thought to be martensitic in microstructure, that appears as a thin light-colored line after etching, because it is more corrosion resistant than the other sample cross section zones).
- A hardness of up to 550 HV was measured at the fusion boundary and was thought to be caused by carburization.
- Chemical composition of the butter, stainless steel clad, and base metal were as-expected (typical) with no reportable abnormalities.
- No micro cracking and no significant welding defects such as slag, inclusions, lack of fusion or blowholes were noticed.
- In addition, examination of Sample C confirmed that the accuracy of UT detection from the channel head inside was approximately $\left[\frac{A,B}{A,B} \right]$ and from the channel head outside was more than $\left[\frac{A,B}{A,B} \right]$.



Note: Where the terms "as-expected" and "typical" are used, the data obtained from the separation area cannot be distinguished from the data from the area with no separation (normal bond).

Examination of the seven samples revealed no obvious abnormalities and did not identify butter/clad separation initiation area that would aid in identification of the root cause of the separation. The investigation showed that the hardness in the transition zone was elevated. Such elevated hardness is expected in the welds involving dissimilar metals. Higher hardness probably facilitated propagation of butter/clad separation along the fusion boundary. However, the examination of these samples alone was not sufficient to identify the root cause of separation.

It is noteworthy that Samples D and E showed a distinct imprint of the butter/clad-to-base metal interface (see photos in Attachment-A). Examination of that interface on all the samples indicated as-expected chemistry and hardness and characterized the surface condition at the separation boundary as being typical of a brittle fracture; but without any specific indication of its origin.



3.2 I-Type Sample Tests

The purpose of the I-Type sample tensile tests was to reproduce the butter/clad separation along the fusion boundary that occurred in the Unit-3 RSGs, in order to obtain the necessary data for evaluation of the cause of failure in general, and of the effect of gouging on susceptibility to failure in particular.

A single block made of SA-533 low alloy steel was prepared by applying the stainless steel clad, removing the clad by machining or gouging to simulate the fabrication processes used on the Unit-2 and Unit-3 RSGs, and then applying the Alloy 152 butter. Smooth and notched tensile samples were then prepared by machining the "slices" cut from this block.

The tensile tests were performed at room temperature in air and after the tests the fracture surfaces were examined. The test matrix is shown in Table 3.2-1.

Table 3.2-1 I-Type Sample Preparation

Purpose	Fabrication process			Tensile test
	Electroslag welding	Gouging + grinding	Machining	
Effect of gouging (Simulating Unit-3)	TP No.①-1 Macro structure Micro structure Hardness	TP No.②-1 Macro structure Micro structure Hardness Surface etching	-	TP No.②-2 Macro structure Micro structure Hardness Tensile test
Effect of removal of HAZ by gouging		TP No.④-1、④-2 Macro structure Micro structure Hardness	-	-
Effect of machining (Simulating Unit-2)		-	TP No.③-1 Macro structure Micro structure Hardness Surface etching	TP No.③-2 Macro structure Micro structure Hardness Tensile test



-I-Type Tensile Test Results

All smooth specimens fractured within the Alloy 152 butter. All notched specimens fractured at the notch location. These tests did not reproduce a brittle fracture surface observed on the samples collected from the Unit-3 RSGs. No differences were evident between the samples regardless of whether the clad was removed by gouging or by machining.

-I-Type Metallurgical Examination Results

Hardness near the fusion boundary on the samples with the clad removed by gouging was lower than that measured on the samples collected from the Unit-3 RSGs. The metallurgical structure and hardness near the fusion boundary on the samples with the clad removed by gouging and machining were not significantly different.

The test design is shown and the test results are described in detail in Attachments-B and C.

-Additional I-Type Sample Tests

Additional I-Type samples were fabricated with Alloy 152 butter applied onto the base metal after gouging without grinding. Smooth and notched test samples were prepared. The tensile tests were performed at room temperature in air and after the tests the fracture surfaces were examined.

All smooth specimens fractured within the base metal. All notched specimens fractured at the notch location. These tests did not reproduce a brittle fracture surface observed on the samples collected from the Unit 3 RSGs.

The metallurgical structure and the tensile strength of the I-Type samples with the clad removed by gouging, but without grinding, were no different than those of the samples that included grinding.

The test results are described in detail in Attachment-D.

3.3 T-Type Sample Tests

The purpose of the T-Type sample tensile tests was to reproduce the butter/clad separation along the fusion boundary that occurred in the Unit-3 RSGs, in order to obtain the necessary data for evaluation of the cause of failure in general, and of the effect of gouging on susceptibility to failure in particular.

Two test samples were fabricated as shown in Figure 3.3-1 using the low alloy steel plates to simulate both the divider plate and channel head pieces. The piece simulating the divider plate had an Alloy 152 butter applied to one end and was welded to the butter applied to the piece simulating the channel head, which had stainless steel clad applied



and then removed prior to butter application. On Sample A, the clad was removed by gouging and on Sample B the clad was removed by machining.

The tensile tests (to failure) were performed at room temperature in air and after the tests the fracture surfaces were examined.

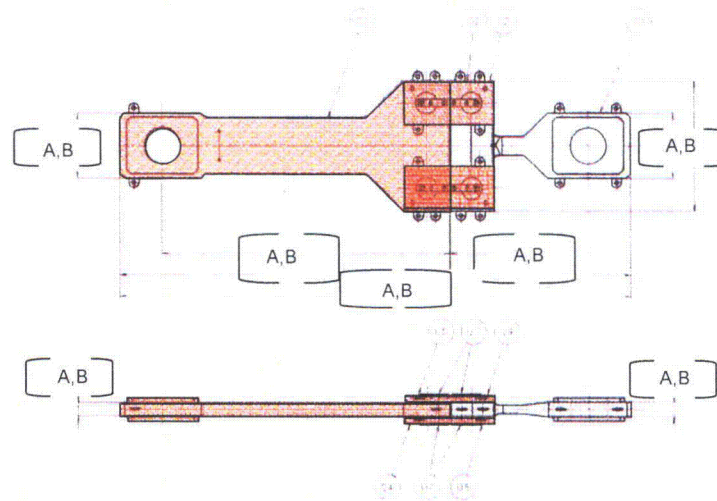


Figure3.3-1 T-Type Full-Scale Test Configuration

Sample A (gouged) fractured within the divider plate simulated by the Alloy 152 butter under a load of [A,B]. Sample B (machined) also fractured within the divider plate simulated by the Alloy 152 butter under a load of [A,B]. Metallurgical structure near the fusion boundary of Sample A (gouged) was similar to that found on the samples collected from the Unit 3 RSGs, including the presence of the "white zone."

These tests did not reproduce a brittle fracture surface observed on the samples collected from the Unit-3 RSGs. The reason for this was inability to model the configuration of the divider plate-to-channel head weld joint in full scale and faithfully replicate during sample preparation all conditions present during fabrication of the actual RSGs.

The test design is shown and the test results are described in detail in Attachment-E.

3.4 Hydrogen Induced Cracking Investigation

3.4.1 Fracture Toughness Tests

The purpose of the fracture toughness tests was to reproduce the butter/clad separation along the fusion boundary that occurred in the Unit-3 RSGs, in order to obtain the necessary data for evaluation of the cause of failure in general, and of the effect of gouging and residual hydrogen concentration on susceptibility to failure in particular.

The test samples were prepared by removing the stainless steel clad by gouging or machining to simulate the fabrication process used on the Unit-2 and Unit-3 RSGs. The samples were prepared to simulate the flawed bond between the Alloy 152 butter and the base metal in order to examine the effect of most likely flaws on susceptibility to brittle fracture along the fusion boundary.



The toughness tests were performed at room temperature in air and after the tests the fracture surfaces were examined. The test matrix is shown in Table 3.4-1.

Table 3.4-1 Test matrix

Pre-crack	Hydrogen pre-charge ^{*1}	Orientation of crack	Fracture Test No.	
			Machining	Gouging
No pre-crack ^{*2}	Yes	S-L	M-1	G-1
Fatigue pre-crack ^{*3} ~1.5mm (0.06")	No	S-L	M-2	G-2
		S-T	M-3	G-3
No pre-crack ^{*2}	No	S-L	M-4	G-4
		S-T	M-5	G-5
Hydrogen pre-crack ^{*4}	No	S-L	M-6	G-6

**1 The sample was pre-charged with hydrogen just before the load was applied.*

**2 Pre-crack was not introduced at the end of notch.*

(All samples have notch shown in Attachment-F, Figure F.3.)

**3 Fatigue pre-crack was introduced with cyclic loading at the end of notch.*

**4 Pre-crack was introduced with hydrogen pre-charged and application of loading, and then heat treatment was performed to remove hydrogen from the samples.*

In summary, fracture at the fusion boundary occurred on the sample with hydrogen pre-charge but fracture did not occur under hydrogen-free conditions. There is not a large difference in fracture resistance at the fusion boundary (J-R curve) between the "M" samples (machined) and "G" samples (gouged).

The test design is shown and the test results are described in detail in Attachment-F.

3.4.2 Buttering Mock Up Tests

The purpose of the buttering mockup tests was to reproduce the butter/clad separation along the fusion boundary that occurred in the Unit-3 RSGs under extreme conditions in terms of butter application environment, in order to obtain the necessary data for evaluation of the cause of failure in general, and of the effect of gouging on susceptibility to failure in particular.

Two types of test samples were fabricated under the following extreme conditions reflecting the Unit-2 and Unit-3 RSGs clad removal methods (machining and gouging, respectively) and butter groove configurations:

- No pre-heating
- No post-baking
- Wet welding rods

In this mock up tests, the butter/clad separation phenomenon was not reproduced.



The test design is shown and the test results are described in detail in Attachment-G.

3.4.3 Tensile Restraint Cracking (TRC) Tests

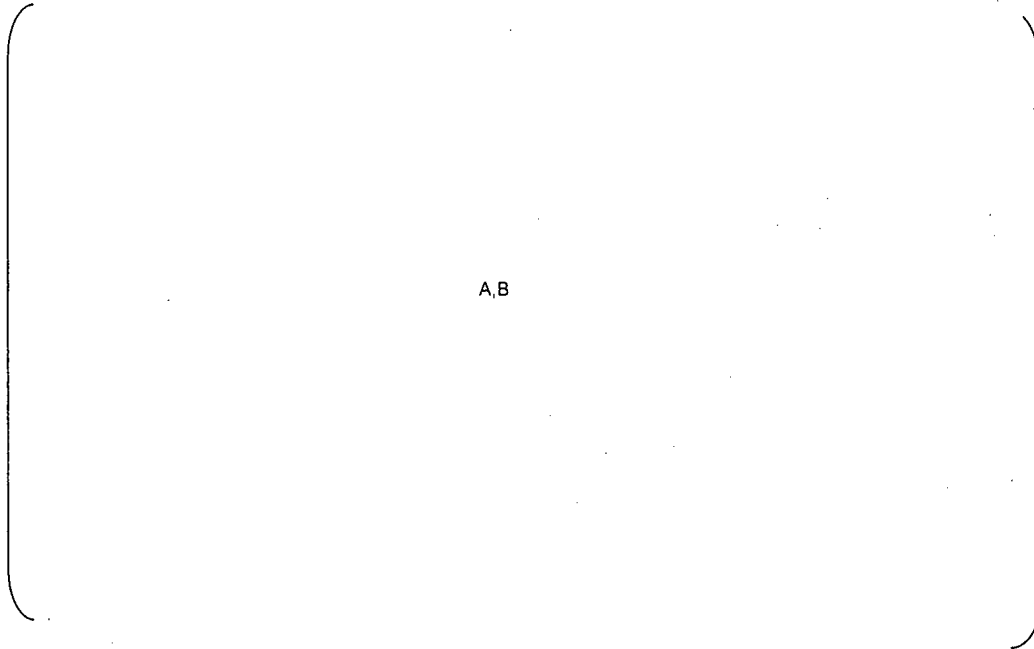
The purpose of the TRC tests was to reproduce the butter/clad separation along the fusion boundary that occurred in the Unit-3 RSGs, in order to obtain the necessary data for evaluation of the cause of failure in general, and of the effect of gouging and carbon deposition on susceptibility to failure in particular.

Three types of test samples were prepared with a "normal groove", "carbon added" and "gouged surface."

The test was performed under the following conditions:

- No pre-heating
- No post-baking
- Wet welding rods
- Tensile load applied immediately after welding

Figure 3.4-1 shows the results of the TRC tests. In these tests, the butter/clad separation phenomenon was reproduced; under a certain load each sample exhibited a brittle fracture along the fusion boundary.



A,B

Figure3.4-1 TRC Test Results

The test design is shown and the test results are described in detail in Attachment-H.

3.4.4 Residual Hydrogen Evaluation

The purpose of this evaluation was to measure residual hydrogen concentration in the Alloy 152 butter and stainless steel cladding in the samples prepared in the laboratory conditions and in the samples collected from the 3A RSG, and to estimate the effect of the post-baking temperature on the residual hydrogen concentration. Table 3.4-2 shows the measurement matrix.

**Table 3.4-2 Evaluation Samples**

Sample type	Sample Name	Sample Condition/Location
New lab sample	A1	Pre-heated and no post-baking
	P1	Add post-baking to A1, simulating RSG-2A
	P2	Add post-baking to A1, simulating RSG-2B
	P3	Add post-baking to A1, simulating RSGs-3A and 3B
Samples collected from 3A RSG	R1	Alloy 152 buttering
	R2	Stainless steel cladding by SMAW
	R3	Stainless steel cladding by ESW

The evaluation of the RSG-3A samples showed that they contained hydrogen in the butter and that the difference in the post-baking temperatures as seen between the Unit-2 and Unit-3 RSGs did not produce a measureable difference in the residual hydrogen concentrations in the butter.

The evaluation results are described in detail in Attachment-I.

3.4.5 Carbon Deposition Effect Evaluation

3.4.5.1 Carbon Effect on Fusion Boundary Hardness

The purpose of this test was to reproduce the hardened layer at the butter-to-base metal fusion boundary by embedding carbon onto the base metal surface prior to buttering. The result of this test was significantly higher hardness at the fusion boundary. This result confirmed that carbon residue left behind after gouging, if not completely removed, would have had a significant effect on fusion boundary hardness.

The test design is shown and the test results are described in detail in Attachment-J.

3.4.5.2 Carbon Induced Cracking Tests

The purpose of these test was to evaluate the effect of the presence of carbon at the butter-to-base metal fusion boundary on susceptibility to HIC. The test samples were prepared by embedding carbon in the weld joint and adding a carbon coating to the base metal surface prior to butter application. These tests confirmed that carbon addition increases the susceptibility of the joint to failure. (See Figure 3.4-1).

The test design is shown and the test results are described in detail in Attachment-H.



3.5 Reheat Cracking Investigation

The purpose of the reheat cracking tests was to determine whether heat input during gouging could initiate reheat cracking. The test matrix is shown in Tables 3.5-1 and 3.5-2.

Table 3.5-1 Test Samples

Item	Type-S	Type-E
Amount	4	4
Cladding process	SMAW	ESW
Label on samples	SM1, SM2, ST1, ST2	EM1, EM2, ET1, ET2
Removal process of clad	Gouging + grinding	
Buttering process	SMAW	
Base metal	Channel head archive sample (MHI stock material)	
Weld metal for buttering	Alloy 152 [A,B]	
Dimension	[A,B]	

Table 3.5-2 Investigations Performed

Item	Method	Purpose
Macro-structure	Visual examination of the cross-section at low magnification after etching	- Evaluate the macro-structure of the materials
Micro-structure	Visual examination of the cross-section at high magnification after etching	- Evaluate the micro-structure around the fusion boundary - Examine the existence of micro-cracking in low alloy steel (LAS) - Measure the grain size of HAZ
Hardness	Measurement for Vickers hardness	- Evaluate the hardness distribution of heat affected zone (HAZ)
Tensile test	Tensile Test on the Round Bar Specimen	- Evaluate whether the reheat cracking initiation occurs on the welding boundary area.

MITSUBISHI HEAVY INDUSTRIES, LTD.



No micro-cracking, including reheat cracking or any other related defects were found in the heat affected zone of the tested samples. The grain size distribution in the samples clad by ESW and SMAW was not significantly different. There was no abnormality in the hardness near the butter-to-base metal fusion boundary. The tensile test samples fractured within the base metal. These tests did not produce reheat cracking and the sample fracture surface characteristics did not duplicate those present in the samples collected from the Unit-3 RSGs.

The test design is shown and the test results are described in detail in Attachment-K.

3.6 Additional Investigations

As a result of the agreements from the working meeting with Edison on this report, additional investigations were performed. They included SEM and EPMA of the boat samples A, B and C.

These investigations did not generate any additional evidence supporting or refuting the conclusions provided in this report, nor did they provide any additional insight on the root cause. The results of these investigations are described in Attachment-S.



3.7 Design Comparison

Figure 3.7-1 shows the dimensions within the divider plate-to-channel head weld joint for all four SONGS RSGs, including the key butter groove dimensions that were considered essential to this evaluation.

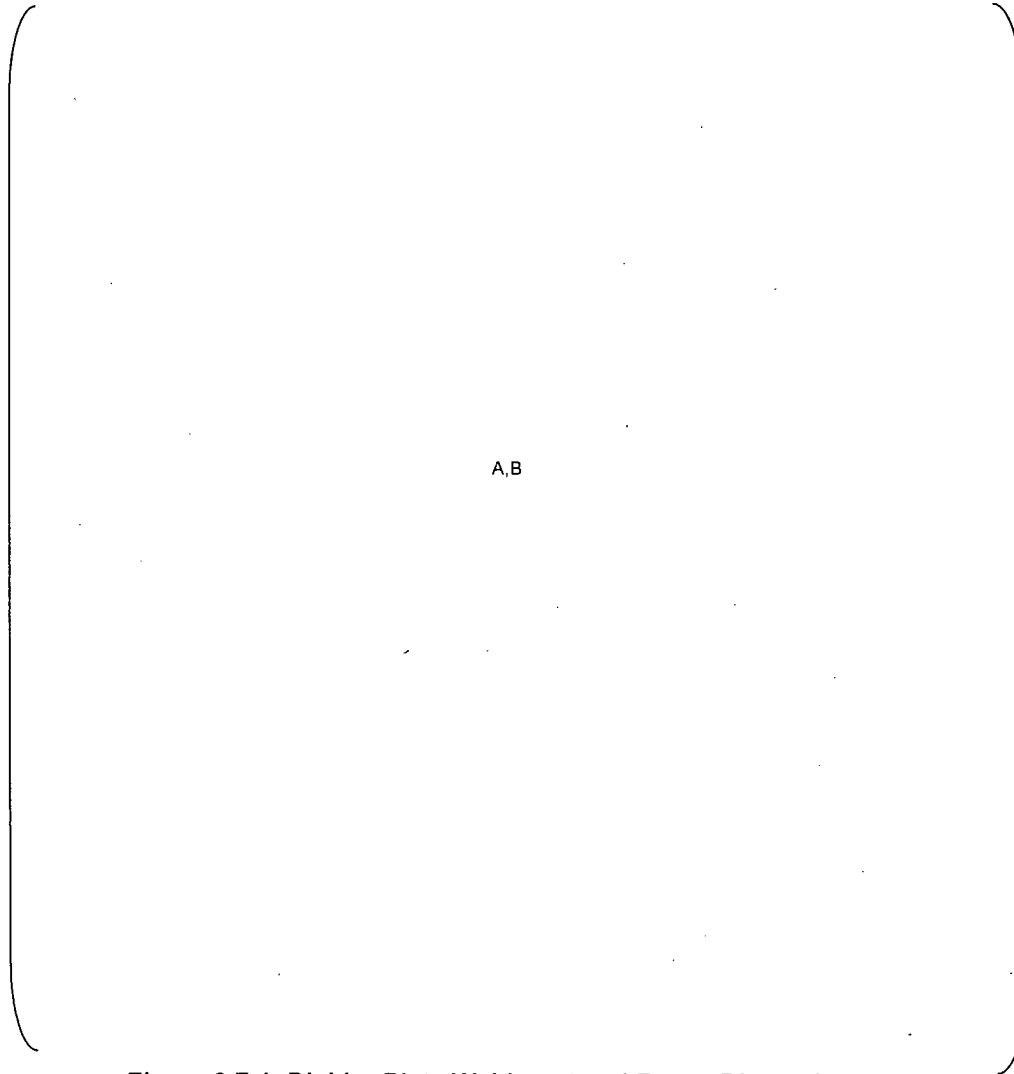


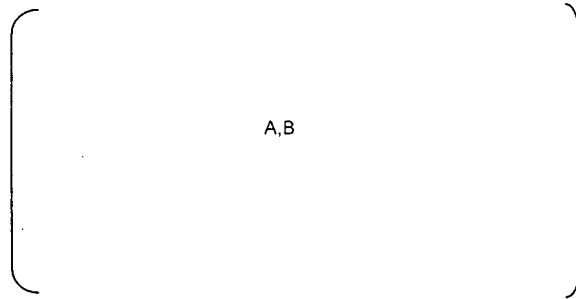
Figure 3.7-1 Divider Plate Weldment and Butter Dimensions

The sketches above show that the butter groove corner radius is considerably smaller and the groove side angle is considerably steeper on the Unit-3 RSGs than on the Unit-2 RSGs.

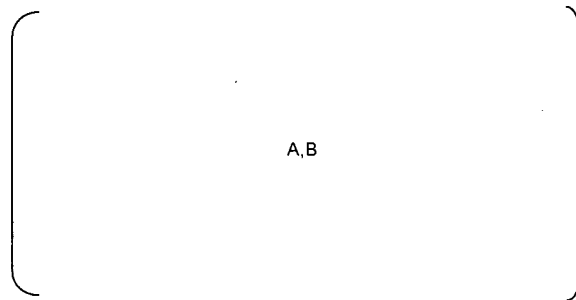


(*) Note: The interface angles between the clad and the butter at the channel head inner surface were estimated from the following samples:

-Unit 2 a mockup sample was specifically prepared to determine the U2 butter groove configuration



-Unit 3 an as-built section of separated material from the 3A RSG (Sample D)





3.8 Analytical Investigations

The Certified Design Report (CDR) for the SONGS RSGs evaluated the divider plate/tubesheet/channel head configuration and demonstrated that the ASME Code, Section III requirements for these components were satisfied. The evaluation did not include fabrication induced conditions such as weld shrinkage or internal residual stresses produced by assembly processes, as this was not required by the Code.

The analytical investigations described in this section began with evaluation of the as-built RSG divider plate-to-channel head weld joint configuration, i.e. the new analytical model included the butter and clad, and actual butter groove dimensions and material properties. The following paragraphs describe the analyses which were performed to determine the residual stresses in the Unit-3 RSGs divider plate-to-channel head weld joints during and after essential fabrication steps.

3.8.1 Channel Head Butter

As mentioned in the preceding section, the butter groove corner radius is smaller and the side angle is steeper on the Unit-3 RSGs than on the Unit-2 RSGs (see Table 3.8-1).

Table 3.8-1 Comparison of the Groove Dimensions and Analysis Results

Dimension	2A	2B	3A	3B	A,B
Depth, mm (inch)					
Corner radius, mm (inch)					
Side slope, degrees					
Maximum tensile stress normal to the fusion boundary, ksi					

An analysis was performed to evaluate the residual stress levels along the butter-to-base metal fusion boundary resulting from the application of the Alloy 152 butter in the groove where the stainless steel clad had been removed. A key element in this analysis was the difference in the dimensions of the groove corner and side.

The analysis indicated that the smaller corner radius and steeper side slope of the Unit-3 RSG butter groove produced significantly higher tensile stresses perpendicular to the fusion boundary. These dimensional differences caused that the groove corner area acted as a stress riser resulting in the residual weld (butter) shrinkage stresses due to buttering to be higher in this area by a factor of three on the Unit-3 RSGs than on the Unit-2 RSGs.

[A,B] as shown in Fig. 3.8-1.

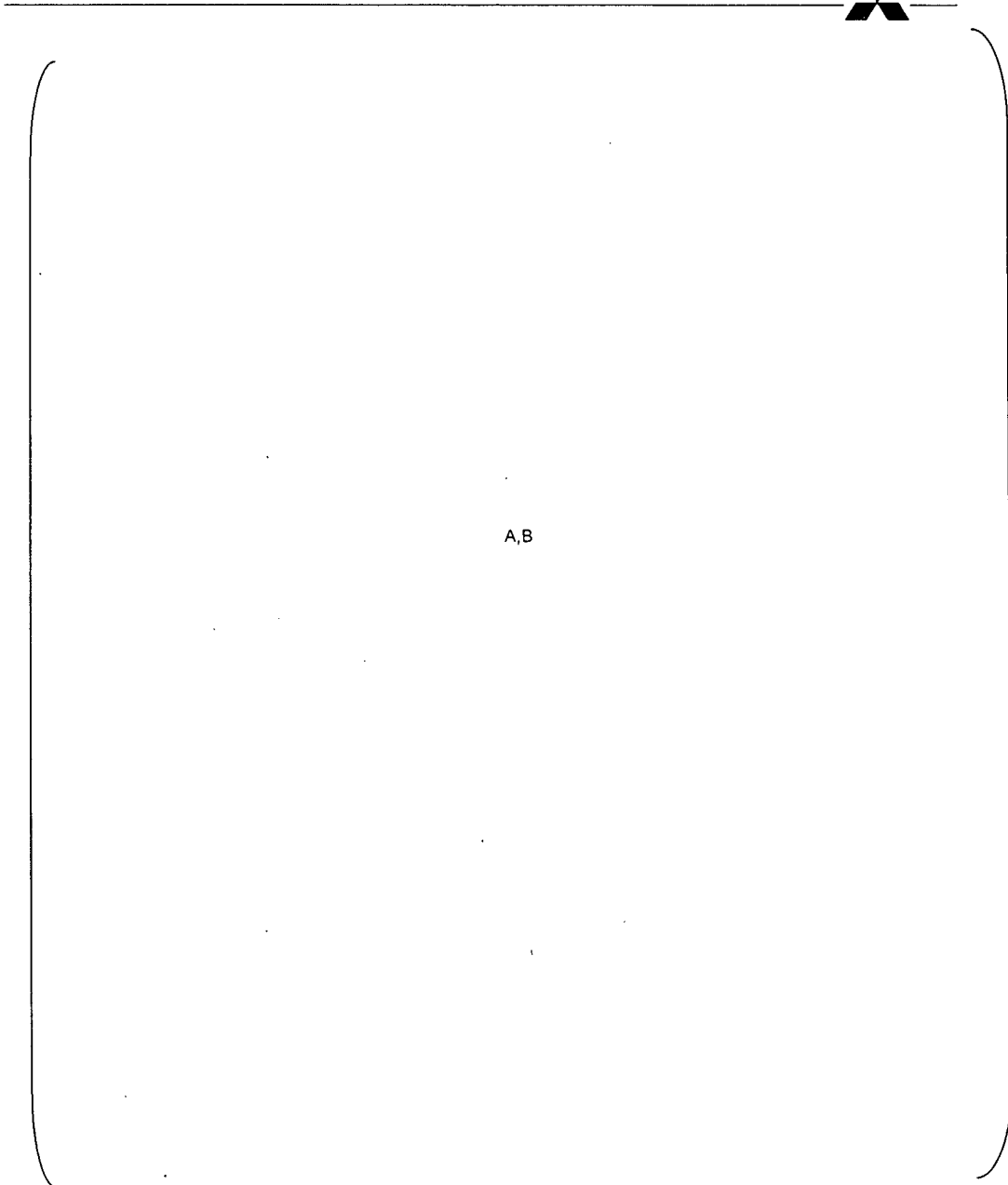


**Figure 3.8-1 Residual Stresses Normal to the Butter-to-Base Metal Fusion Boundary
(under the divider plate at channel head center)**



Because hydrogen preferentially diffuses into the high stress areas, these high stress levels could have contributed to HIC, which might have resulted in an initiating crack(s) in the groove corner area.

This analysis is described in detail in Attachment-L.

3.8.2 Divider Plate Fit Up

An analysis was performed to evaluate the effect of a 10 mm (0.4") divider plate offset from being perpendicular to the channel head bottom on the stress levels in the divider plate-to-channel head weld joint. This analysis showed that there was no significant difference between the stress levels in this condition and with the divider plate being perfectly perpendicular. It was concluded from this analysis that the divider plate potential lack of perpendicularity was not essential, therefore, it could be ruled out as a root or contributing cause of butter/clad separation.

This analysis is described in detail in Attachment-M.

3.8.3 Channel Head-to-Tubesheet Weld

An analysis was performed to evaluate the effect of the channel head-to-tubesheet weld shrinkage on the stress levels in the divider plate-to-channel head weld joint. This analysis did not show high stress levels at the divider plate-to-channel head weld. It is possible, however, that this weld shrinkage contributed to the propagation of the separation initiated in a weak bond area(s), or to propagation of a pre-existing crack(s).

This analysis is described in detail in Attachment-N.

3.8.4 Channel Head-to-Tubesheet Weld PWHT

An analysis was performed to evaluate stress levels in the divider plate-to-channel head weld joint during the PWHT of the channel head-to-tubesheet weld. This analysis showed that the stress on the surface of the flat bottom area, near the divider plate was very low - lower than [A,B]. It is possible, however, that the PWHT contributed to the propagation of the separation initiated in a weak bond area(s), or to propagation of a pre-existing crack(s).

This analysis is described in detail in Attachment-O.

3.8.5 Hydrostatic Test

An analysis was performed to evaluate the stress levels in the divider plate-to-channel head weld joint during the primary side hydrostatic pressure test. This analysis included the material properties of the Alloy 152 butter, the stainless steel clad, and the as-built weld fillet and butter groove corner configuration at the divider plate-to-channel head weld. The tensile stress normal to the butter-to-base metal fusion boundary was the highest near the butter groove corner area. It was concluded, however, that these stresses alone were not sufficient to result in butter/clad separation. However, the hydrostatic test loading



most likely contributed to the propagation of the separation initiated in a weak bond area(s) or to propagation of a pre-existing crack(s).

This analysis is described in detail in Attachment-P.

3.8.6 Hydrogen Diffusion

An analysis was performed to evaluate concentrations of the residual hydrogen remaining after application of the Alloy 152 butter. The analysis showed that the butter and clad materials contained hydrogen on the order of ppm even after the PWHT and that the difference in post-baking temperatures, such as seen between the Unit-3 and Unit-2 RSGs, did not have a discernable effect on these hydrogen concentrations.

This analysis is described in detail in Attachment-Q.

3.9 Fabrication Process Investigation

The fabrication sequence for the Unit-2 and Unit-3 RSG channel heads was reviewed and all its steps were compared in the course of this evaluation. Although the comparison showed that majority of the fabrication methods and parameters were common to all four RSGs, there were some steps when they were different. Of the greatest interest are those steps where a method or parameters used on the Unit-2 RSGs were different than those used on the Unit-3 RSGs.

For the detailed fabrication step comparison, refer to Attachment-R.

3.9.1 Channel Head Cladding

Stainless steel clad was applied to the entire inner surface of the LAS channel head in order to provide its compatibility with the reactor coolant system (resistance to corrosion).

The stainless steel clad was applied on the channel head bowl by the Electro-Slag Welding (ESW) process except at the center of the channel head bottom where the Shielded Metal Arc Welding (SMAW) process was used. One of the causes of weld quality degradation is "migration of detrimental materials into the base metal, which could lead to degradation of the base metal material properties". Another cause can be improper welding conditions (e.g., exceeding the heat input limit).

Actions taken to address such causes included review of the welding records and welding processes. The reviews concluded that the welding process parameters such as current, voltage, speed, pre-heat/inter-pass temperatures were all within the specified ranges and the welding materials met the specification requirements.

The in-process clad PT examinations on the 2A RSG resulted in some unacceptable indications, but none of these indications was near the divider plate. These indications were reworked in accordance with the approved standard procedure. The clad PT examination results for the other three RSGs were acceptable.



The in-process clad UT examinations on the 3A RSG resulted in both unacceptable indications and acceptable but recordable indications, but none of these indications was near the divider plate. The unacceptable indications were reworked in accordance with the approved standard procedure. The clad UT examination results for the other three RSGs were acceptable.

3.9.2 Clad Removal Prior to Buttering

The SONGS RSG design utilizes a divider plate, which is a structural attachment credited for supporting the tubesheet during limiting transients. This necessitated that a structural butter be applied on the channel head, to which the divider plate was welded. The Alloy 152 butter also allowed for not performing PWHT of the divider plate-to-butter weld. In order to apply the butter, the stainless steel clad had to be removed from the area where the butter were to be applied.

The stainless steel clad was removed by machining on the Unit-2 RSGs and by air carbon-arc gouging on the Unit-3 RSGs. The change from machining to gouging was made in order to avoid a schedule delay due to machine unavailability. [

A,B

] Both processes were followed by grinding and buffing to produce a smooth base metal surface suitable for PT examination and butter application. The channel head surface on the Unit-3 RSGs was also acid-etched to confirm that the clad was removed completely.

Gouging vs. machining is a major difference between the Unit-2 and Unit-3 RSG fabrication process. An important feature of the gouging process is that it uses a carbon electrode. If a carbon residue deposited on the base metal surface during gouging is not completely removed by subsequent grinding, the hardness at the base metal surface will increase significantly due to carburization. Also, the elevated hardness lowers the threshold stress needed for initiation of HIC and makes it more likely to occur.

3.9.3 Buttering

The review of the welding records indicated that the welding materials were used correctly and buttering was performed properly. Welding parameters such as current, voltage, speed and preheat/inter-pass temperatures were within the specified ranges. There was no evidence or record of carbon residue on the surfaces where the butter was applied, however, such residue could have been present, especially in the butter groove corner areas where its removal by grinding was difficult due to a small corner radius.

There were differences in the number of weld layers and weld beads noted between the four RSGs but these differences were judged not to be essential to the butter/clad separation.

The in-process butter VT inspection, and PT and UT examination results were acceptable for all four RSGs and there were no recordable UT indications. Identical inspection/examination methods, procedures and acceptance criteria were used for all four RSGs.



The duration of the pre-heating period during buttering was much longer for the Unit-2 RSGs than for the Unit-3 RSGs [^{A,B}]. The temperatures during post-baking after buttering were higher for the Unit-2 RSGs than for the Unit-3 RSGs [^{A,B}]. This difference suggests that after completion of buttering more hydrogen might have been present in the butter-to-base metal transition zone on the Unit-3 RSGs than on the Unit-2 RSGs.

3.9.4 Welding of Divider Plate to Channel Head

The review of the welding records indicated that the processes and sequences used for welding the divider plate to the channel head buttered surface were the same for all four RSGs. An evaluation of the differences in fitting/bracing of the divider plate during welding concluded that they had no effect on the stress levels in the divider plate-to-channel head weld.

The divider plate was welded to the channel head and the tubesheet by GTAW and SMAW processes. The welding sequences and parameters were identical for all four RSGs and were strictly controlled in order to minimize weld shrinkage and distortion.

The weld VT inspection, and PT and UT examination results were acceptable for all four RSGs and there were no recordable UT indications. Identical inspection/examination methods, procedures and acceptance criteria were used for all four RSGs.

3.9.5 Other Fabrication Steps

The processes, sequences and parameters used for welding the divider plate to the tubesheet clad surface and for welding the channel head to the tubesheet were the same for all four RSGs.

The PWHT of the channel head-to-tubesheet weld was tightly controlled and monitored. The process results were essentially the same for all four RSGs with the 2A RSG having the longest accumulated holding time and the 3A RSG having the second longest holding time.

3.9.6 Hydrostatic Test Records

The review of the test records verified that the test pressure and temperature were within the limits required by the ASME Section III Code and hydrostatic test procedure. No unusual pressure changes were identified. All four RSGs were tested in accordance with the same procedure with the only exception being that the 3A RSG underwent two primary and two secondary side hydrostatic tests, while the 3B RSG underwent one primary and two secondary hydrostatic tests as a result of the leaking tube-to-tubesheet joints (seal welds) that needed to be reworked.

3.9.7 Flaw Detection Accuracy

After application, the Alloy 152 butter was examined on all four RSGs by straight beam UT to verify absence of cracks or lack of fusion. As stated in Section 3.9.3, no UT indications



were found on any of the four RSGs. These examinations would have detected any flaws oriented parallel to or at a shallow angle from the channel head inside surface. However, if a flaw were oriented at a relatively steeper angle from the channel head inside surface, it is possible that such a flaw would have escaped detection by straight beam UT.

Figure 3.9-1 shows the test results for straight beam UT detection accuracy as a function of the flaw orientation angle relative to the base metal surface. The 20% DAC threshold corresponds to an angle of approximately [A,B]. Please note that the most likely flaw location is at the butter groove corner (bottom of groove) which is the location with the highest residual stress (after butter application). Therefore, the angle of [A,B] is taken as a slope angle at the groove corner, and not at the groove edge (top of groove).

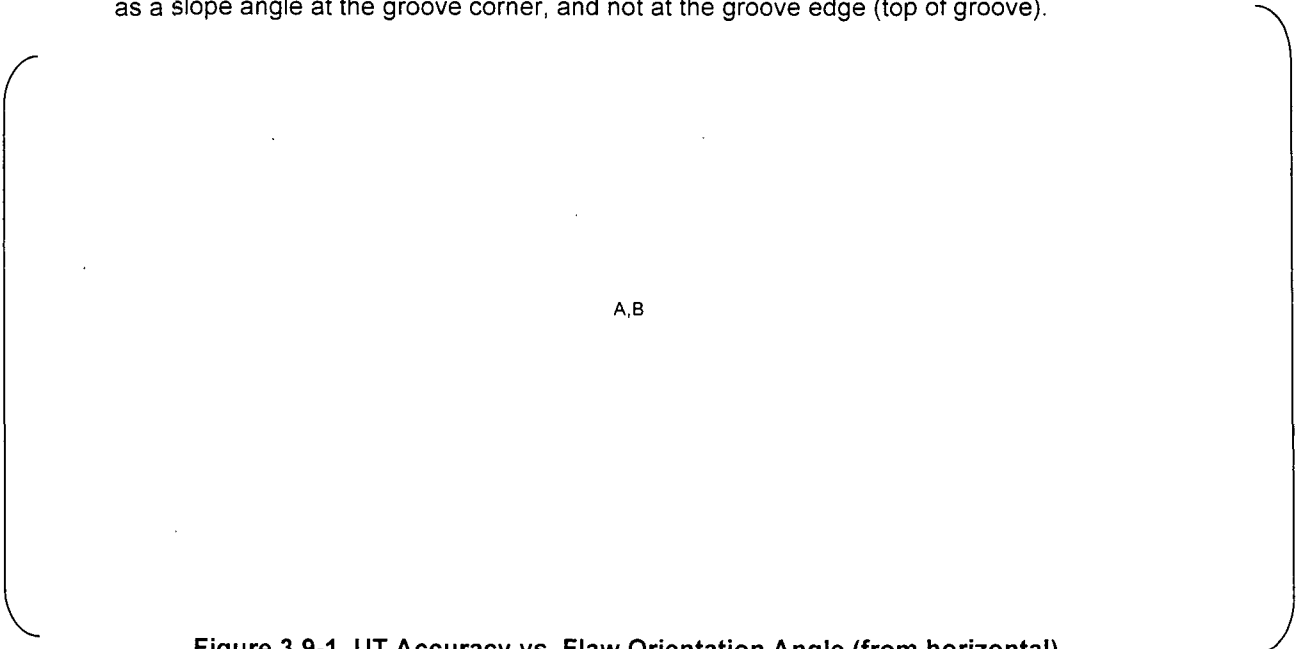


Figure 3.9-1 UT Accuracy vs. Flaw Orientation Angle (from horizontal)

For the Unit-2 RSG geometry, cross-sections of the butter grooves show the angles at the groove corners to be about [A,B]. This is considered reasonable as the angles at the groove edge are about [A,B] (see Figure 3.7-1). [Note: Even though the butter groove on the 2B RSG is narrower than on the 2A RSG, both 2A and 2B RSGs have the same groove corner geometry.] For the Unit-3 RSG geometry, cross-sections of the butter grooves show the angles at the groove corners to be well over [A,B], which is to be expected given that the angles at the groove edge are about [A,B] (See Figure 3.7-1).

Based on the above and the results of the straight beam UT detection accuracy test, it was concluded that on the Unit-2 RSGs the straight beam UT would have produced reportable indications if there were flaws larger than [A,B] present in the butter groove corner area; however, such flaws may not have been detected on the Unit-3 RSGs.



3.10 Materials

Chemical composition and mechanical properties of the base metal, and the butter/ clad welding materials were all within the specified range with no discernable differences between those used on the Unit-2 and on the Unit-3 RSGs.

Figure 3.10-1 contains a textbook figure describing the effect of material hardness on the stress level needed for onset of the HIC. This data is for materials different than the channel head low alloy steel base metal. However, the trend is believed to apply to the materials used on the RSGs. The stress ratio shown in Figure 3.10-1 is the ratio of the stress needed to produce a tensile failure, divided by the material ultimate tensile strength (UTS). For elevated hardness the stress level needed for failure is reduced from ~85% UTS to ~25% UTS, i.e. by a factor of ~3. If carbon deposits were left behind by the air carbon-arc gouging process on the base metal surface, then especially high hardness areas could be present at the butter-to-base metal fusion boundary.

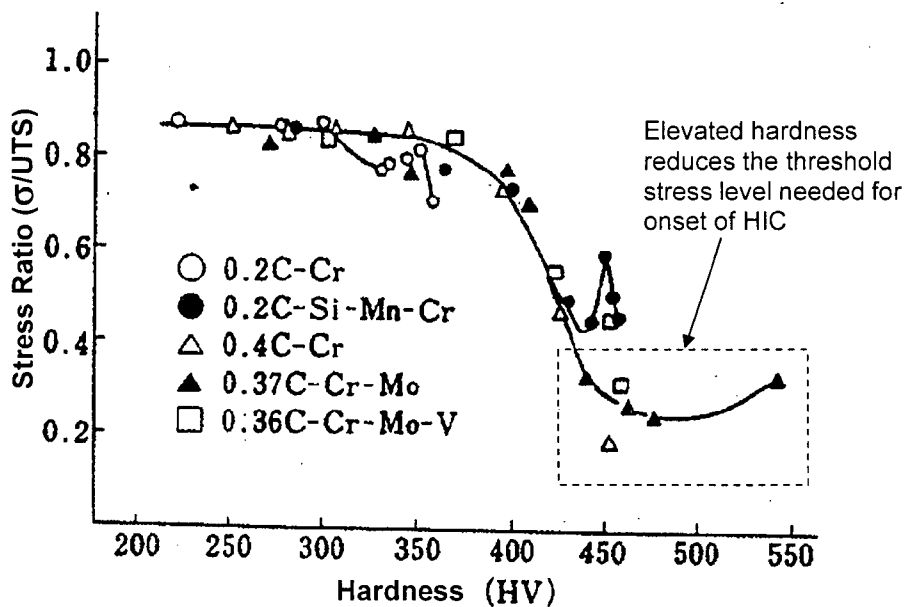


Figure 3.10-1 HIC Sensitivity to Hardness

Note; This figure is taken from "鉄と鋼 Vol. 55, No.2 (1969) page 151, Syoichi Fukui" with additional description.



4.0 EVALUATION OF RESULTS

Evaluation of the fillet weld external cracks found on the 3A and 3B RSGs divider plate-to-channel head welds concluded that they were ductile fractures. Examinations of the samples taken from the 3A and 3B RSGs indicated that the butter/clad separation from the base metal was a brittle fracture along the butter-to-base metal fusion boundary. It is believed that the external cracks in the welds occurred during the primary side hydrostatic tests and that the brittle butter/clad separation might have propagated during these tests. The origin of the butter/clad separation is believed to be a weak butter-to-base metal bond and possibly hydrogen embrittlement induced cracks.

4.1 Principles of Dissimilar Metal Welding

The microstructure of the fusion boundary between the dissimilar metals (LAS and austenitic filler metal) is characterized by the columnar austenitic dendrites perpendicular to the weld fusion line and truncated at the fusion line by Type II boundaries that form parallel to the fusion line. Adjacent to the Type II dendrites is a hardened layer thought to be martensitic in microstructure, but appears as a thin white phase. Next comes the heat affected zone (HAZ) that develops from the heat of welding. The hard white layer that occurs along the fusion boundary of dissimilar weldment is characteristic of such welds and is due to the normal dissolution and localized mixing that occurs during the welding process. The mixed microstructures result from localized heating and cooling following solidification. Micro-hardness values were measured in the studies that ranged from 400 Hv to more than 550 Hv. The open literature has reported even higher values in similar dissimilar metal welds. The key element determining hardness in a martensitic microstructure (the thin white layer) is carbon. In this case, the hard layer may have been made harder by the incorporation of residual carbon deposits left from the manual arc gouging process used to create the cavity in which the Alloy 152 butter material was deposited. It should be noted that no evidence for such a mechanism was observed in the destructive examinations of the samples removed from the Unit-3 channel heads. It may be possible that such evidence exists under the divider plate butter weld but such samples could not be taken without damaging the potential for repairing the generators.



4.2 Mechanism of Separation

Although air carbon-arc gouging is an efficient process for removing material, it can create localized regions of case hardening on a surface of the channel head from which the material is being removed. Carbon from the electrode is absorbed into the molten metal layer at the surface of the base metal. Additionally, the base metal mass provides an excellent heat sink, generating a very high quenching rate in the thin molten layer. The increased carbon content and rapid quenching are sufficient to form martensite, which is often harder than the martensite that forms in the parent metal.

Case hardened layers produced by gouging are difficult to remove by manual grinding. Variations in the rate of electrode travel, depth and angle, and an irregular arc produce hardened layers with non-uniform thickness. Additionally, the case hardened layer can be significantly harder than the surrounding base metal. The lack of accurate positioning and variability in material hardness often result in incomplete removal of the case hardened layer by manual processes and result in islands of case hardened material remaining on the pre-weld base metal surface. This was observed in the mock up tensile test samples produced by MHI (*Appendix C, Figure C.5 and C.6*).

Any vestige of the case hardened layer on the pre-weld surface would create conditions problematic for subsequent buttering. It is believed that several of these conditions might have contributed to the butter/clad separation from the channel head low alloy steel base metal in the Unit-3 RSGs. The two most important conditions are described below.

4.2.1 Weak Bond

Local variation in composition of the base metal could alter weld pool characteristics that could result in poor bonding between the butter and base metal. Areas where case hardened material is not completely removed would have much higher carbon content.

Composition variations can affect fluid flow in the weld pool. Highly localized changes in composition can make it difficult for a welder to make any adjustments during welding to compensate for this. This can lead to small intermittent areas of poor bonding (known as "cold lap"). There is evidence supporting the presence of localized areas of poor bonding in the fractography work performed by MHI. Figures in the Attachment-A (*Figure A.8(2) and A.10(1), Figure A.20(2) and A.21(1)*) show regions of flat, featureless fracture surface which is indicative of a poor bond.

Evidence of poor bonding was also observed via optical metallography. *Figure A.22(1)* shows a micrograph of the interface along the butter layer. The fracture in this location is smooth, propagating along the butter-to-base metal fusion boundary. Similar morphologies were observed along the fusion boundary in *Figure A.23(1)*. The fracture morphologies shown in these figures suggest that there was little bonding between the butter and the base metal, as evident by the absence of ductility or surface perturbations. This was most likely the result of poor bonding in these areas.



Properly bonded areas should exhibit a more tortuous, higher energy crack path, such as seen in *Figures A.23(2), A.24(2)*, and others. In these figures, the crack transverses the fusion boundary in multiple locations showing no preference to any particular location or microstructure. Crack morphologies like these indicate good bonding between the butter and the base metal.

4.2.2 Hydrogen Induced Cracking (HIC)

The HIC can be caused by a combination of elevated hardness at the butter-to-base metal transition zone, presence of residual hydrogen in the weld (in this case the butter) and high residual stresses at the fusion boundary. These three factors, if combined together, may result in an initiating crack(s) as early as during cool down after butter application.

Residual case hardening may not be fully consumed by arc welding. Case hardening not consumed by the arc will persist along the fusion boundary. In this region of the transition zone, dilution between the butter and base metal occurs by diffusion only. Any remaining case hardened material present along the fusion boundary will become enriched in Cr and Mo from the filler metal, increasing the hardenability.

Upon cooling, martensite forms along the fusion boundary between the butter and the base metal. Those regions containing any remnant case hardened material may exhibit higher hardness as a result of increased hardenability, i.e. material in these areas has *fully* transformed into martensite. This was evident in the mock up samples produced by MHI where hardness as high as [A,B] was measured (see *Attachment-J, Figure J.2-6*). Hardness values in this range increase susceptibility to hydrogen embrittlement and low energy fracture, in other words susceptibility to HIC. Additionally, material of this hardness has little potential for inhibiting crack propagation. The quasi-cleavage fracture surface morphologies on the fracture surface on the samples collected from the Unit- 3 RSGs and on the test samples produced by MHI support this statement.

The presence of residual hydrogen in the welds is normal, because welding rods (electrodes) always contain some hydrogen, and hydrogen is available from the atmosphere. Hydrogen content in the finished weld is minimized by proper pre-heating and post-baking (the longer the time and the higher the temperature, the better), so that the hydrogen concentrations are typically insufficient to cause HIC, by itself.

However, the concentration of hydrogen required for initiating hydrogen embrittlement decreases with increasing hardness and residual stress. Although hydrogen concentrations do not appear to be an issue for the SONGS RSGs (as the Unit-2 RSGs passed the hydrostatic tests without an incident) they could be a factor if these high levels of hardness and stress were present along the fusion boundary. In addition, less than ideal welding conditions (welding material, welding environment and heat treatment) could result in elevated residual hydrogen concentrations.

The high residual stress at the fusion boundary is associated with the geometry of the butter groove corner area acting as a stress riser. The high stress areas also contribute to a localized increase of hydrogen concentration, as hydrogen diffuses preferentially into the high stress areas.



Figure 4-1 summarizes the conditions necessary to produce HIC.

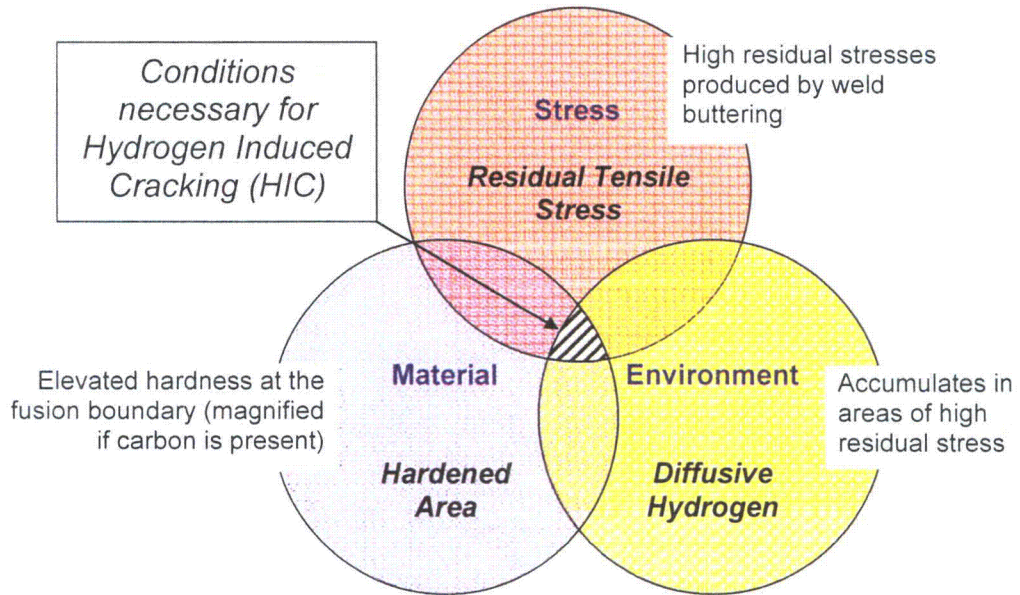


Figure 4-1 Hydrogen Induced Cracking (HIC) Diagram



4.3 Root Cause Determination

Table 4-1 contains the logic developed in the course of the investigation that led to the determination of the root cause, direct causes and contributing causes.

Table 4-1 Root Cause Determination Logic

	Conclusions from Investigations	Reference
1.	Examinations performed on the Unit-2 RSGs did not identify separation of the butter/clad from the base metal.	Section 2.2
2.	The purpose of all fabricated sample tests was to reproduce the butter/clad separation along the Alloy 152 butter-to-LAS base metal fusion boundary discovered on the Unit-3 RSGs.	Section 3.2 through 3.5
3.	Separation at the fusion boundary could not be reproduced, except for the fracture toughness test with the sample pre-charged with hydrogen and the tensile restraint cracking test (all other tensile test samples failed in the ductile mode on either side of the fusion boundary).	Section 3.2 through 3.5
4.	Hardness measured on the as-built samples collected from the Unit-3 RSGs and on the I-Type samples indicated increase of hardness in the transition zone.	Section 3.1 and 3.2
5.	Higher than typical hardness was found on samples that were contaminated with carbon.	Section 3.1 and 3.4.5.1
6.	Microstructure examinations of samples collected from the Unit-3 RSGs concluded that the separation surface was typical of brittle fracture, similar to that of hydrogen induced cracking (i.e. quasi-cleavage, Type II grain boundaries).	Section 3.1
7.	Review of the design configuration identified that the butter groove corner radius and side slope on the Unit-3 RSGs were considerably different from those on the Unit-2 RSGs: <div style="text-align: center;"> [A,B] </div>	Section 3.7
8.	Stress analyses indicated that these butter groove dimensional differences resulted in considerably higher tensile stresses perpendicular to the fusion	Section 3.8.1

**Table 4-1 Root Cause Determination Logic**

	Conclusions from Investigations	Reference
	boundary [A,B] in the groove corner areas.	
9.	Review of the fabrication sequence identified the steps that were different between the Unit-3 and Unit-2 RSGs.	Section 3.9
10.	One of the fabrication steps –air carbon-arc gouging – performed using a carbon electrode had a potential for introducing carbon deposits on the base metal surface that might have not been completely removed by subsequent grinding (especially in the groove corners)	Section 3.9.2
11.	Another step – hydrogen bake-out – was performed at a lower temperature on the Unit-3 RSGs than on Unit-2 RSGs.	Section 3.9.3
12.	Carbon deposition in what then became the transition zone between the butter and the base metal might have resulted in a higher than typical hardness.	Section 3.4.5.1
13.	High carbon resulted in the local areas of poor butter-to-base metal bond and might have increased susceptibility to HIC.	Section 3.4.5.2
14.	Residual hydrogen is always present in welds even with properly handled (dry) welding rods, but lower bake-out temperatures might have resulted in a higher than typical residual hydrogen concentration in the transition zone, especially in high residual stress areas.	Section 3.4.4
15.	The combination of high stress due to the butter groove configuration, high hardness due to carburization and higher residual hydrogen concentration might have resulted in formation of a hydrogen induced crack(s) in the groove corner areas.	Section 4.2
16.	The weak bond and/or HIC initiated extensive butter/clad separation under thermal or pressure loads during the fabrication steps following butter application, such as channel head FPWHT, divider plate-to-channel head and tubesheet welding, and primary side hydrostatic pressure test.	Section 3.8.1 through 3.8.6



5.0 EVALUATION SUMMARY

Based on the information presented in Section 4.2 and the logic presented in Table 4-1, the evaluation identified the following root cause, direct causes and contributing causes.

5.1 Root Cause

The evaluation concluded that the root cause of butter/clad separation from the channel head base metal on the U3 RSGs was the air carbon-arc gouging.

Gouging was performed using a carbon electrode and left carbon deposits on the base metal surface. Gouging was followed by grinding, which was designed to remove the heat affected zone and should, but did not, remove the carbon deposits completely. The carbon deposits left behind on the base metal surface resulted in the localized areas of high carbon and high hardness caused by carburization of the base metal surface.

5.2 Direct Causes

The evaluation concluded that the root cause promoted a direct cause that led to butter separation initiation. This cause was a localized weak butter-to-base metal bond in the areas of high carbon/high base metal hardness. Butter separation in the areas of the weak bond caused also limited area separation of the channel head clad. The relationship between the root cause and the direct cause is described in detail in Section 4.2.

The evaluation concluded that it was also possible, but less probable, that the root cause promoted HIC in the high base metal hardness/high stress areas, most likely in the butter groove corner areas, due to hydrogen preferentially diffusing into the high stress areas. This is supported by the fact that there were samples pre-charged with hydrogen which failed in the way similar to that seen on the as-built samples collected from the U3 RSGs. However, the investigations performed under this evaluation did not reveal any hydrogen-induced cracks on the as-built samples in the area of concern, nor it provided quantitative evidence that the hydrogen was present in the as-built samples in harmful concentrations due to improper performance of the fabrication processes or handling of the welding materials.

5.3 Contributing Causes

The evaluation concluded that the contributing causes which led to extensive butter separation were: 1) weld joint loading during thermal transients (IPWHT, PWHT) and 2) weld joint loading during primary side hydrostatic testing.

The evaluation also concluded that the following causes could contribute to HIC that possibly could have occurred on the U3 RSGs and did not occur on the U2 RSGs: (1) high stress butter groove corner geometry, (2) lower post-bake temperature and (3) shorter



pre-heat time during butter application, as all of them could possibly result in harmful hydrogen concentrations in the butter groove corner areas.

5.4 Extent of Condition

The evaluation concluded that the extent of condition described herein was limited to the Unit-3 RSGs divider plate-to-channel head weld joints for the following reasons:

- a) The clad was removed by gouging only on the Unit-3 RSGs; on the Unit-2 RSGs, it was removed by machining. Therefore, only on the Unit-3 RSGs there was a potential for carbon deposition and elevated hardness due to carburization, and hence a potential for a weak bond between the butter and the base metal and for increased susceptibility to HIC.
- b) For the Unit-3 RSGs, the pre-heat duration was only about one-third of that for the Unit-2 RSGs, and the post-baking temperature was lower than those for the Unit-2 RSGs. Therefore, only on the Unit-3 RSGs there could be higher hydrogen concentrations in the butter, potentially leading to HIC.
- c) The Unit-3 RSG butter groove has a smaller corner radius and a steeper side slope than the Unit-2 groove, causing the residual stresses in the corner areas to be higher by a factor of three in the Unit-3 RSGs than in the Unit-2 RSGs, and making removal of the carbon residue difficult. Therefore, only on the Unit-3 RSGs a potential existed for localized elevated hydrogen concentrations and localized high hardness, both increasing susceptibility to HIC.
- d) The Unit-2 RSGs passed the primary side hydrostatic pressure test without an incident.
- e) The UT examinations of the Unit-2 RSGs, the same as for the Unit-3 RSGs, did not identify any separation of the butter or clad from the base metal.

Based on the above, it is further concluded that the evaluated condition did not apply to the Unit-2 RSGs or to any other dissimilar weld joint within the SONGS RSGs.



Attachment-A

Unit 3 As-built Sample Investigation



I. First Investigation

1. Purpose

The purpose of this report is to provide results of investigation of the samples collected from the U3B and U3A RSG.

2. Background

Cracks were discovered on the divider plate-to-channel head weld (Figure A.1), during the inspections of tube-to-tubesheet welds in secondary side hydrostatic test of Unit 3B RSG. The cracks were caused by the separation of the divider plate and channel head. The same separation was also confirmed in Unit 3A RSG.

3. Investigation Methodology

3 boat samples were obtained from the Unit 3B RSG at the location as shown in Figure A.2. 2 samples were also obtained from the Unit 3A RSG at the location as shown in Figure A.3. The detail of the each sample was shown in Table A.1.

Table A.1 Locations and purpose of boat samples

Sample No.	Location	Purpose
Sample A	Area including crack on fillet weld	To investigate the situation of the crack on fillet weld as well as separation.
Sample B	Area of typical 152 buttering with separation	To investigate the situation of the separation between 152 buttering and LAS (low alloy steel).
Sample C	Area of stainless steel cladding around the end of separation by UT	To investigate the situation of the separation between stainless steel cladding and LAS (low alloy steel). To confirm the difference in situation between the area with and without crack.
Sample D	Large area of 152 buttering and stainless steel clad with separation in hot side of U3A	To investigate the situation of the separation between 152 buttering and LAS (low alloy steel) or between stainless steel clad and LAS in U3A.
Sample E	Large area of typical 152 buttering and stainless steel clad with separation in cold side of U3A	To investigate the situation of the separation between 152 buttering and LAS (low alloy steel) or between stainless steel clad and LAS in U3A.



The investigation methodology matrix was summarized in Table A.2

Table A.2 Investigation Methodology

Item	Method	Purpose
Sample appearance	Visual examination	Confirm that the sample conditions (contains expected materials)
Separation surface	Visual examination at low magnification	Evaluate the macro-structure of the separation/crack surface
Separation surface	SEM (Scanning Electron Microscope) examination at high magnification	Evaluate the micro-structure of the separation/crack surface
Macro-structure	Visual examination of the cross-section at low magnification after etching	Evaluate the macro-structure of the materials constituting the sample
Micro-structure	Visual examination of the cross-section at high magnification after etching	Evaluate the micro-structure of the materials constituting the sample
Hardness	Measure Vickers hardness	Evaluate the hardness distribution near the separation/crack surface
Chemical analysis	EPMA (Electron Probe Micro Analyzer) analysis	Evaluate chemical composition of the material near the separation/crack surface

4. Results of investigation

A. Sample A

Figure A.6 shows appearance of boat sample A. The cracks corresponding to Visual inspection and UT indication were observed.

Figure A.7 shows appearance of fracture surface of TP A-1 cut from sample A. The TP A-1 was divided into 2 pieces. The fracture surface of TP A-1 consists of three areas. First one is fracture surface of 152 buttering, second one is fracture surface of stainless steel cladding and the last one is fracture surface between stainless steel cladding and LAS (low alloy steel).

Figures A.8 show SEM pictures of fracture surface of TP A-1. The cracks observed in 152 weld metal and stainless steel cladding revealed ductile fracture surface with dimple pattern (at location A and location B shown in Figure A.8(1)). The crack between 152 buttering and LAS revealed quasi-cleavage fracture surface and relatively flat surface with grain boundary like feature(at location C shown in Figure A.8(2)).



Figure A.9 shows appearance of fracture surface of TP A-2 cut from sample A. The TP A-2 was divided into 2 pieces. The fracture surface of TP A-2 consists of two areas. One is fracture surface between 152 buttering and LAS, another one is fracture surface between stainless steel cladding and LAS.

Figures A.10 show SEM pictures of fracture surface of TP A-2. The fracture surface between 152 buttering and LAS revealed quasi-cleavage fracture surface and flat surface with grain boundary like feature (at location A shown in Figure A.10(1)). The fracture surface between stainless steel cladding and LAS revealed quasi-cleavage fracture surface and relatively flat surface with dendrite boundary like or grain boundary like feature (at location B shown in Figure A.10(2)).

Figures A.11 show macro-structure and micro-structure of cross section of sample A. The crack observed on the surface of fillet weld of divider plate propagated in 152 weld metal and stainless steel weld metal (at location A shown in Figure A.11(1)).

The crack which causes UT indication locates along the fusion boundary between LAS base metal and 152 weld metal (at location B and location C shown in Figure A.11 (2) and A.11(3)) or along the fusion boundary between LAS base metal and stainless steel weld metal (at location D shown in Figure A.11(4) and A.11(5)).

There is no abnormality in microstructure of LAS base metal, 152 weld metal and stainless steel weld metal as shown in Figure A.11(6).

Figures A.12 through A.15 show results of hardness measurement. Hardness value is high (HV300 to 350) near the crack in weld metal (Figure A.12). Plastic deformation during ductile fracture could results in this hardening. Hardness value is also high (HV300 to 425) in stainless steel cladding adjacent to fusion boundary (Figure A.13) and (HV300 to 350) in white zone near fusion boundary (Figure A.14). Supposedly, these hardened zones could be generated by carburization during PWHT. There is no abnormality in hardness of LAS base metal and heat affected zone of LAS (Figure A.13(2) and Figure A.14), even though the hardness of heat affected zone of LAS varied widely (Figure A.15).

Figure A.16 and Table A.3 show the results of chemical composition measurement by EPMA. The chemical compositions of stainless steel cladding and 152 buttering are equivalent to the value of CMTR.

Summary of Sample A;

- (1) The crack observed on the surface of fillet weld of divider plate fractured in ductile mode.
- (2) The separation which caused UT indication propagates along the fusion boundary



between LAS and 152 buttering or between LAS and stainless steel cladding.

(3) There is no abnormality in typical microstructure of LAS base metal, 152 weld metal and stainless steel weld metal.

(4) High hardness was observed in white zone of 152 buttering and stainless steel weld metal just adjacent to the fusion boundary.

(5) There is no abnormality in hardness of LAS base metal and heat affected zone of LAS.

(6) There is no abnormality in chemical composition of 152 buttering and stainless steel cladding.

B. Sample B

Figures A.17 and A.18 show appearance of boat sample B. The sample was divided into 2 pieces, 152 buttering part (Fig.A.17) and low alloy steel part (Fig.A.18), when they were taken.

Figure A.19 shows appearance of fracture surface of both sides of the sample. A rough surface was observed on the fracture surface. It is supposed that the rough surface corresponds to welding bead shape of 152 buttering.

Figures A.20 and A.21 show SEM pictures of fracture surface. Three types of features were observed; the quasi-cleavage (at location A in Figure A.20(1) and location A in Figure A.21(1)), flat surface with dendrite boundary like or grain boundary like feature (at location C in Figure A.20(2) and location B in Figure A.21(2)) and ductile fracture surface (at location B in Figure A.20(2)). Any significant welding defects such as slag inclusion, lack of fusion and blowhole were not observed on the fractured surface.

Figures A.22 and A.23 show macro-structures and micro-structures of cross section of sample B. The crack is located along the fusion boundary between 152 weld metal and LAS base metal. In pictures with higher magnification, different crack paths were observed; crack path in LAS (at location B & C in Figure A.22(2)), crack path in the white zone (at location B in Figure A.23(2)) and crack path between white zone and LAS (at location A in Figure A.22(1) and location A in Figure A.23(1)).

Figures A.24 through A.26 show the results of hardness measurement. Hardness value is high (HV300 to 400) in white zone near fusion boundary (Fig.A.24 and A.26). Hardened zone (HV400 to 550) and softened zone (about HV250) were observed near the fusion boundary (Fig.A.25 and A.26(2)). These hardened and softened zones were considered to be generated by carburization and decarburization during PWHT. There is no abnormality in hardness of LAS (Figure A.25).



Figures A.27, A.28 and Table A.4 show results of chemical composition measurement by EPMA. The chemical compositions of 152 buttering and LAS are equivalent to the value of CMTR. The chemical composition in white zone between 152 buttering and LAS changes gradually.

Summary of Sample B;

- (1) The separation propagated along the fusion boundary between 152 buttering and LAS.
- (2) Any significant welding defects such as slag inclusion, lack of fusion or blowhole were not observed at the fracture surface.
- (3) High hardness was observed in white zone and LAS just adjacent to the fusion boundary.
- (4) There is no abnormality in chemical composition of 152 buttering and LAS.

C. Sample C

Figure A.29 shows the appearance of boat sample C. The separation reached to the middle of the sample in a longitudinal direction.

Figure A.30 shows the appearance of fractured surface of TP C-1 and C-2 cut from sample C.

Figures A.31 show SEM pictures of fracture surface of TP C-1. The crack revealed quasi-cleavage fractured surface and flat surface with dendrite boundary like or grain boundary like feature.

Figures A.32 shows macro-structures and micro-structures of cross section of sample C. The crack propagates along the fusion boundary between stainless steel cladding and LAS base metal. There is no abnormality in typical microstructure of LAS base metal and stainless steel cladding.

Figures A.33 show result of Vickers hardness measurement of cross section of sample C. The stainless steel revealed high hardness (HV360 to 500) in colored zone near the fusion boundary. It is assumed that the hardened zones could be generated by carburization during PWHT.

Figures A.34 show results of EPMA line analysis. It seems that the hardened zone shown in Figure A.33 corresponds to the transition zone between stainless steel cladding and LAS base metal.

Summary of Sample C;

- (1) The separation propagated along the fusion boundary between stainless steel cladding and LAS.



- (2) High hardness value was obtained in the transition zone just beside the fusion boundary.
- (3) There is no abnormality in chemical composition of stainless steel cladding and LAS.

D. Sample D

Figure A.35 shows the appearance of sample D. The sample, which had been separated from LAS channel head when it was collected, contained stainless steel clad part and 152 buttering part.

Figures A.36 show the appearance of fractured surface of sample. There were three areas in fractured surface; 152 buttering by SMAW, stainless steel clad by SMAW and stainless steel clad by ESW. The area welded by SMAW revealed rough surface. Any significant welding defects such as slag inclusion, lack of fusion and blowhole were not confirmed at the fracture surface. The channel head body after removal of sample revealed similar fractured surface morphology to the sample (Figures A.37).

Figures A.38 show the SEM pictures of fractured surface. Three types of features were mainly observed; the quasi-cleavage (location A in Figure A.38(1), location B in Figure A.38(2) and location E in Figure A.38(4)), flat surface with dendrite boundary like or grain boundary like feature (location A in Figure A.38(1) and location E in Figure A.38(4)) and ductile fractured surface (location C in Figure A.38(2)). The direction of crack propagation was not clear from the feature of the fractured surface. In the crack observed between 152 buttering and stainless steel clad revealed ductile fractured surface (location D in Figure A.38(3) and location F in Figure A.38(5)). Any significant welding defects such as slag inclusion, lack of fusion and blowhole were not observed at the fractured surface.

Figures A.39 show the macro-structures and micro-structures of cross section of sample D. The crack is located along the fusion boundary between 152 weld metal and LAS base metal (location C in Figure A.39(2)) or between stainless steel clad and LAS base metal (shown in Figure A.39(1) and Figure A.39(3)). In pictures with higher magnification, the crack paths seem to be similar to the sample A, B and C; crack path in LAS or crack path in the weld metal adjacent to fusion boundary. The direction of crack propagation was not clear from microstructure observation of the cross section of sample.

Figures A.40 show the results of hardness measurement. Hardness value is high (HV300 to 350) in white zone near fusion boundary between 152 buttering and LAS base metal (shown in Figure A.40(2)) as measured in samples collected from U3B. The colored zone observed adjacent to fusion boundary between stainless steel clad and LAS base metal revealed high hardness value (HV300 to 380 as shown in Figure A.40(3)) as measured in samples collected from U3B.



Figures A.37 show the appearance of fractured surface of channel head body after sample was collected. Any significant welding defect or crack in base metal was not observed in fracture surface of LAS base metal.

Summary of Sample D;

- (1) The separation propagated along the fusion boundary between 152 buttering and LAS or between stainless steel cladding and LAS.
- (2) Any significant welding defects such as slag inclusion, lack of fusion and blowhole were not observed at the fractured surface. Any significant welding defect or crack in base metal was not observed in fractured surface of LAS base metal.
- (3) High hardness value was measured in transition zone just beside the fusion boundary.
- (4) The direction of crack propagation was not clear.
- (5) Any significant differences were not observed in sample D collected from U3A compared with other samples collected from U3B in investigation results.

E. Sample E

Figure A.41 shows the appearance of sample E. The sample contained only stainless steel clad and 152 buttering.

Figures A.42 show the appearance of fractured surface of sample. There were three areas in fractured surface; 152 buttering by SMAW, stainless steel clad by SMAW and stainless steel clad by ESW as like as sample D. Some chips were observed on the fractured surface of 152 buttering. It is supposed that those chips resulted from sampling operation. Any significant welding defects such as slag inclusion, lack of fusion and blowhole were not observed on the fractured surface. The direction of crack propagation was not clear from the feature of the fractured surface.

Figures A.43 show the appearance of fractured surface of channel head body after collection of sample. Any significant welding defect or crack in base metal was not observed in fractured surface of LAS base metal.

Summary of Sample E;

- (1) Any significant differences were not observed in fractured surface morphology compared with other samples.
- (2) Any significant welding defects such as slag inclusion, lack of fusion and blowhole were not observed at the fractured surface. Any significant welding defect or crack in base metal were also not observed in fractured surface of LAS base metal.
- (3) The direction of crack propagation was not clear from the feature of the fractured surface.



5. Evaluation of Results

As shown in the results of investigation, crack propagated near fusion boundary and hardening was observed along fusion boundary (white zone/colored zone). It seems that hardening along fusion boundary can affect crack propagation. Mechanisms of the hardening are described as follows;

(1) Hardening by martensite formation (shown in Figure A.4)

- Near fusion boundary between LAS and 152/ stainless steel cladding, chemical composition changes gradually.
- Alloy with chemical composition between LAS and 152/ stainless steel cladding can form martensite, and can be hardened during cooling process after welding.

(2) Hardening by carburization (shown in Figure A.5)

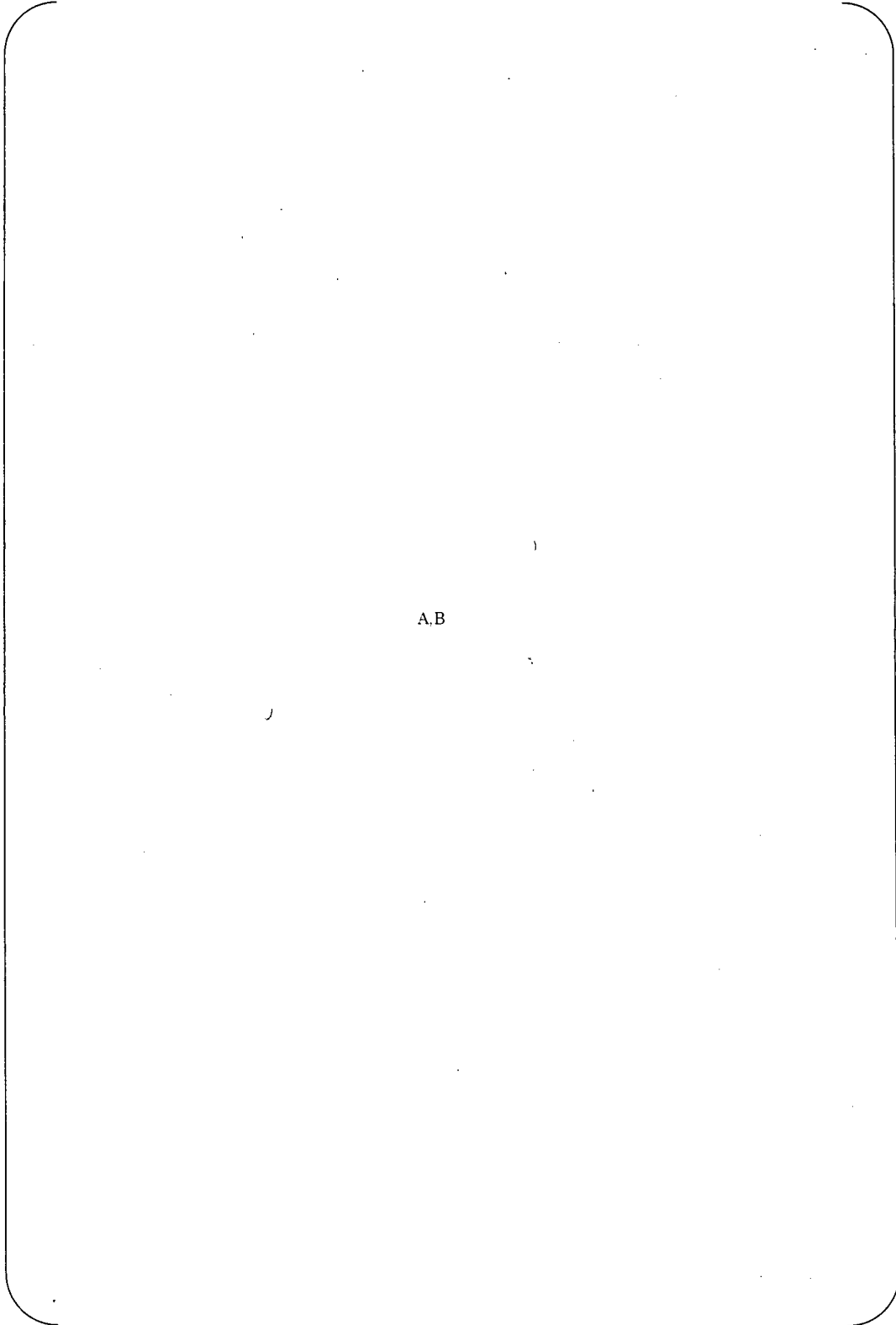
- During post weld heat treatment, decarburization can occur in LAS and carburization can occur in 152/ stainless steel cladding near fusion boundary. Carburization can result carbide precipitation and hardening.
- There is example that hardened zone corresponds high C zone.

6. Conclusions

Three boat samples were collected from Unit 3B RSG and two samples were collected from Unit 3A for investigation. On each sample, hardened area was observed adjacent to the fusion boundary between 152 buttering and LAS base metal. Similar hardened area was also observed near the fusion boundary between stainless steel cladding and LAS base metal. These areas with higher hardness value might have been generated by carburization during heat treatment and would cause the propagation of separation of the buttering/clad from the LAS at or near the fusion boundary.

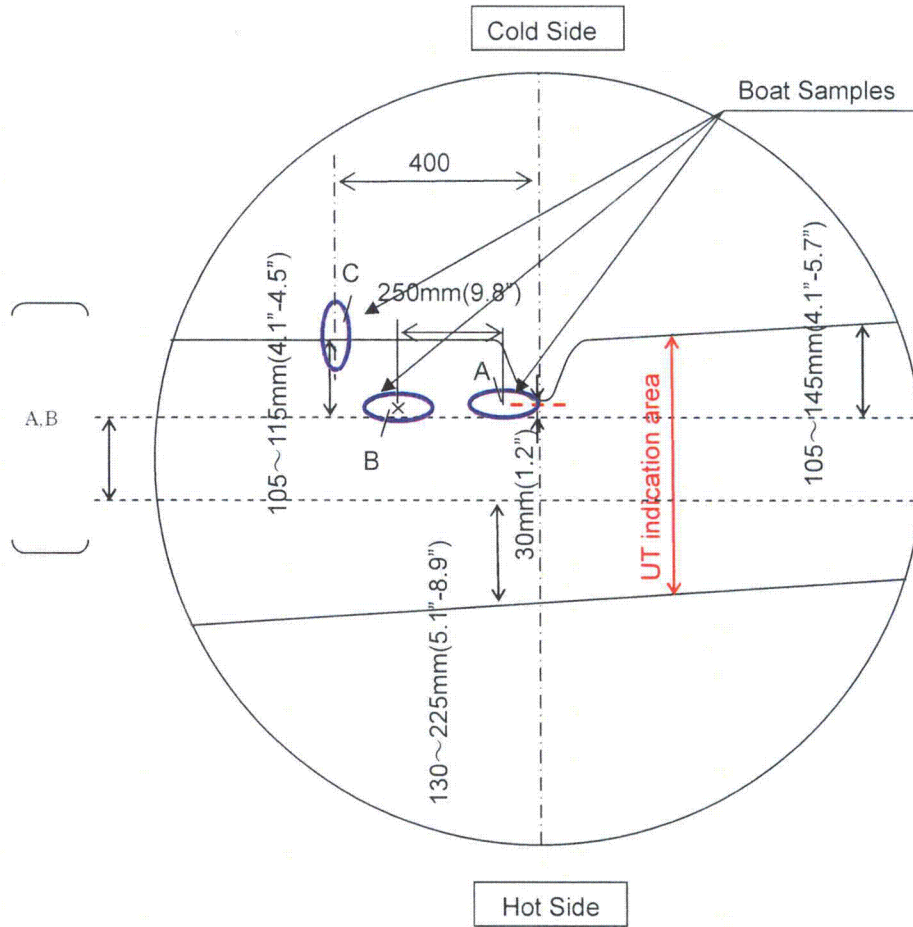
However, the hardening phenomenon near the dissimilar weld boundary is a generally expected phenomenon, and the investigations of these boat samples alone cannot tell the root cause of the separation of the buttering/clad from the base metal.

The surface crack in Unit 3B, which was found during secondary side hydrostatic test, is likely to be the result of the separation that was initiated and propagated between buttering and LAS, because its surface has ductile fractured surface as shown in Sample A.

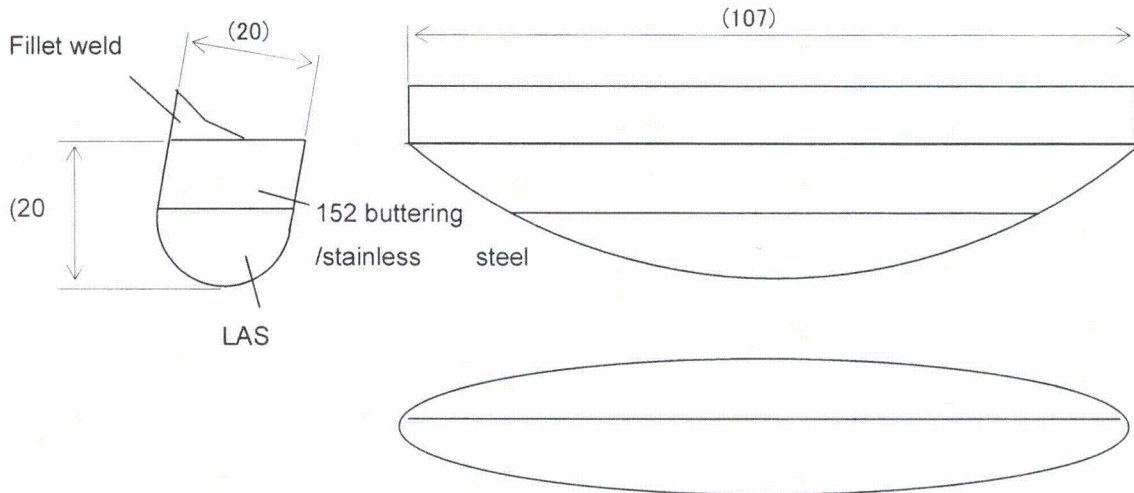


A,B

Fig. A.1 The position of crack in Channel Head

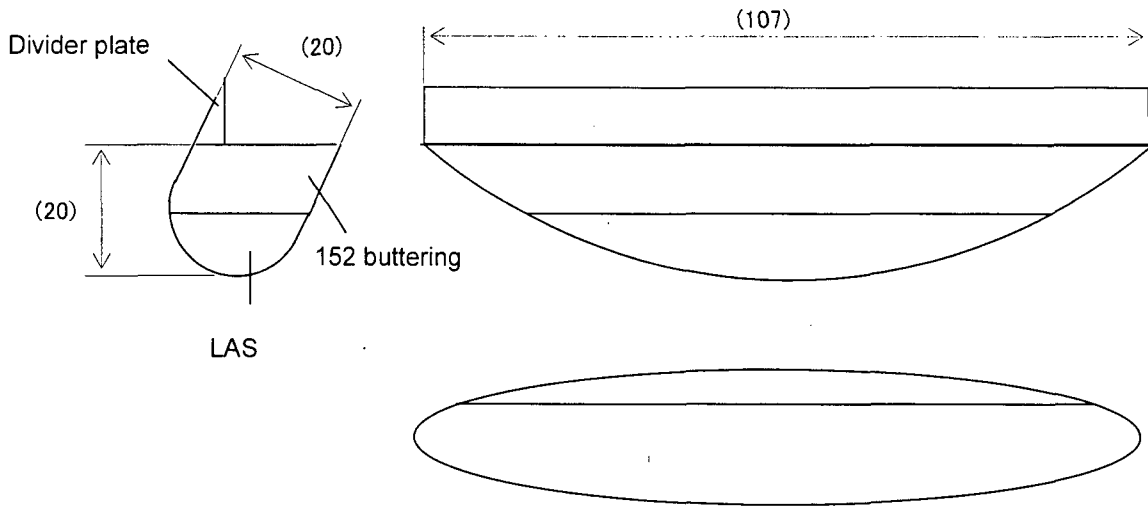


(a) The location of boat sampling

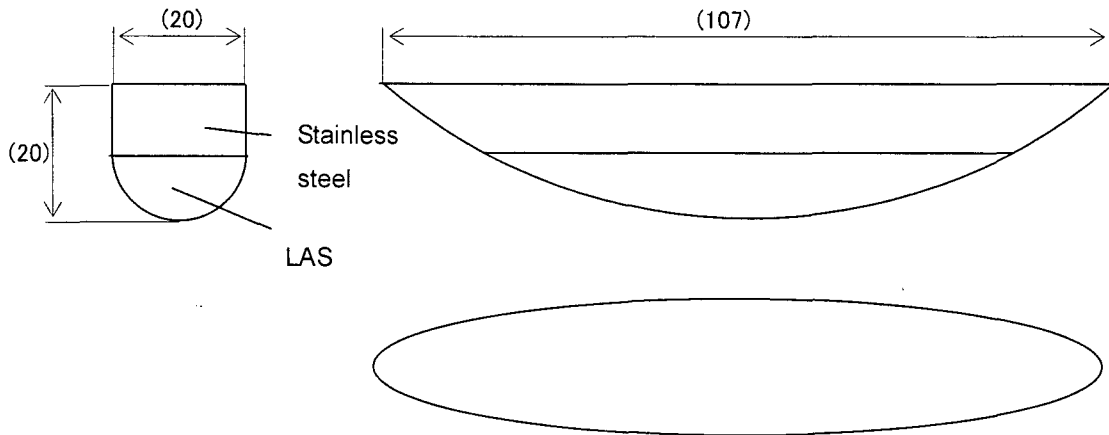


(b) Schematic illustration of Sample A

Fig. A.2(1) The collected location and schematic illustration of boat samples.

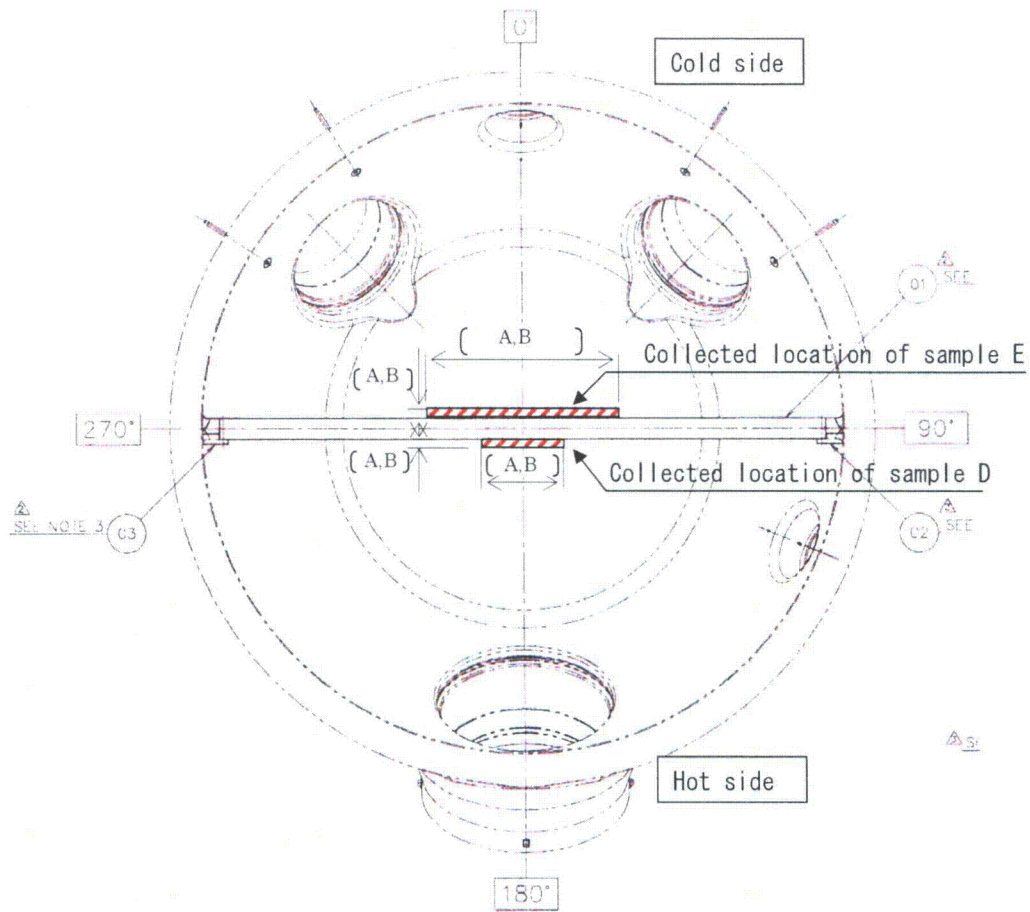


(c) Schematic illustration of Sample B

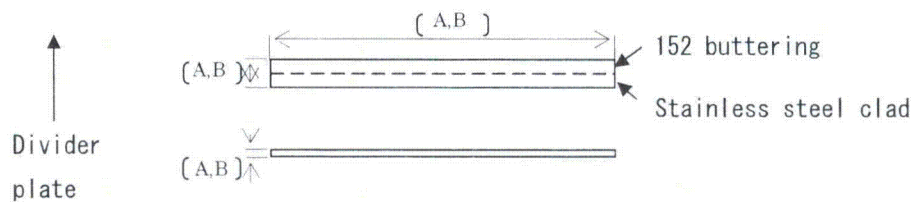


(d) Schematic illustration of Sample C

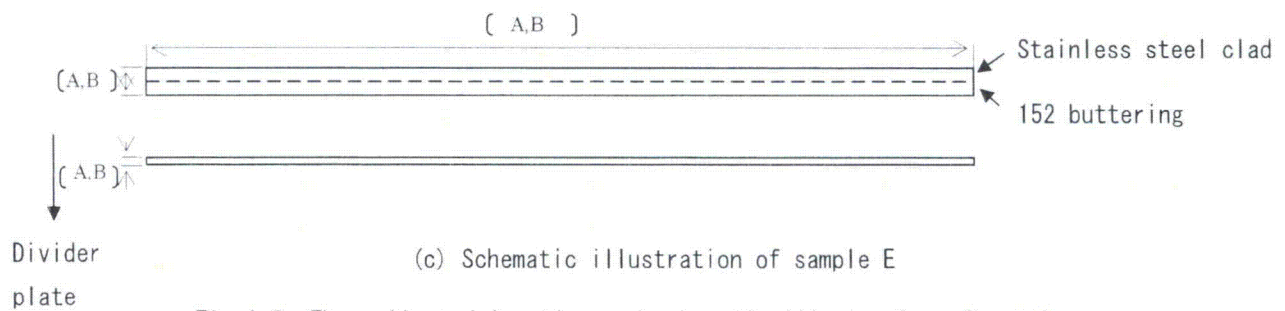
Fig. A.2(2) The collected location and schematic illustration of boat samples.



(a) Collected location of samples



(b) Schematic illustration of sample D



(c) Schematic illustration of sample E

Fig. A.3 The collected location and schematic illustration of samples.

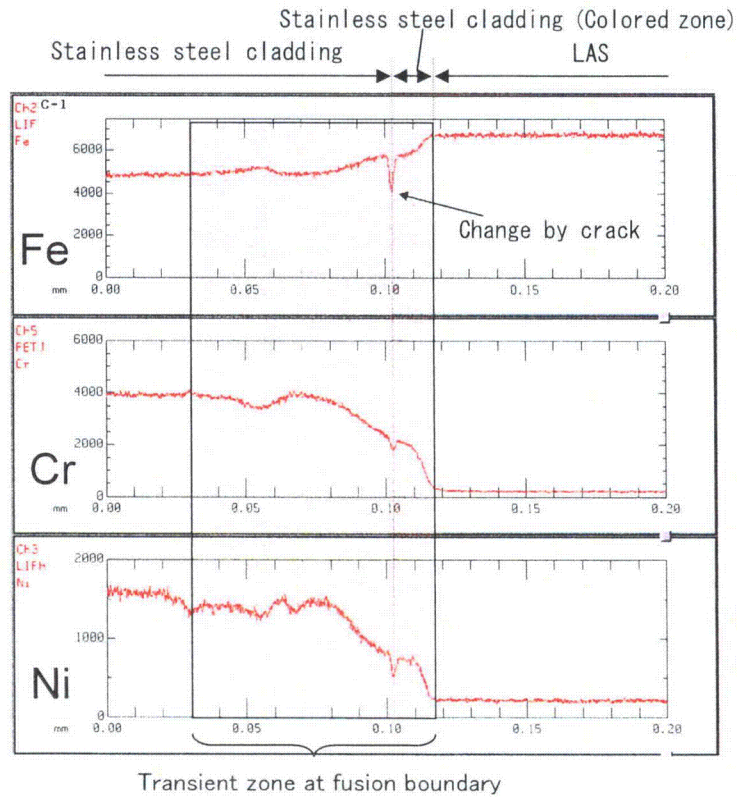
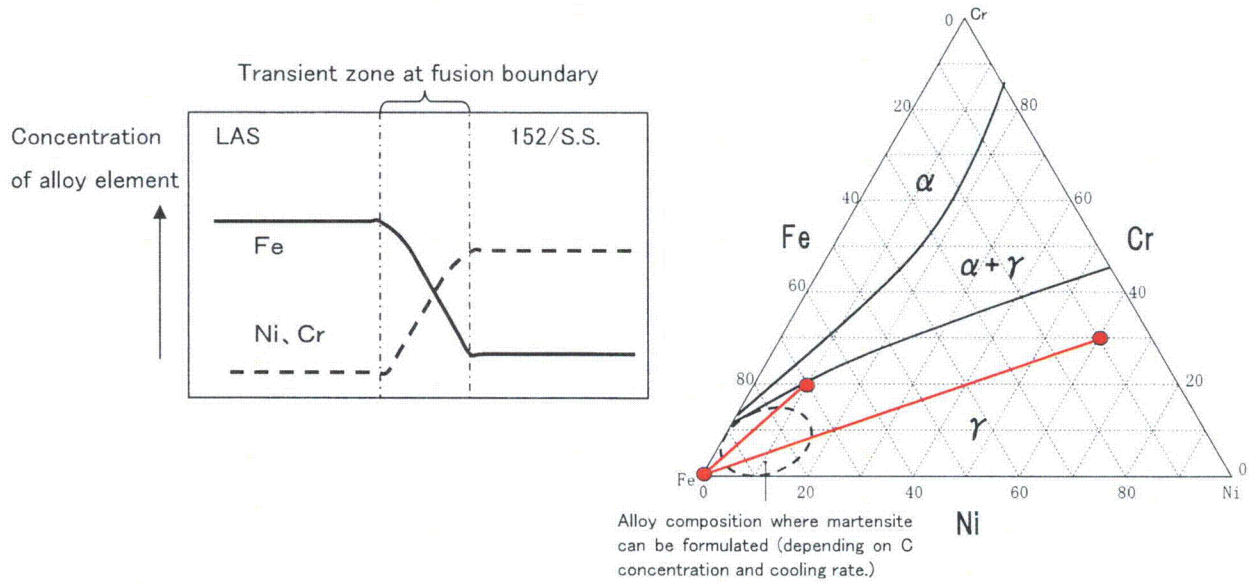


Fig.A.4 Explanation of hardening by martensite formation

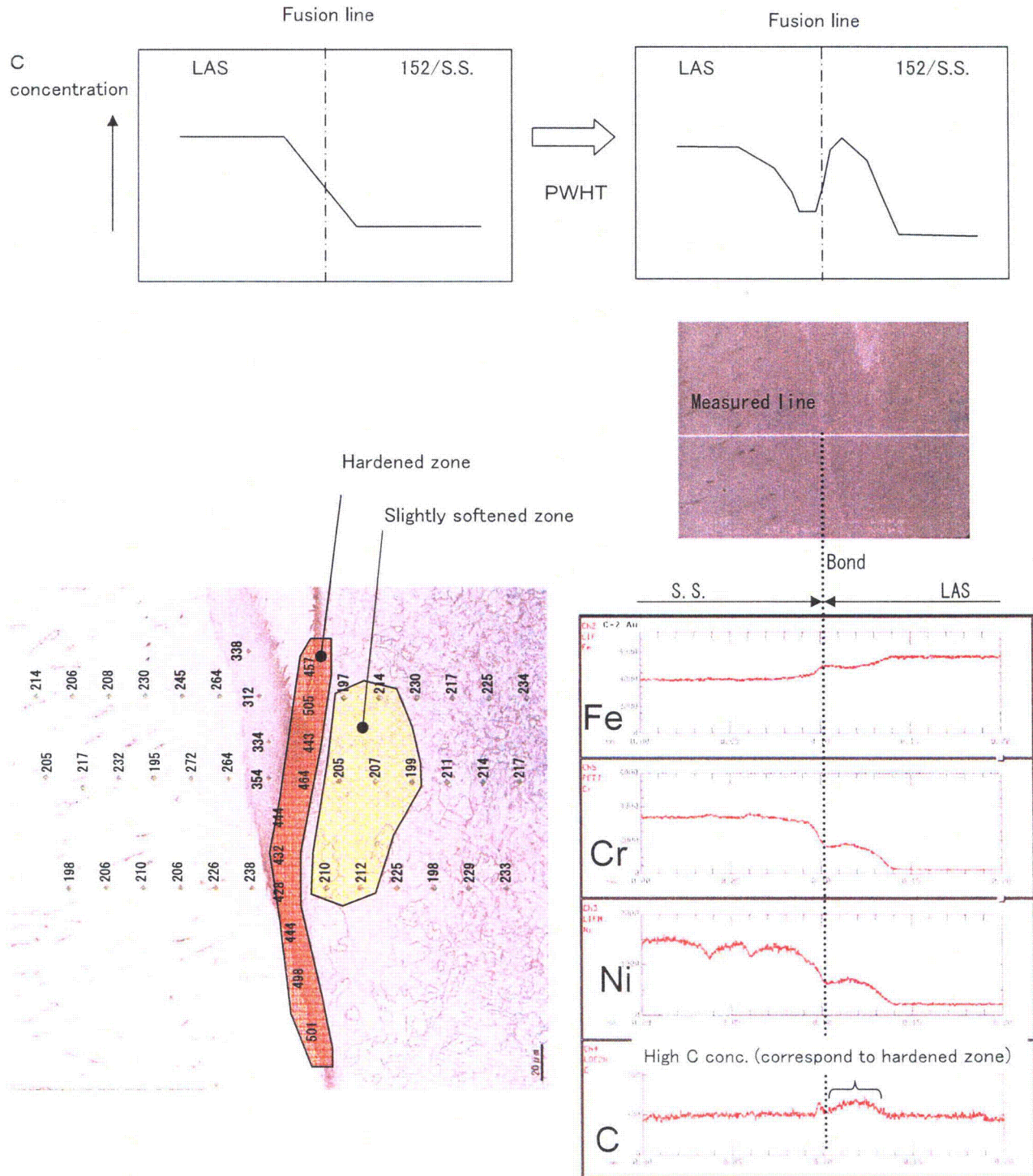
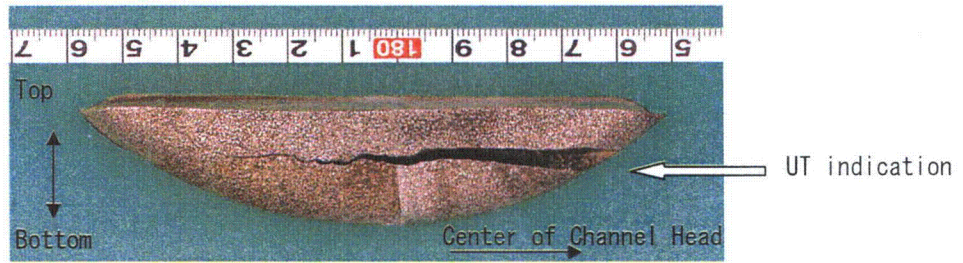
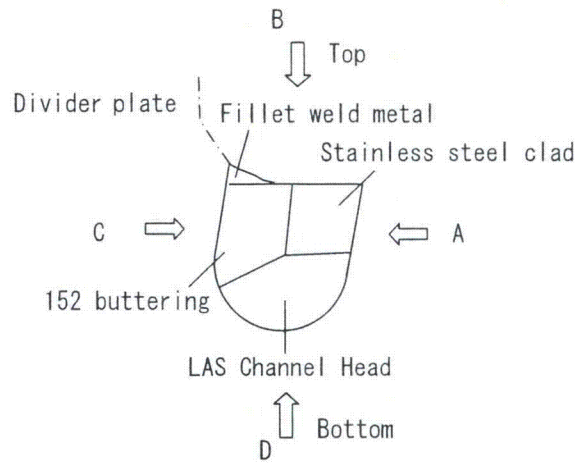
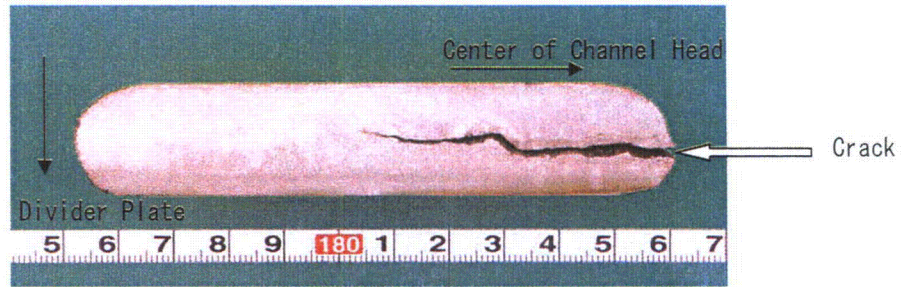


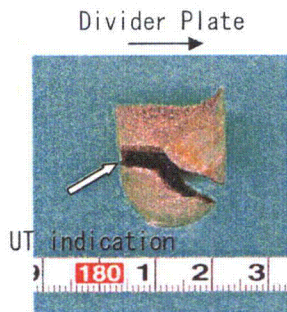
Fig.A.5 Explanation of hardening by carburization



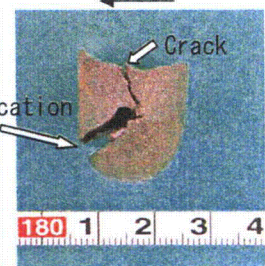
Electron Discharge Machined Surface (Direction A)



Surface of buttering (direction B)

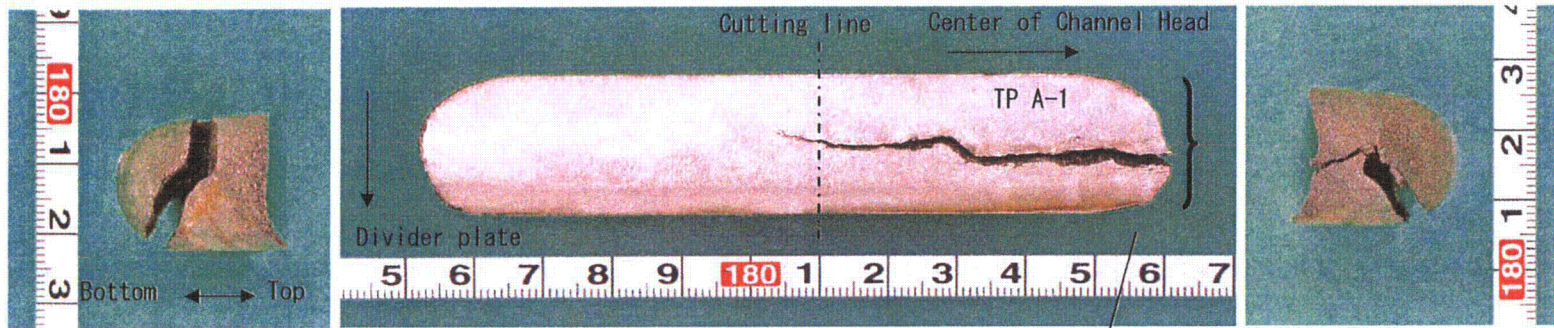


Electron Discharge Machined Surface (Direction C)



Electron Discharge Machined Surface (Direction D)

Fig.A.6 Appearance of sample A

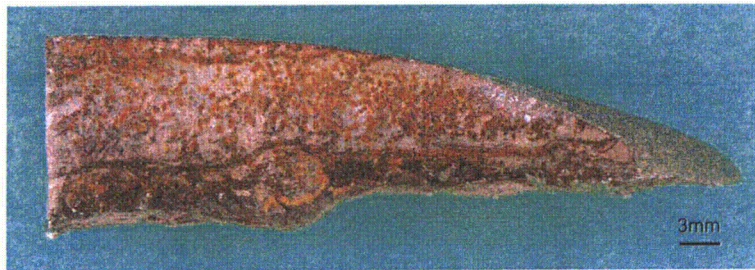
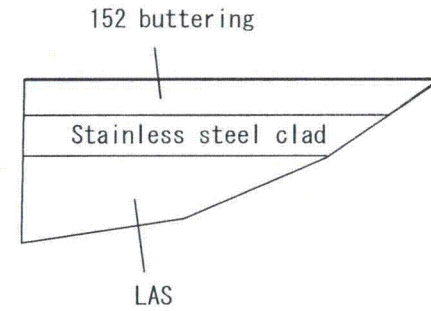


Separated two pieces

TP A-1



Fracture surface (from Direction C)



Fracture surface (from Direction B)

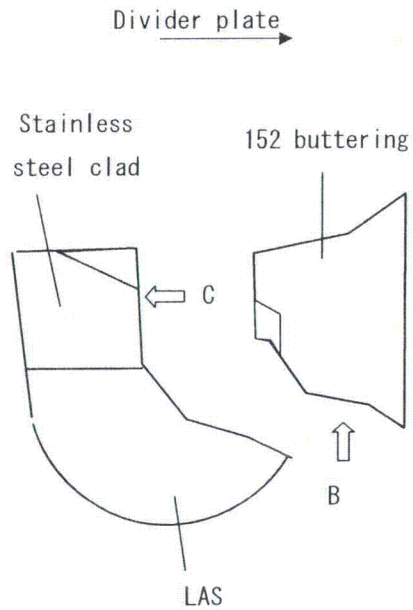
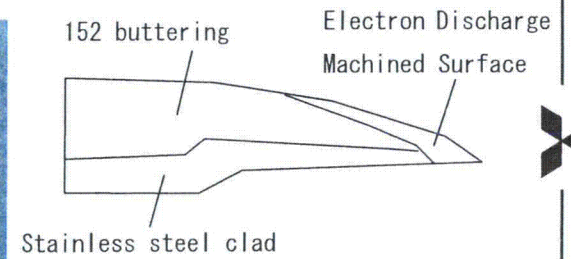
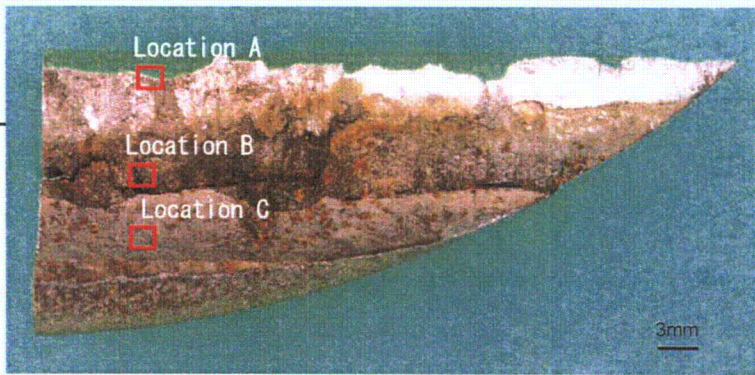
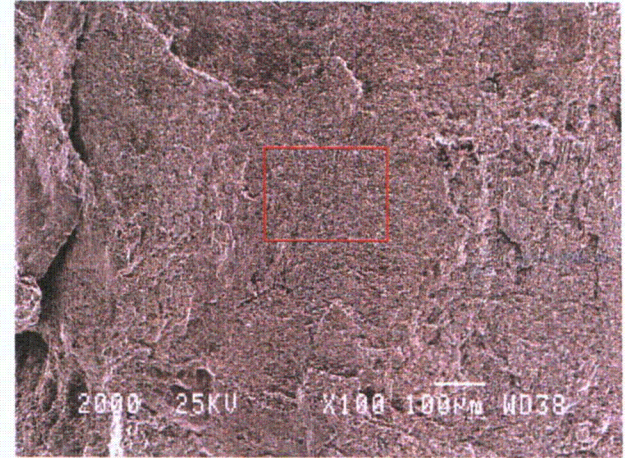
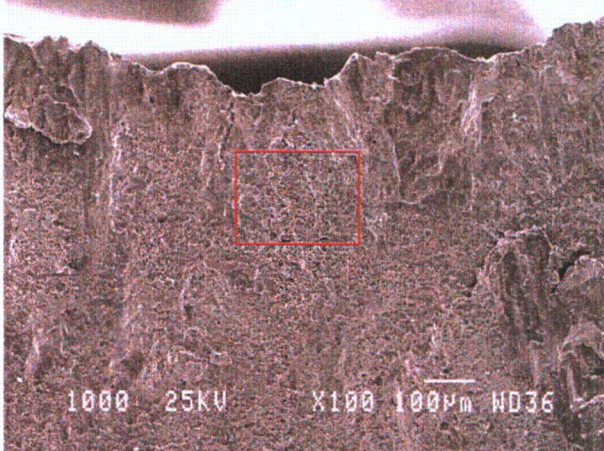


Fig.A.7 Appearance of fracture surface of TP A-1 (sample A)



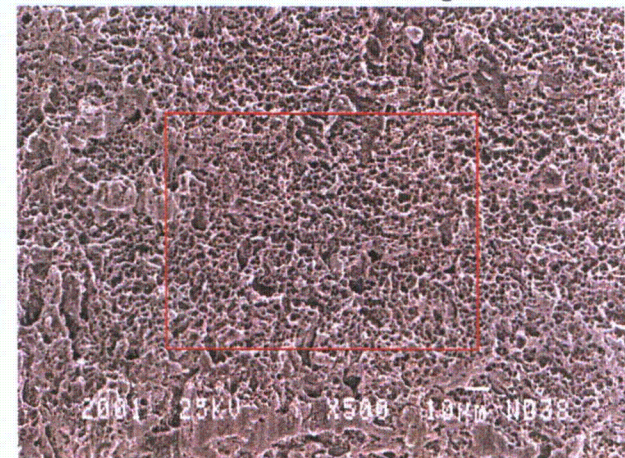
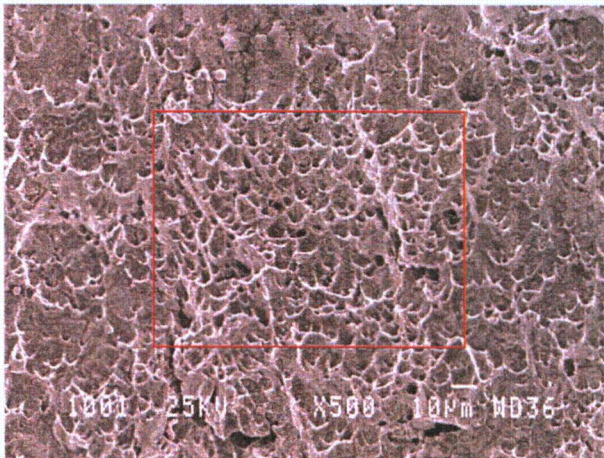
Detail observation of Location A

Detail observation of Location B



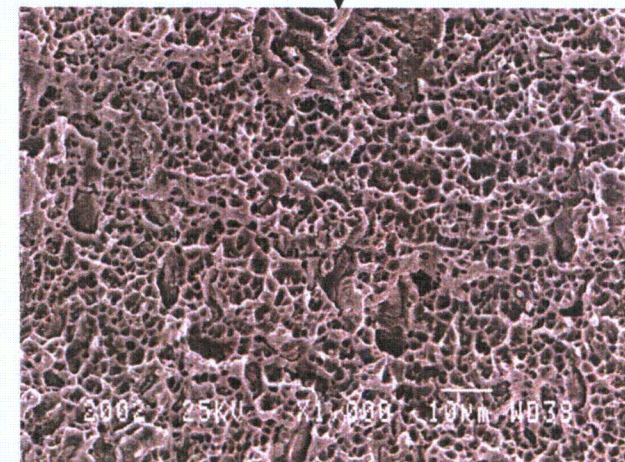
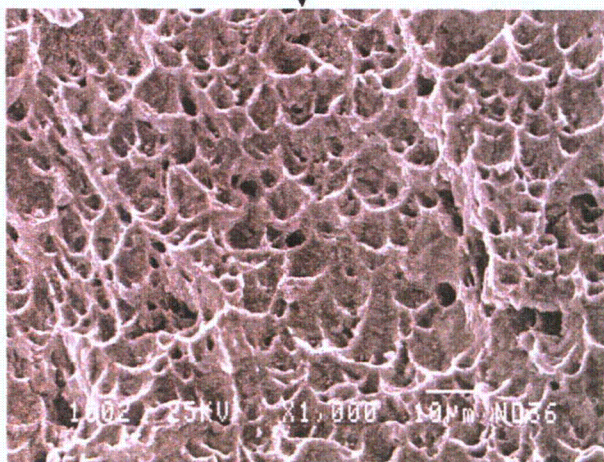
↓ Enlarged

↓ Enlarged



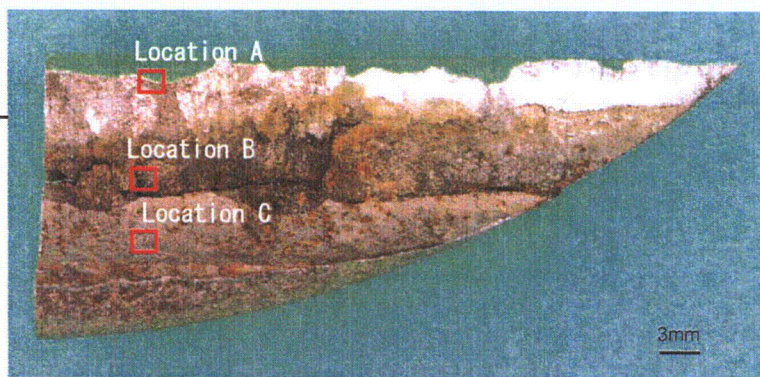
↓ Enlarged

↓ Enlarged

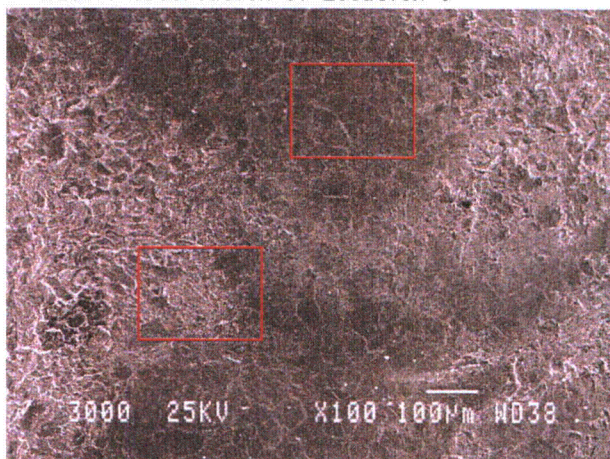


Ductile fracture surface with dimple

Fig. A. 8(1) SEM observation of fracture surface of TP A-1 (sample A)

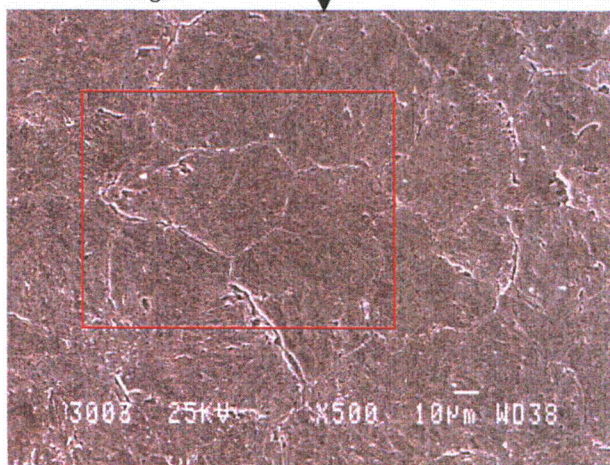


Detail observation of Location C

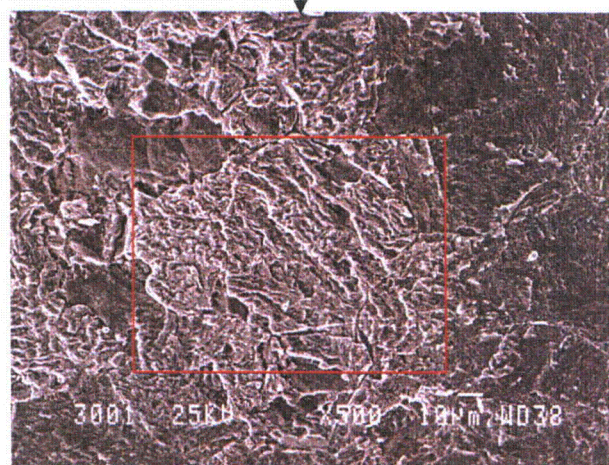


Enlarged

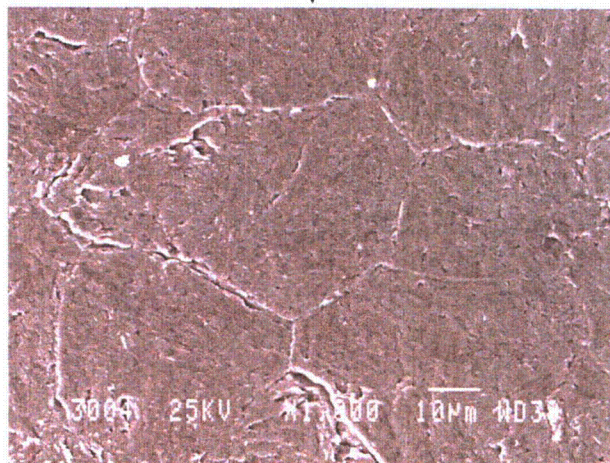
Enlarged



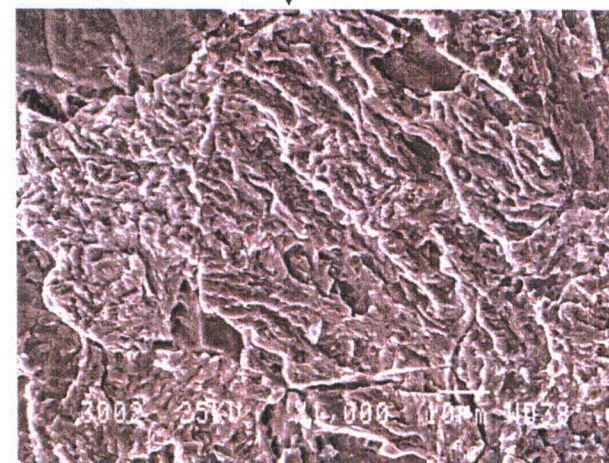
Enlarged



Enlarged



Grain-boundary-like pattern



Quasi-cleavage fracture surface

Fig. A.8(2) SEM observation of fracture surface of TP A-1 (sample A) (Continued)

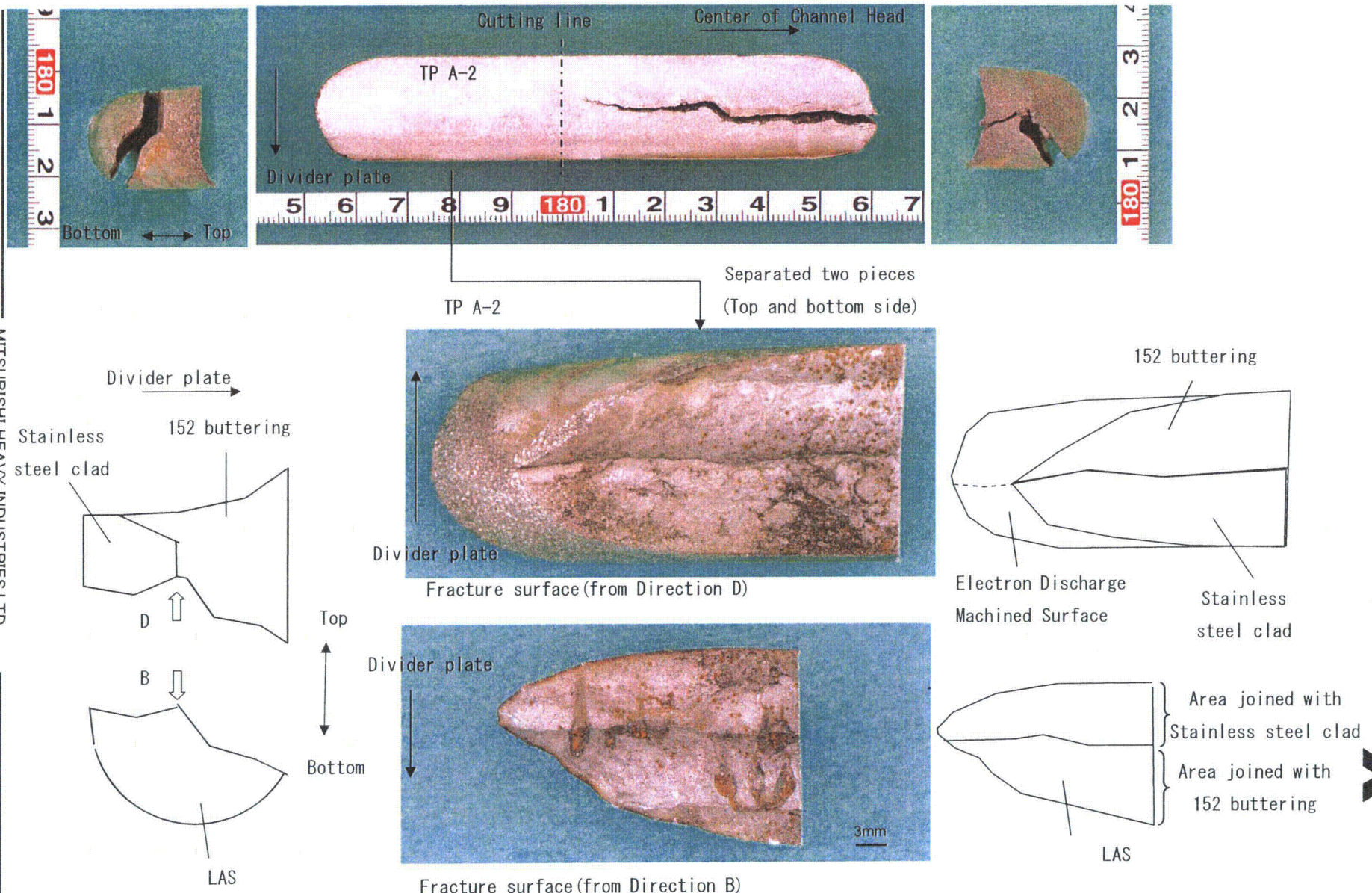
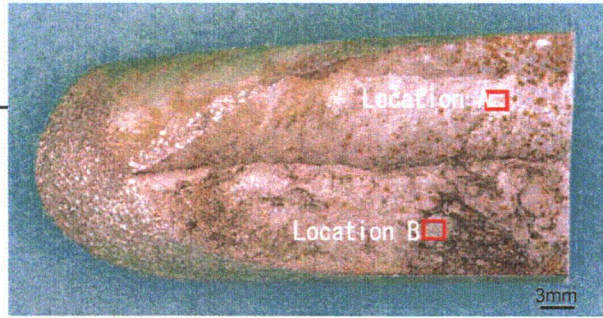
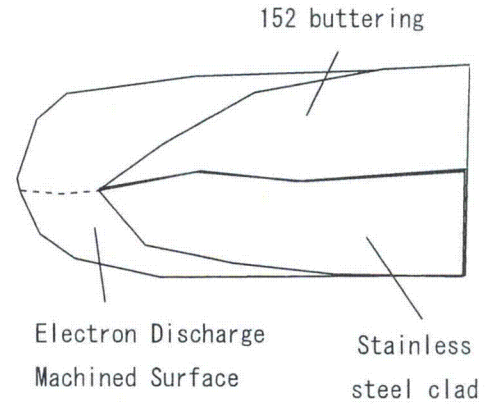
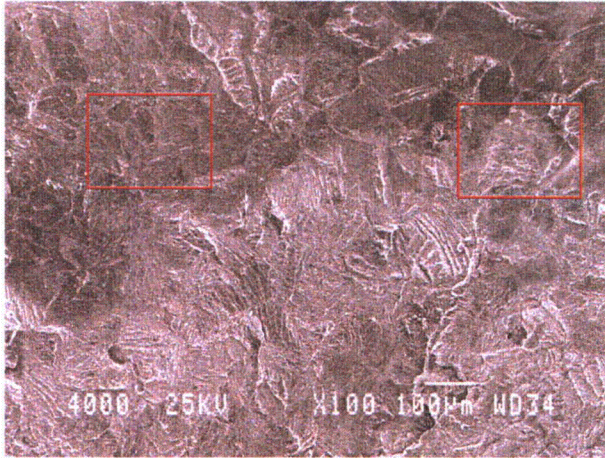


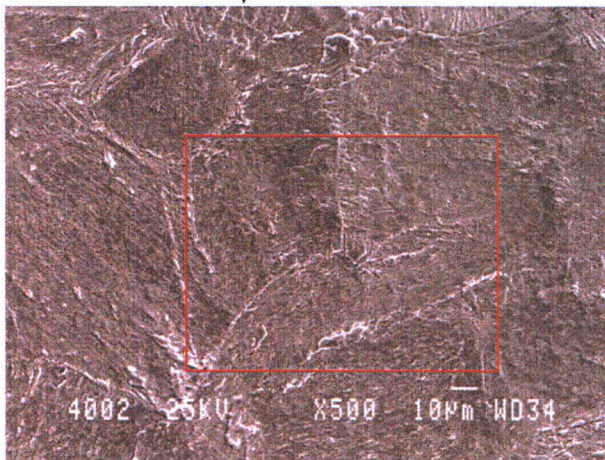
Fig. A.9 Appearance of fracture surface of TP A-2 (sample A)



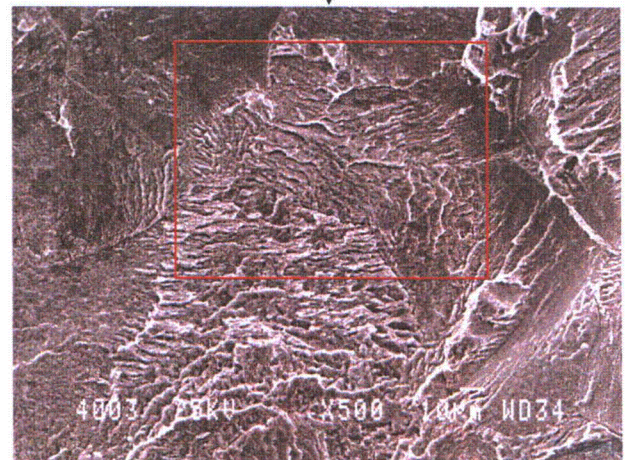
Detail observation of Location A



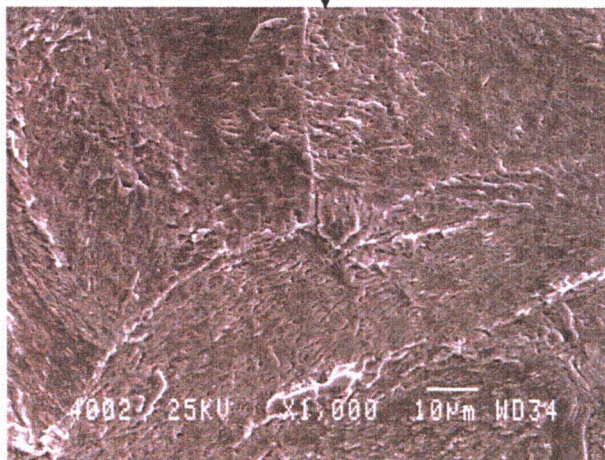
Enlarged



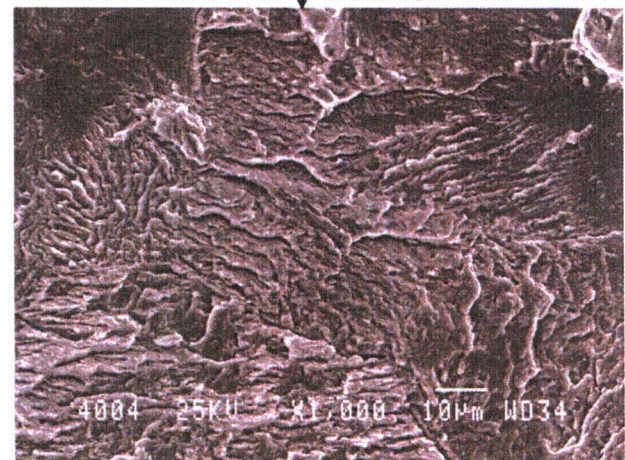
Enlarged



Enlarged

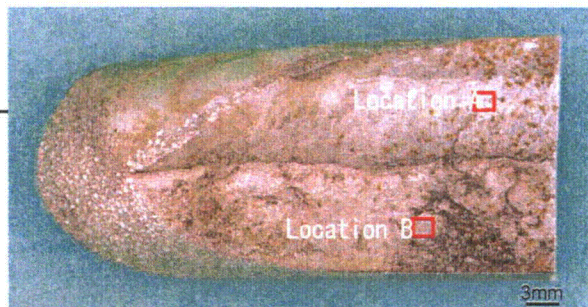


Dendrite-boundary-like pattern

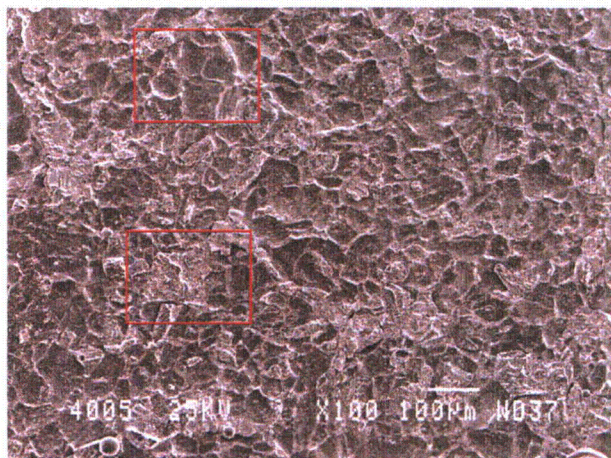


Quasi-cleavage fracture surface

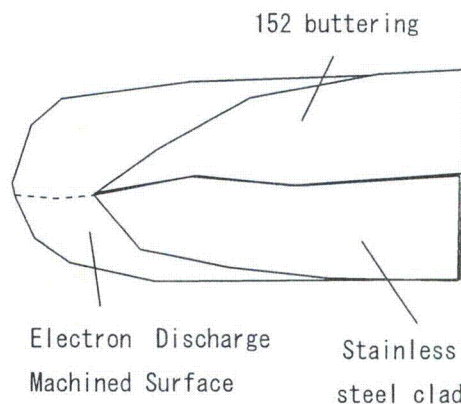
Fig. A.10(1) SEM observation of fracture surface of TP A-2(sample A)



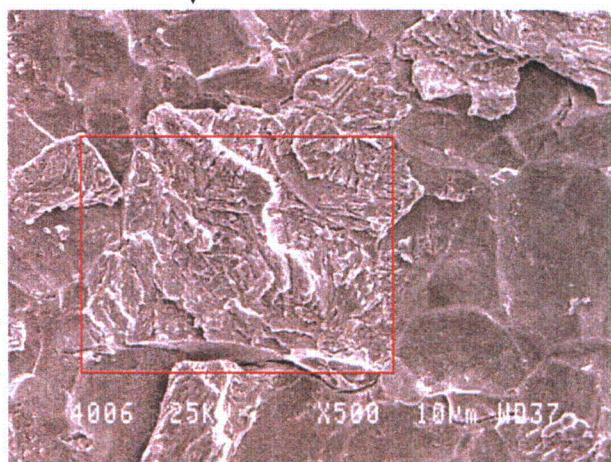
Detail observation of Location B



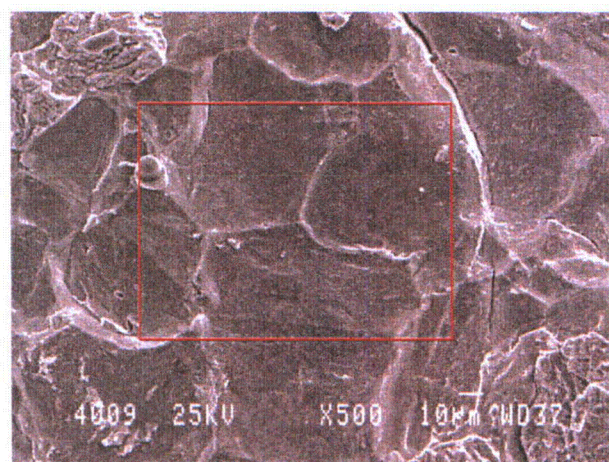
Enlarged



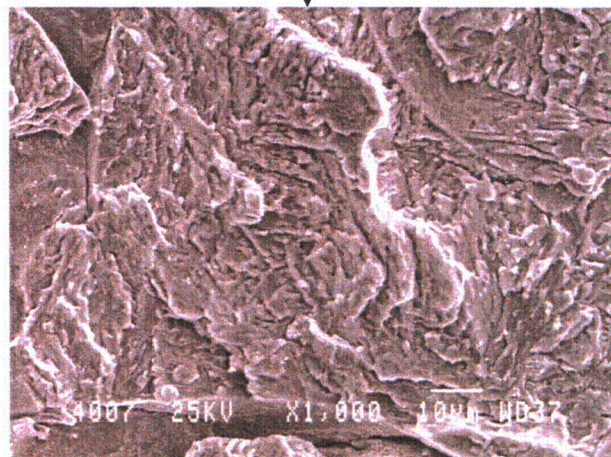
Enlarged



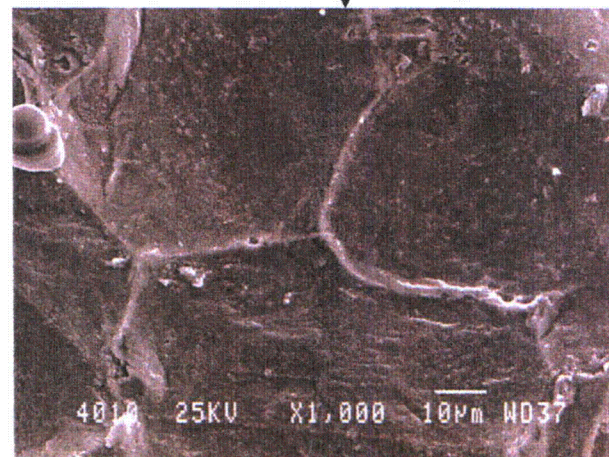
Enlarged



Enlarged



Quasi-cleavage fracture surface

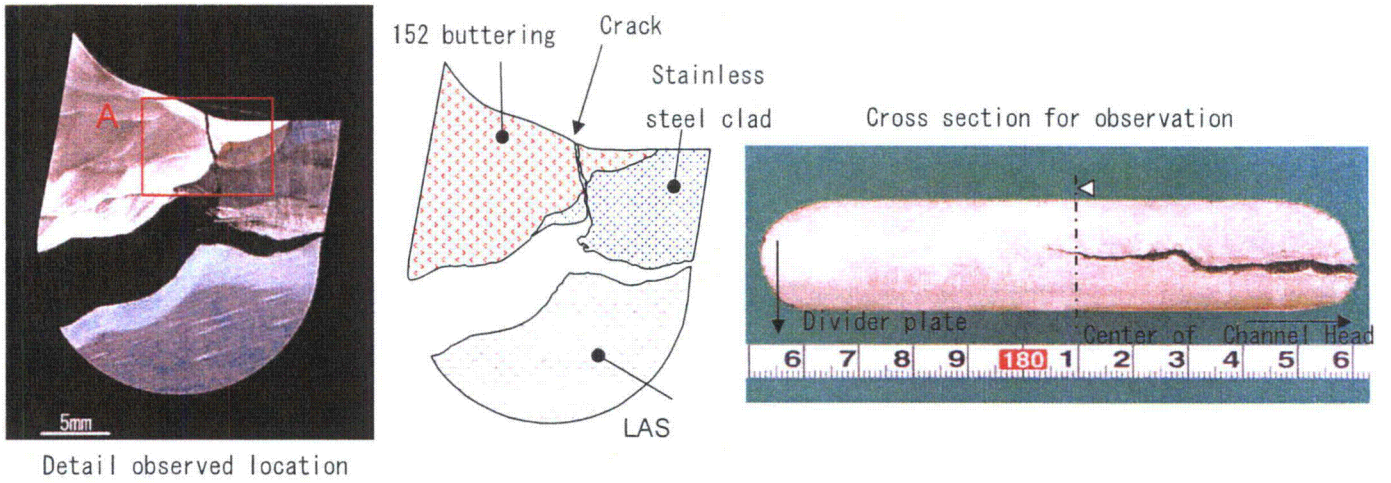


Dendrite-boundary-like pattern

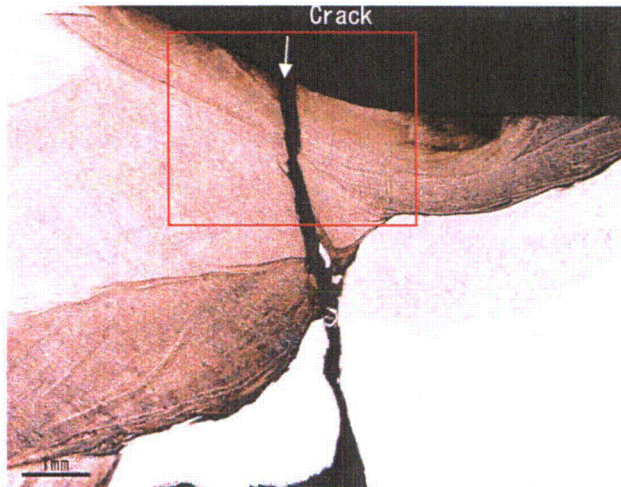
Fig. A.10(2) SEM observation of fracture surface of TP A-2(sample A) (Continued)



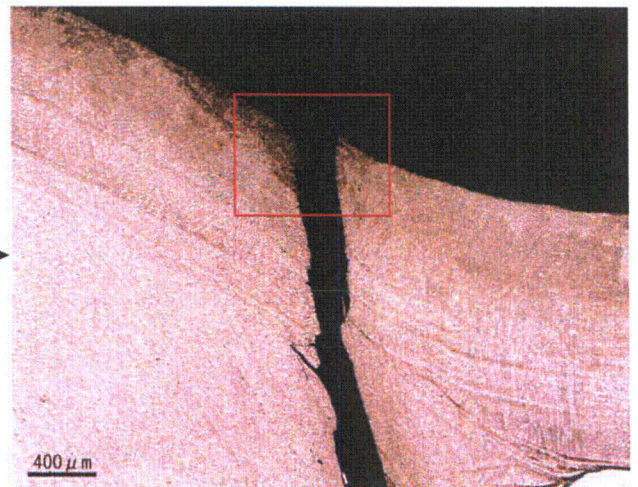
Macro-structure of cross section of sample A



Detail observation of location A

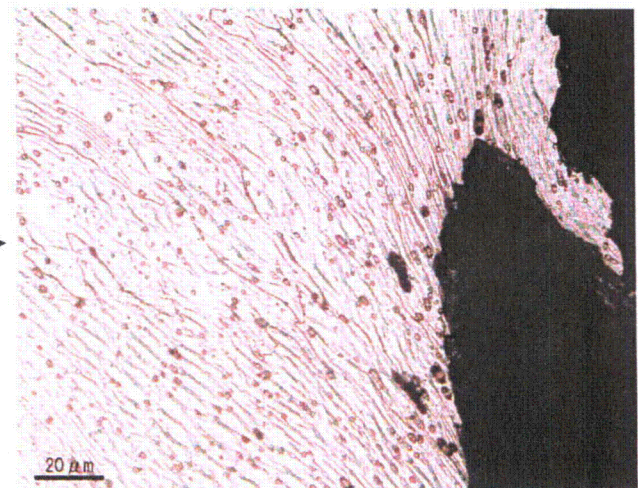
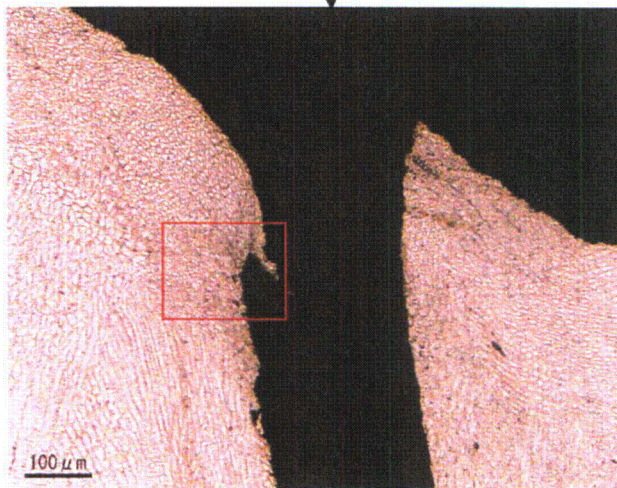


Enlarged



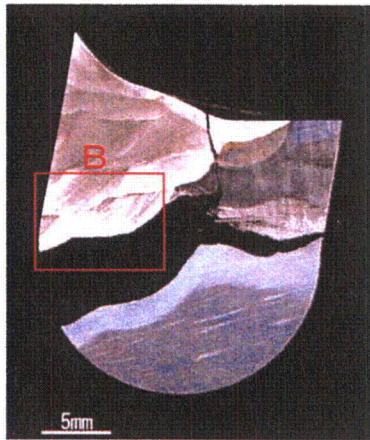
152 buttering ↔ Stainless steel clad

Enlarged

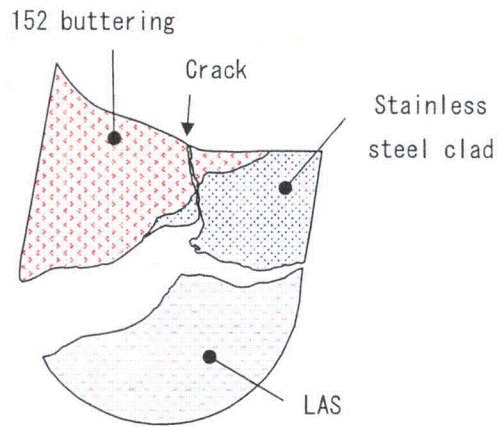


Enlarged

Fig. A. 11(1) Micro-structure observation of cross section of sample A

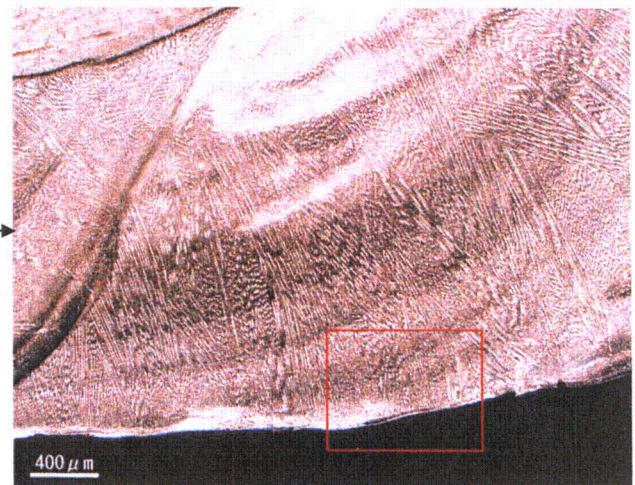
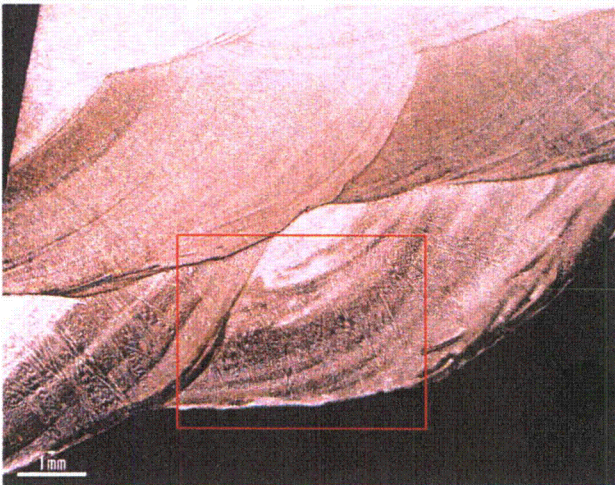


Detail observed location

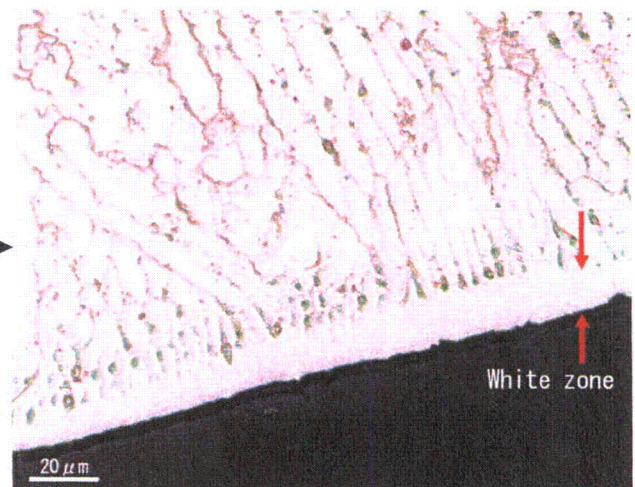
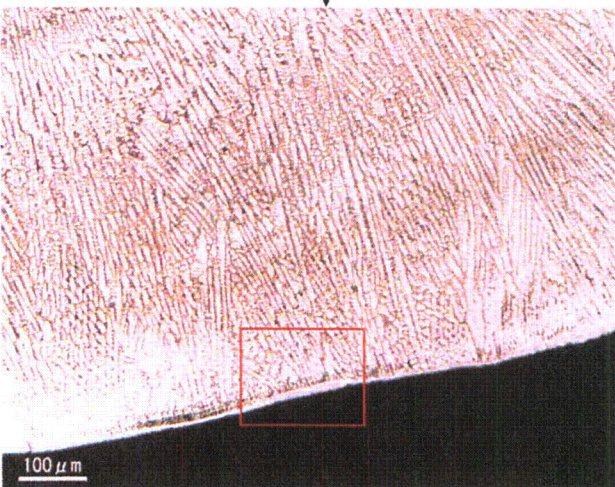


Detail observation of location B

Enlarged

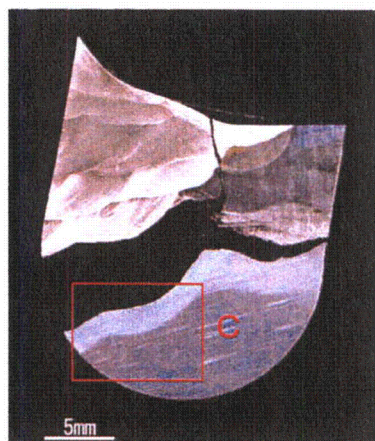


Enlarged

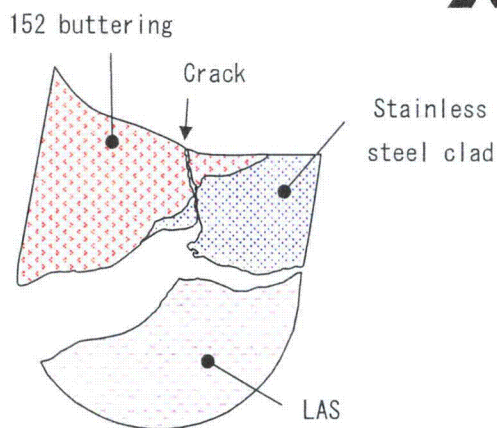


Enlarged

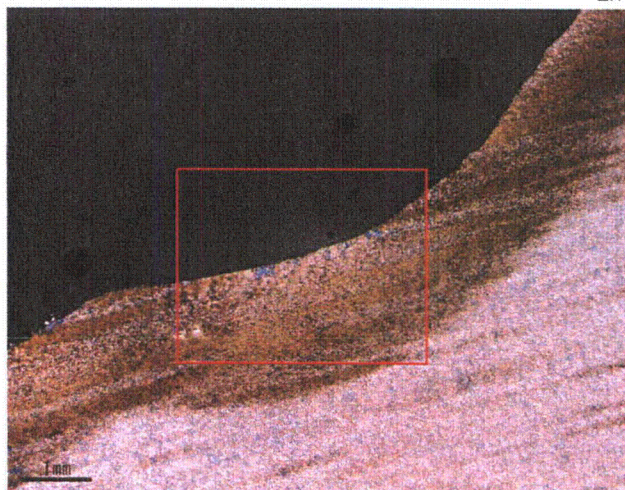
Fig. A.11(2) Micro-structure observation of cross section of sample A (Continued)



Detail observed location



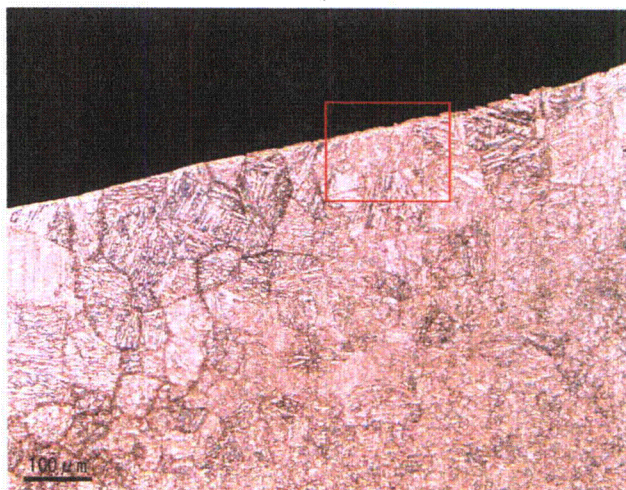
Detail observation of location C



Enlarged



Enlarged



Enlarged

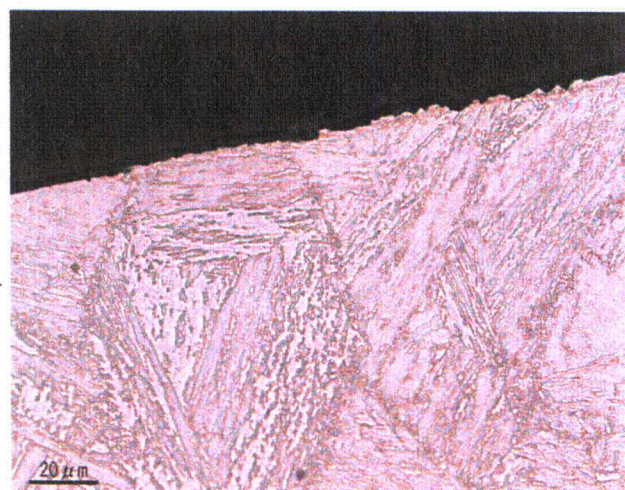
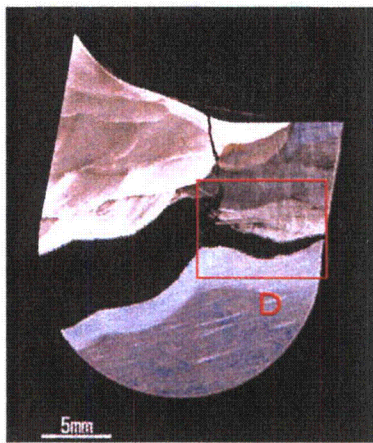


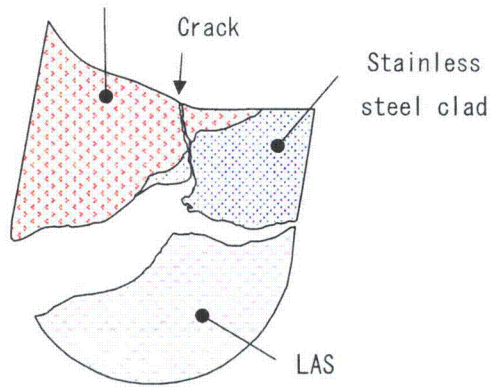
Fig. A.11(3) Micro-structure observation of cross section of sample A (Continued)



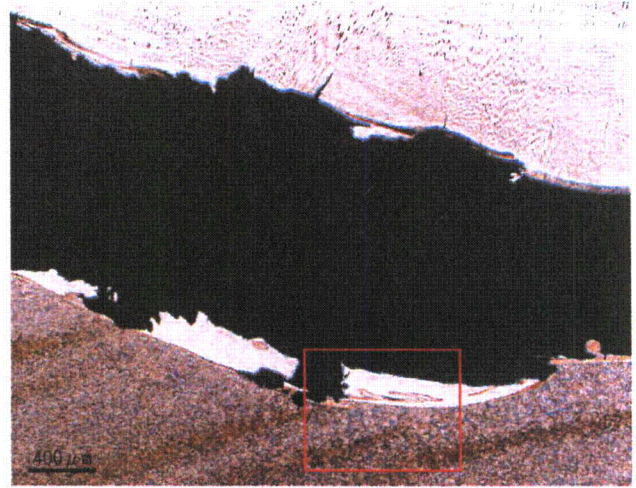
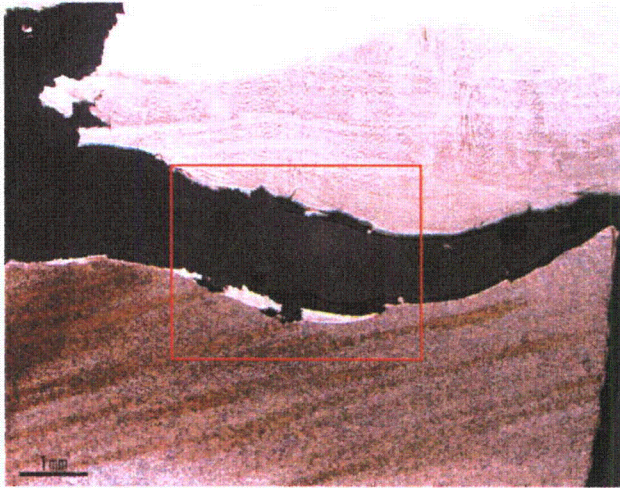
Detail observed location

Detail observation of location D

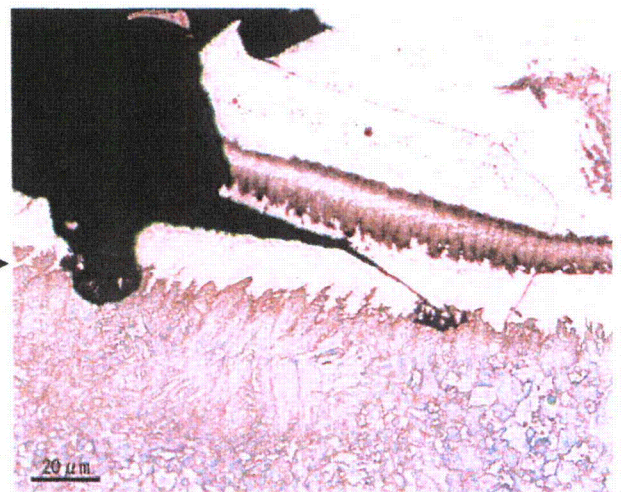
152 buttering



Enlarged



Enlarged

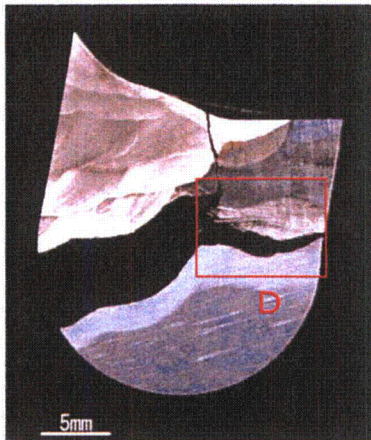


Enlarged

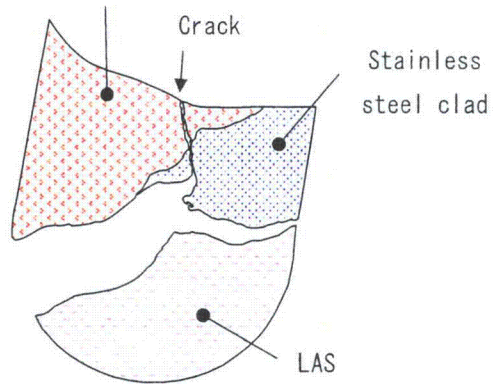
Fig. A.11(4) Micro-structure observation of cross section of sample A (Continued)



152 buttering

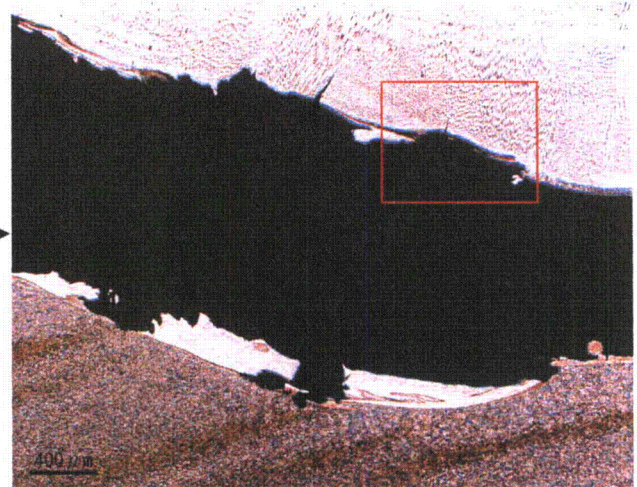
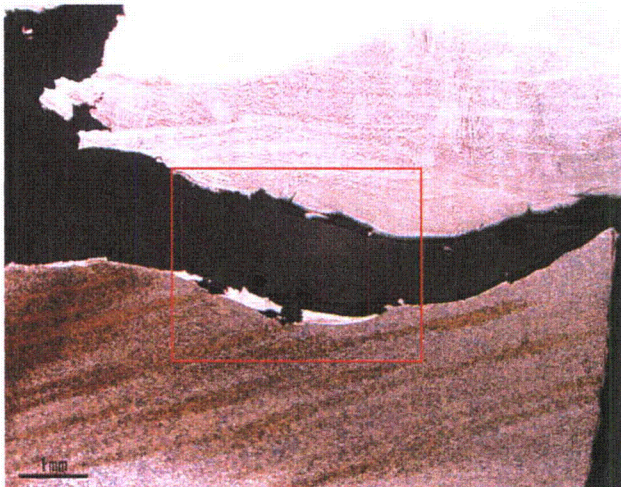


Detail observed location

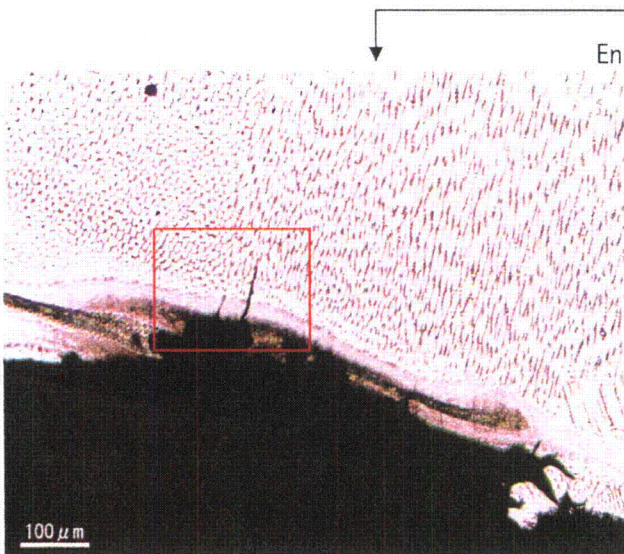


Detail observation of location D

Enlarged



Enlarged



Enlarged

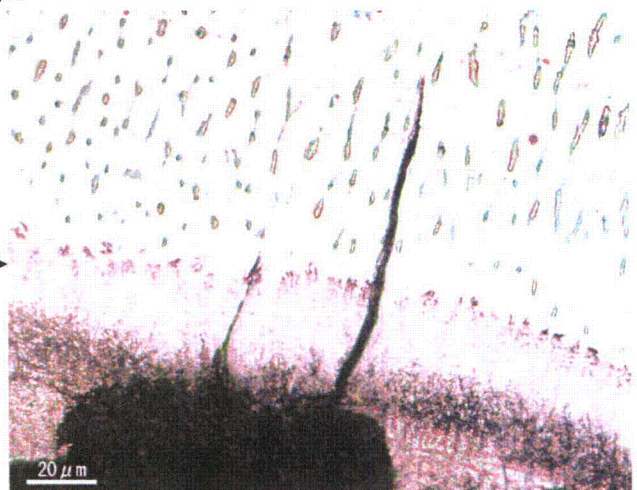


Fig. A.11(5) Micro-structure observation of cross section of sample A (Continued)

Detail observed location

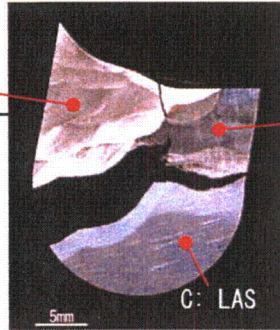
(A-28)

Document No.L5-04GA440 (0)

Attachment-A



A: 152 buttering

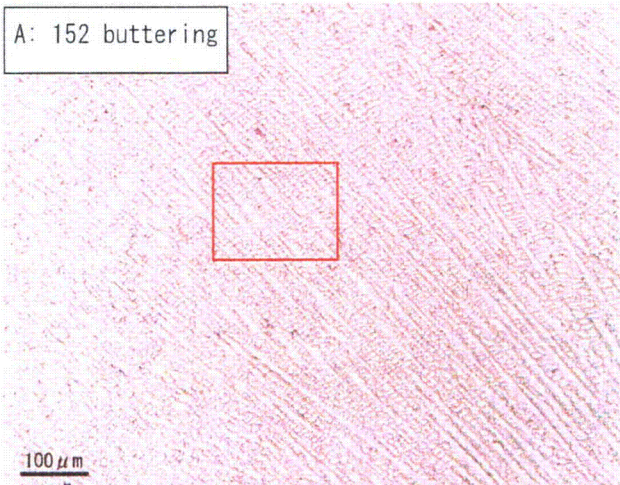


B: Stainless steel clad

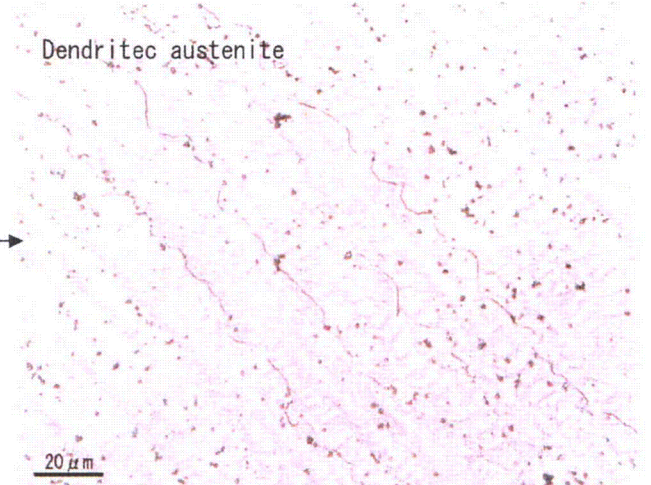
C: LAS

Typical micro-structure of weld metal and base metal

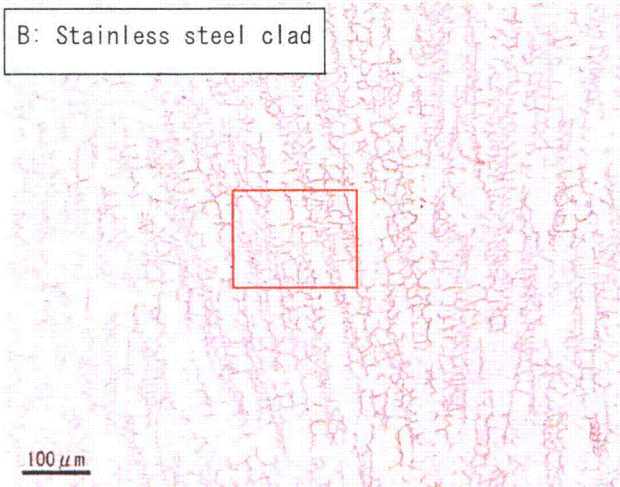
A: 152 buttering



Dendritic austenite

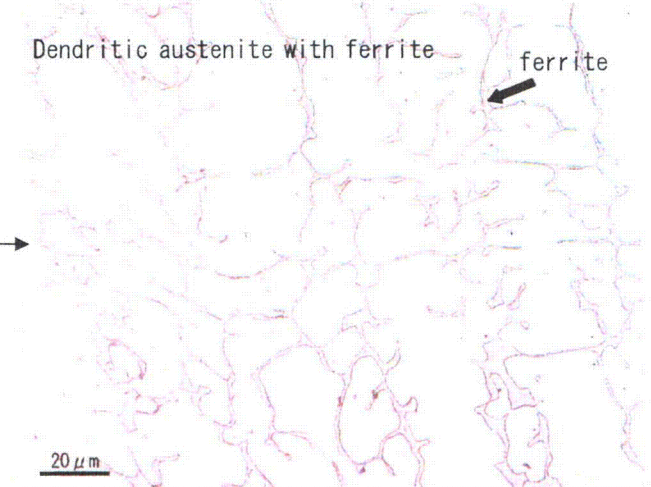


B: Stainless steel clad

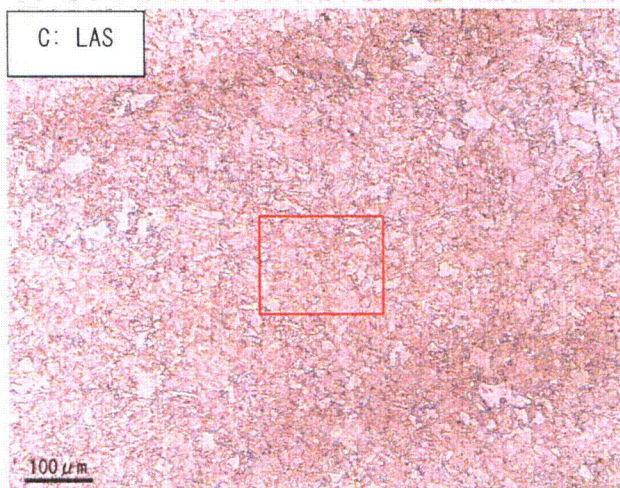


Dendritic austenite with ferrite

ferrite



C: LAS



Bainite

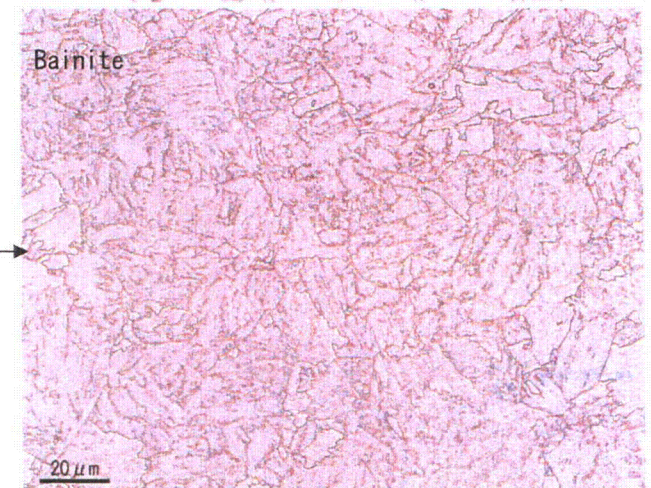
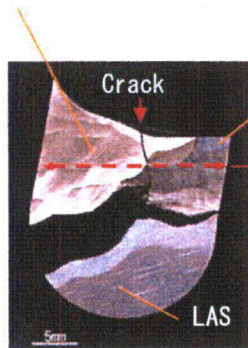


Fig. A.11(6) Micro-structure observation of cross section of sample A (Continued)



152 buttering



Stainless steel clad

The position of hardness test

Crack

LAS

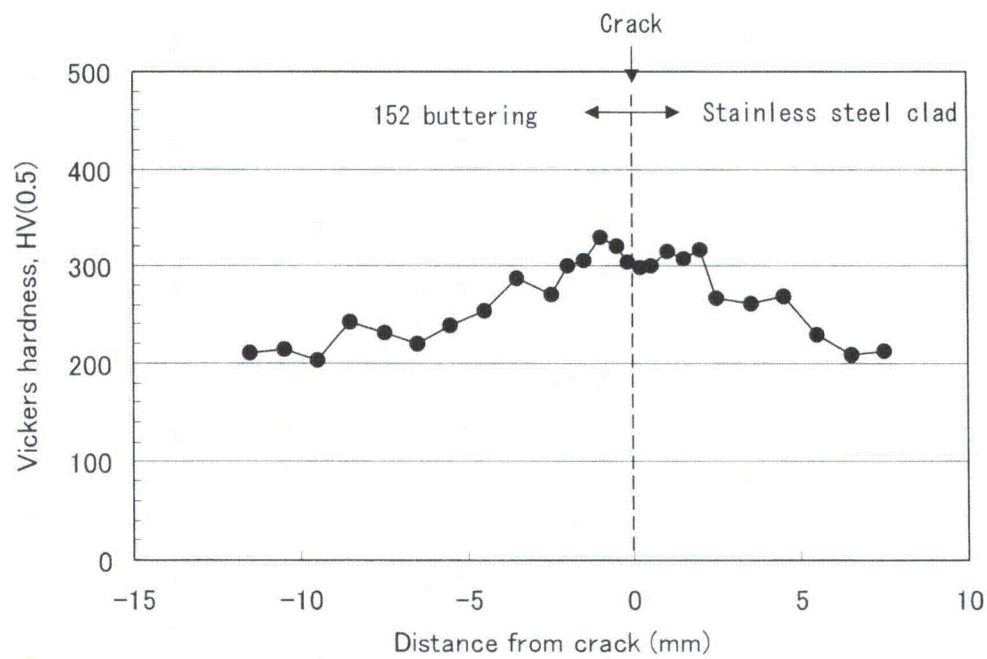
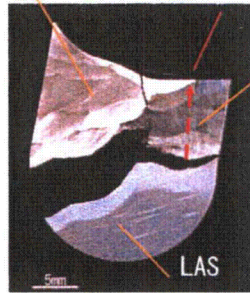


Fig. A.12 Vickers hardness of cross section of sample A (near crack)

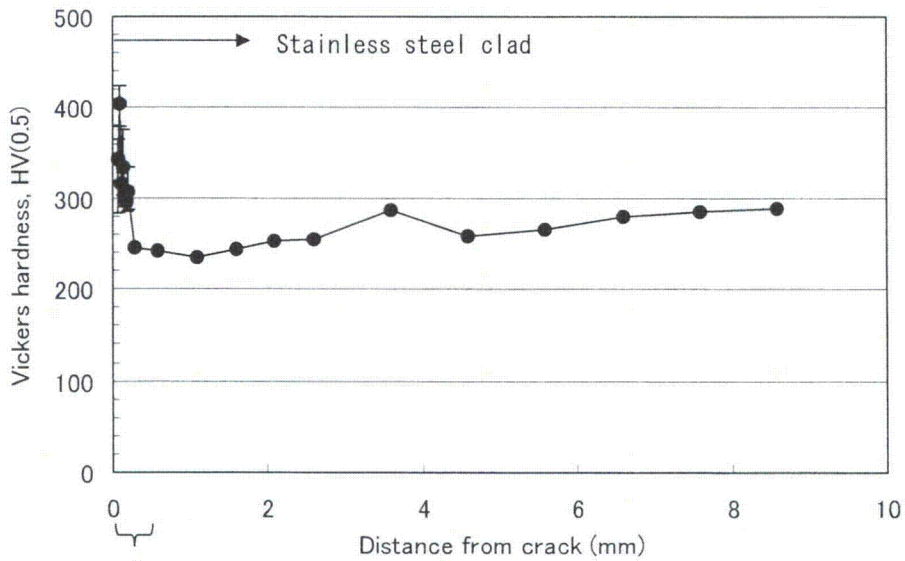


152 buttering

The position of hardness test

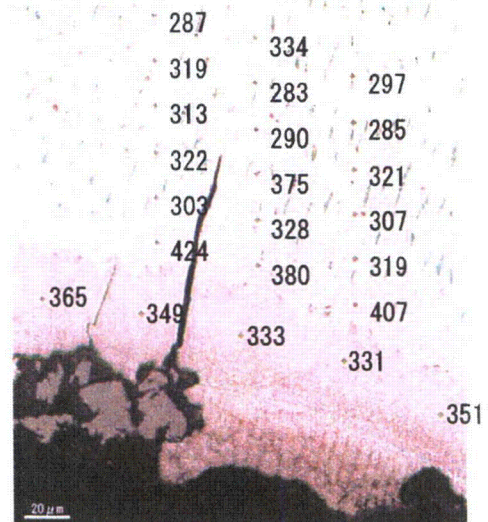
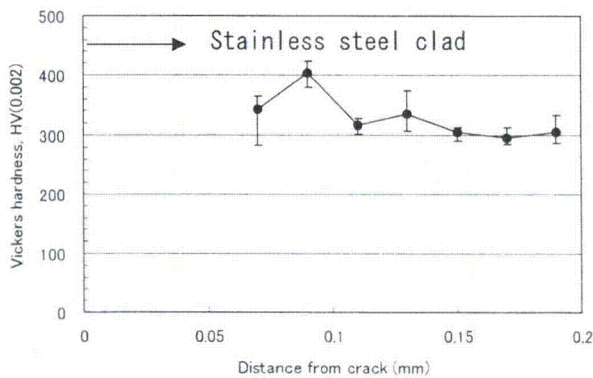


Stainless steel clad



* Testing load is 2g at the distance to 0.2mm

Enlarged

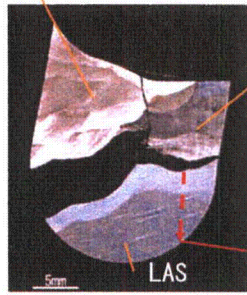


The result of hardness test

Fig. A.13(1) Vickers hardness of cross section of sample A (Stainless steel clad/LAS boundary)

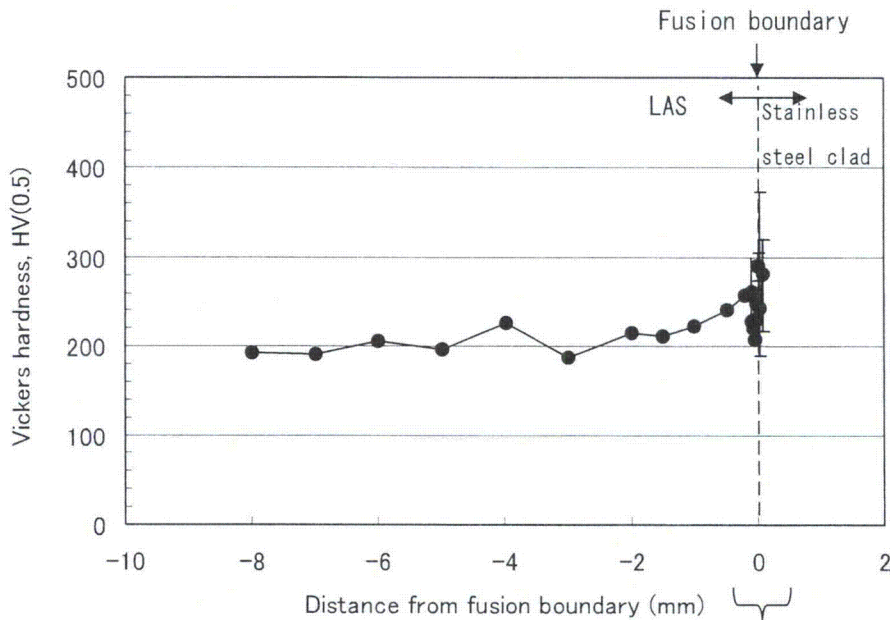


152 buttering



Stainless steel clad

The position of hardness test



* Testing load is 2g at the distance from -0.1 to 0.15mm

Enlarged

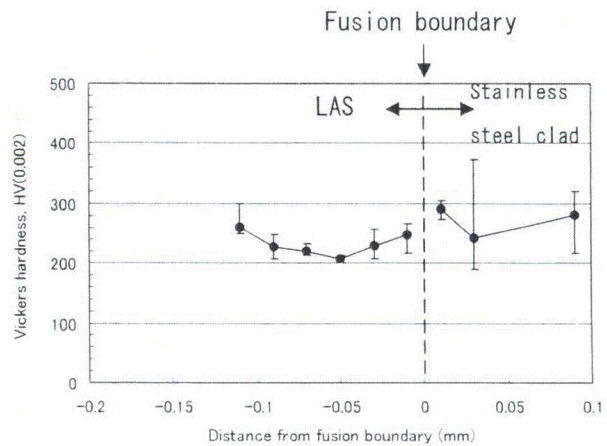
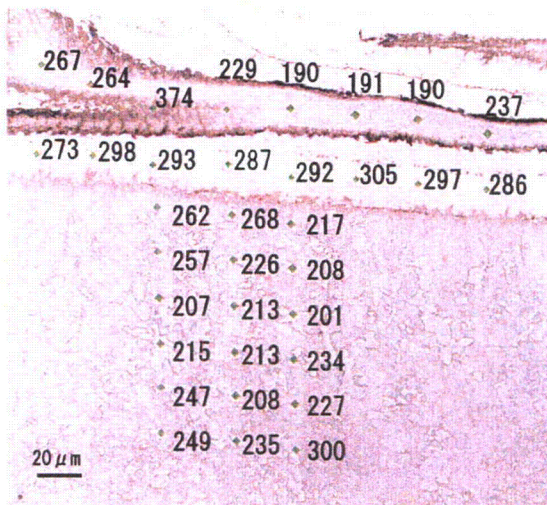
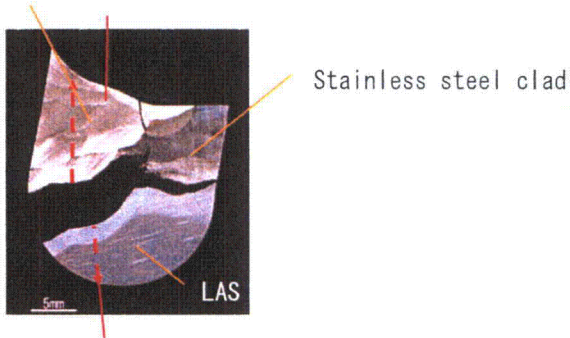


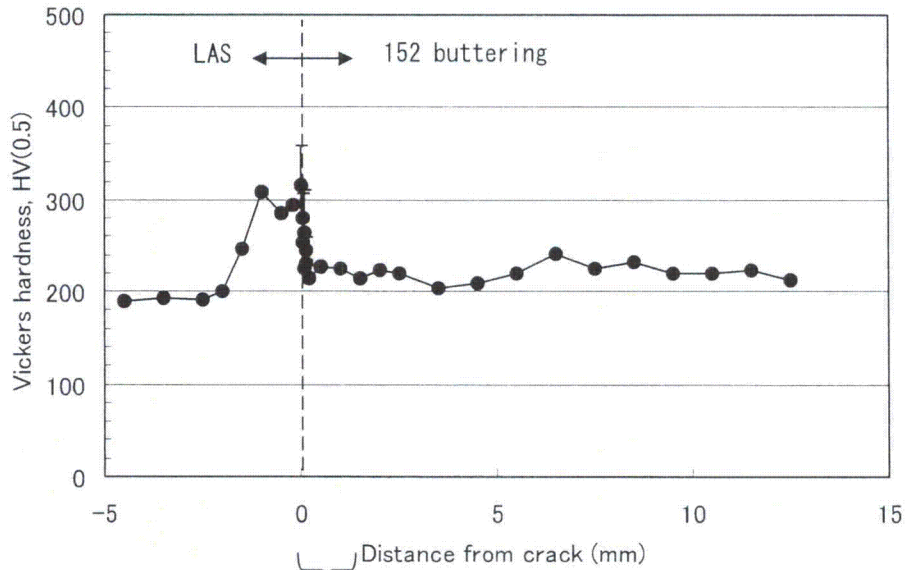
Fig. A.13(2) Vickers hardness of cross section of sample A (Stainless steel clad/LAS boundary) (Continued)



152 buttering



The position of hardness test



Distance from crack (mm)
 * Testing load is 2g at the distance from 0 to 0.15mm
 Enlarged

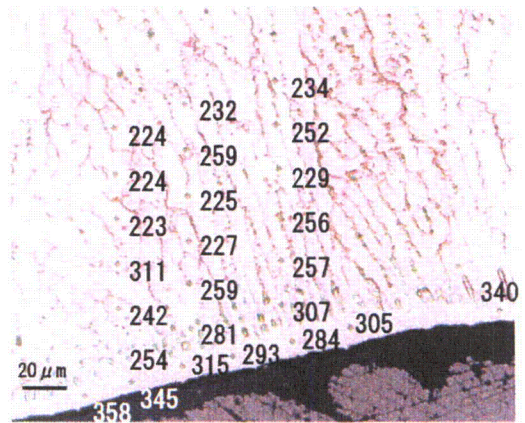
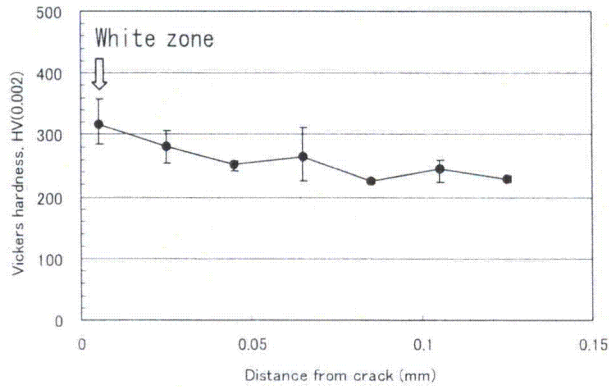
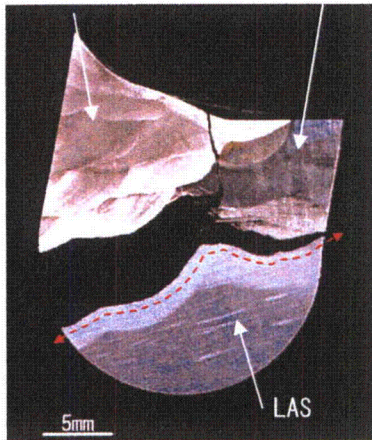


Fig. A.14 Vickers hardness of cross section of sample A (152 buttering/LAS boundary)



152 buttering Stainless steel clad



Testing at a distance of 0.2mm and 0.5mm from fracture surface

The position of hardness test

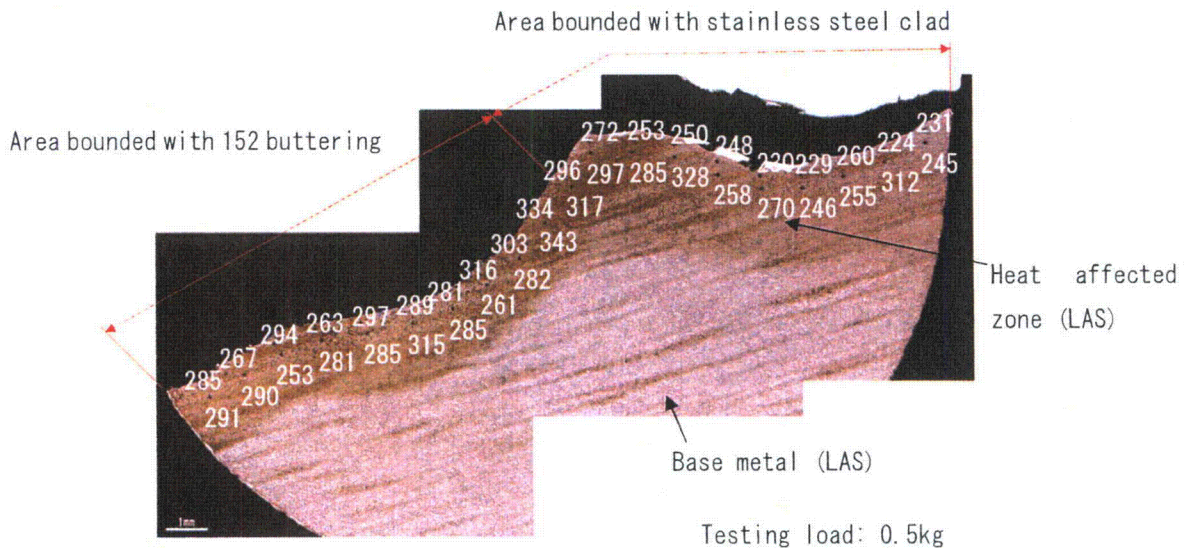
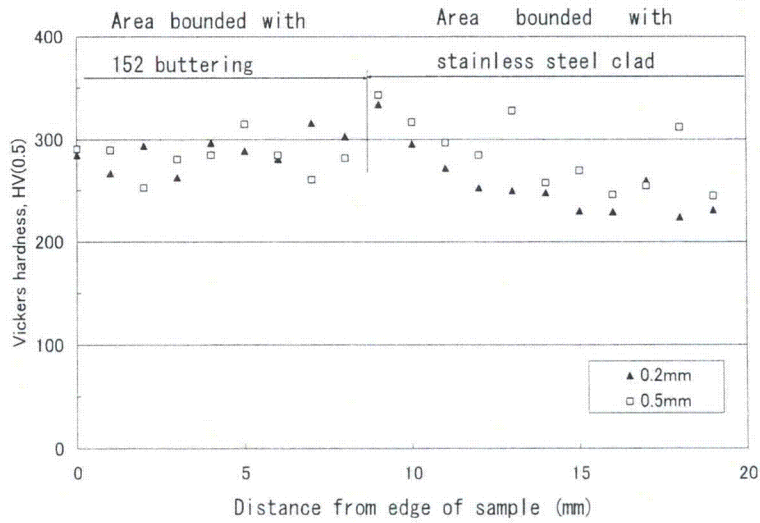
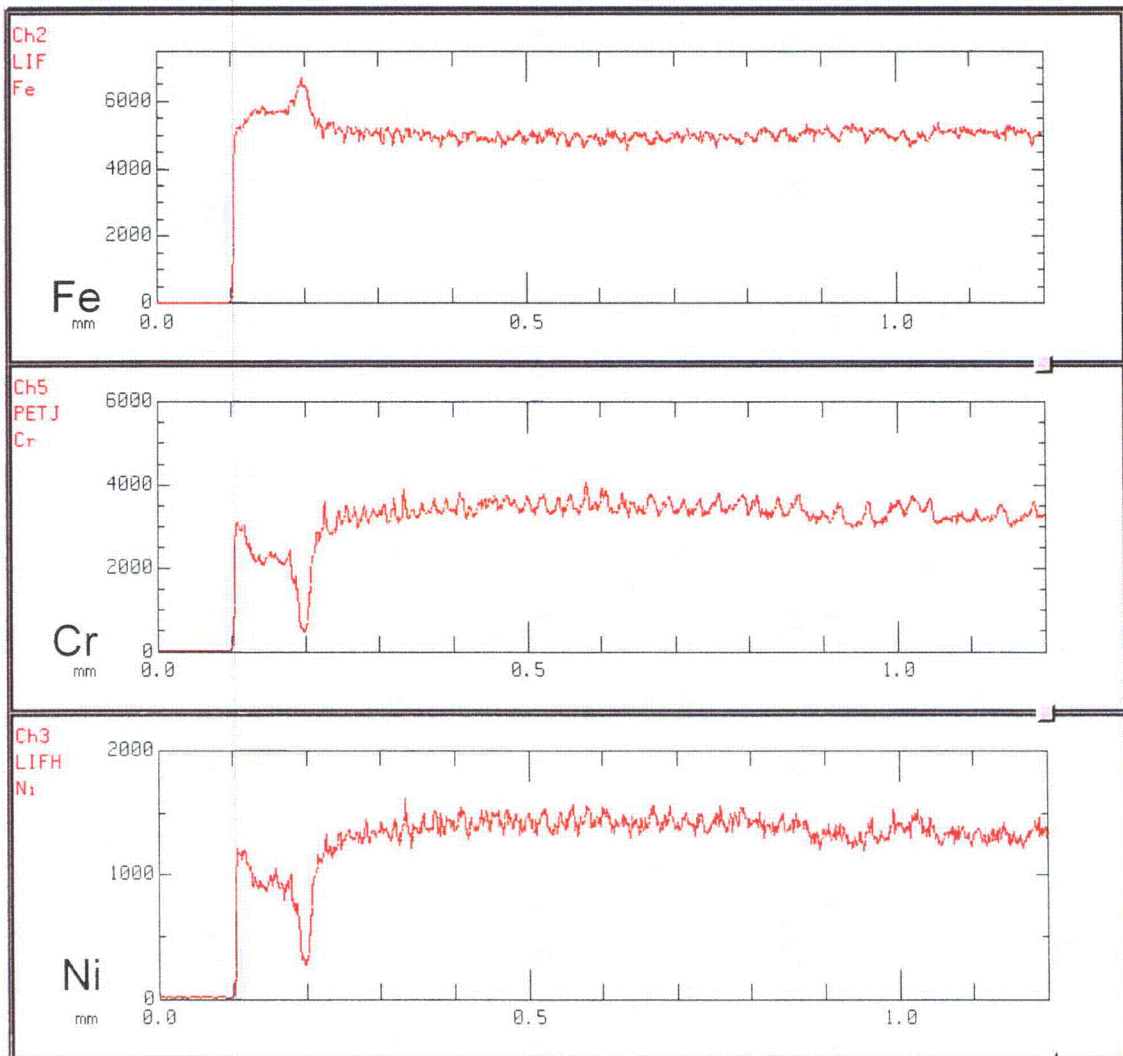
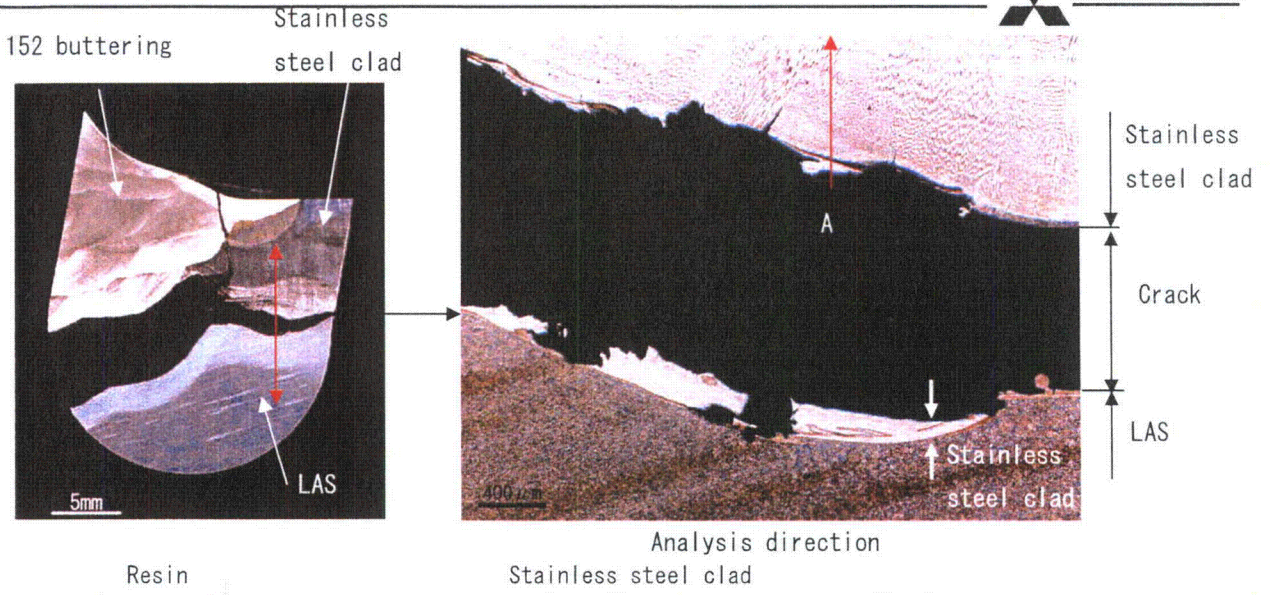
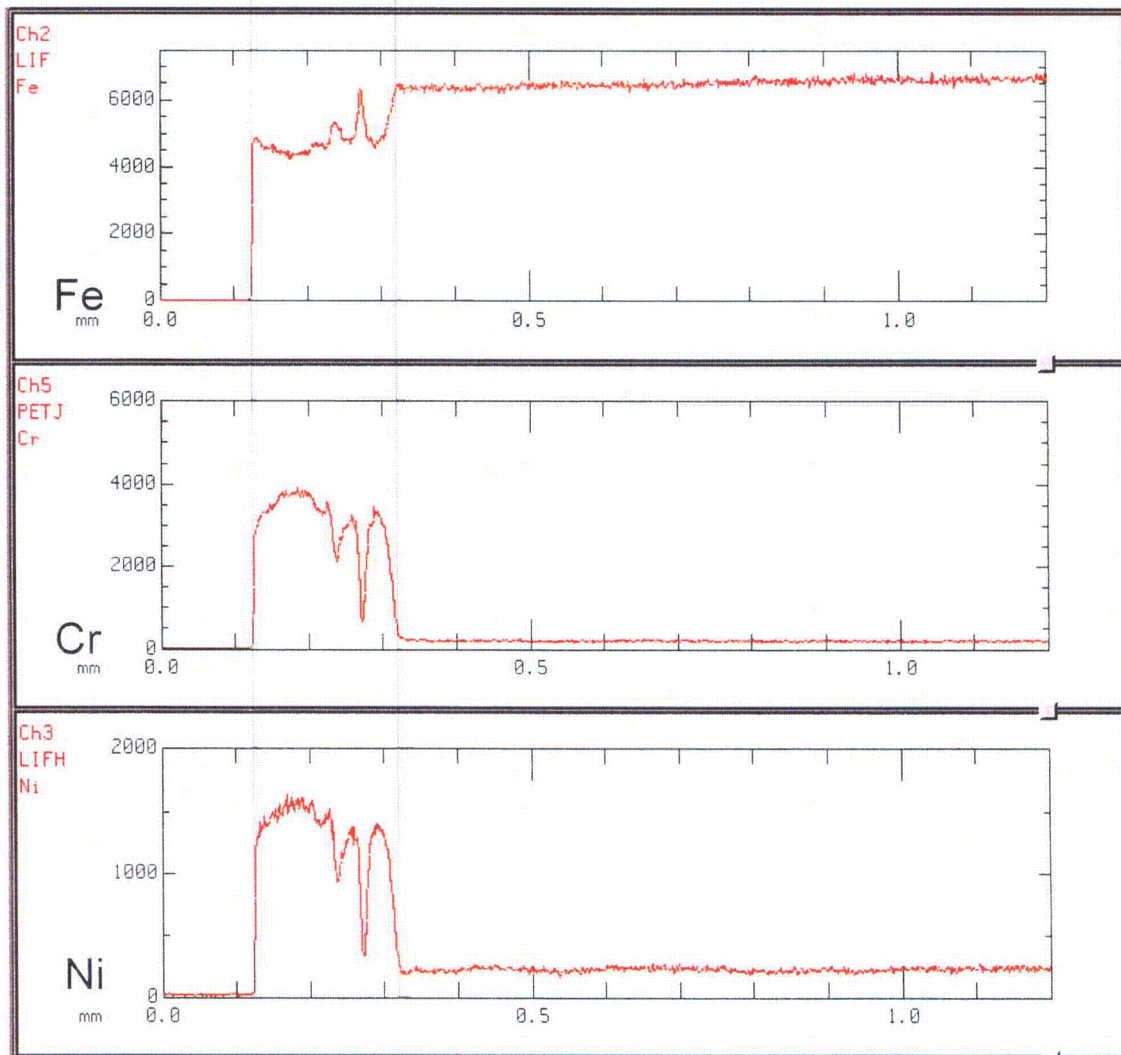
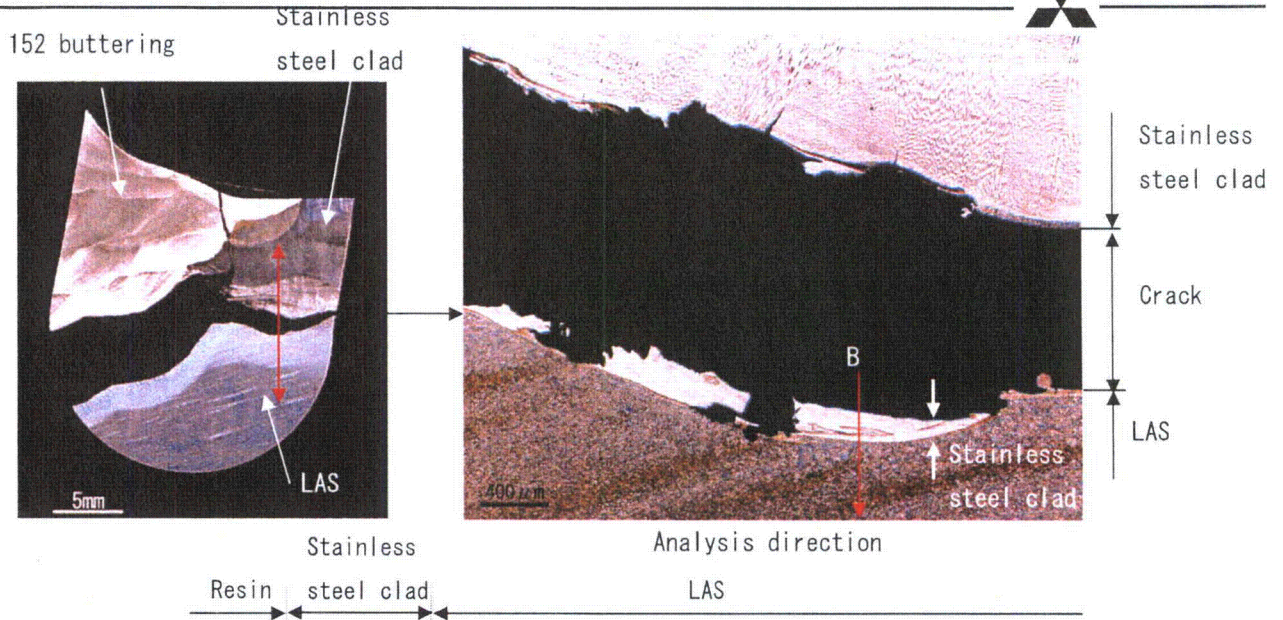


Fig. A.15 Distribution of Vickers hardness of heat affected zone in cross section of sample A



The result of line analysis to depth direction in cross section of sample A (Line A)

Fig. A.16(1) EPMA line analysis of cross section of sample A
 (Stainless steel clad/LAS boundary)



The result of line analysis to depth direction in cross section of sample A (Line B)

Fig. A.16(2) EPMA line analysis of cross section of sample A

(Stainless steel clad/LAS boundary) (Continued)



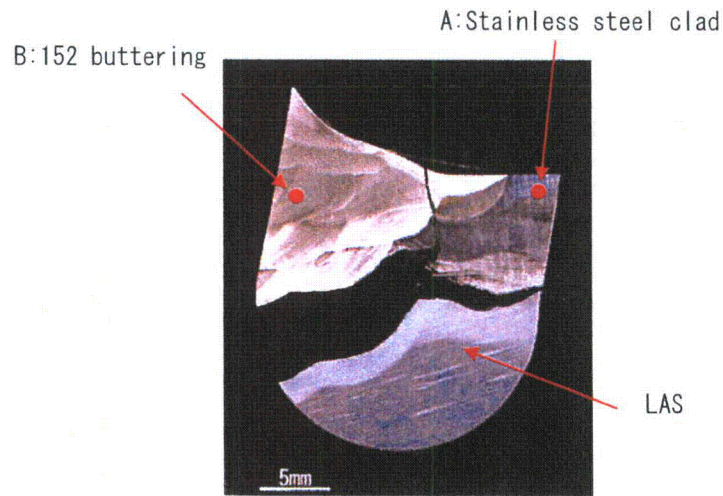
Table A.3 The results of EPMA semi-qualitative analysis (wt.%)

		Al	Si	Ti	Cr	Mn	Fe	Ni	Nb	Mo
Sample A	A: Stainless steel clad	-	0.4	-	21.1	1.8	66.1	10.6	-	-
Stainless steel clad** (A,B)		-	0.20	<0.01	20.2	1.5	Bal.	10.2	<0.01	0.01
Sample A	B: 152 buttering	0.2	0.5	0.2	29.7	4.2	10.8	53.3	1.1	-
152 weld metal** (A,B)		0.11	0.27	0.1	29.57	0.27	10.1	59.6	1.61	0.01

* The value obtained by semi-quantitative analysis was for reference because the effect of background and superposition X-ray were not considered.

** The values in certification sheet of the material.

*** The semi-qualitative analysis of LAS was performed in sample B.



The position of EPMA semi-qualitative analysis

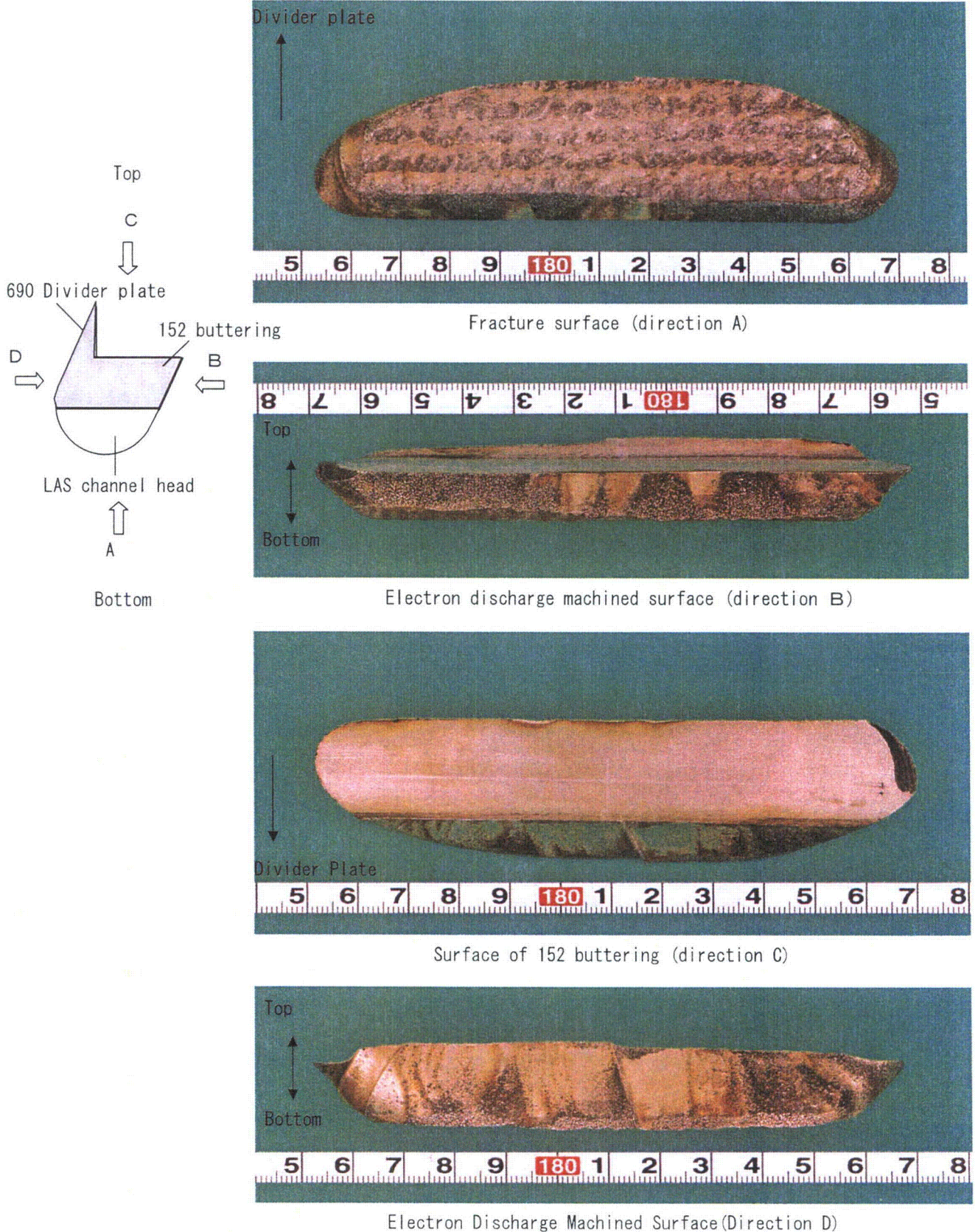


Fig. A.17 Appearance of sample B (152 buttering)

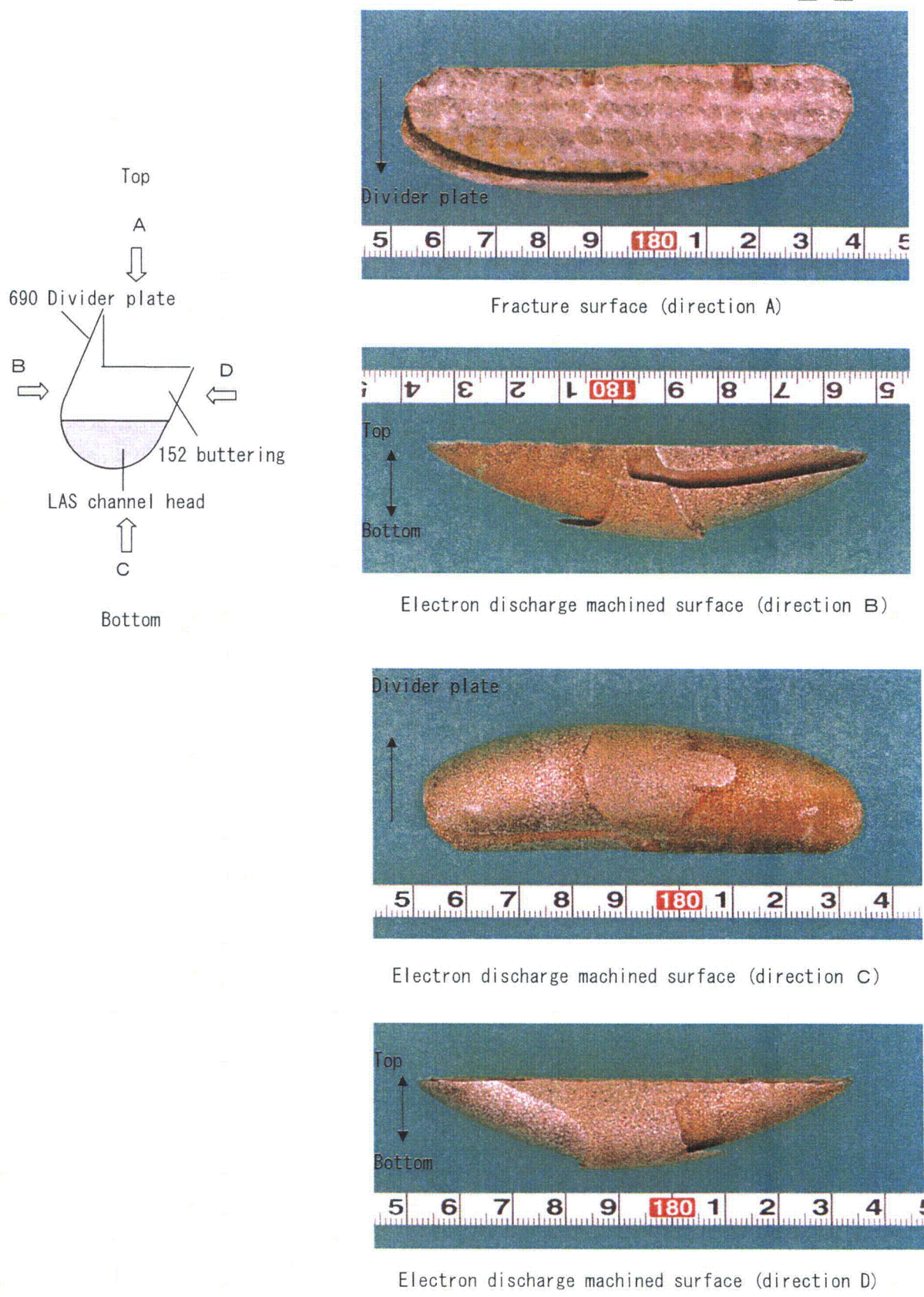


Fig. A.18 Appearance of sample B (Low alloy steel channel head)

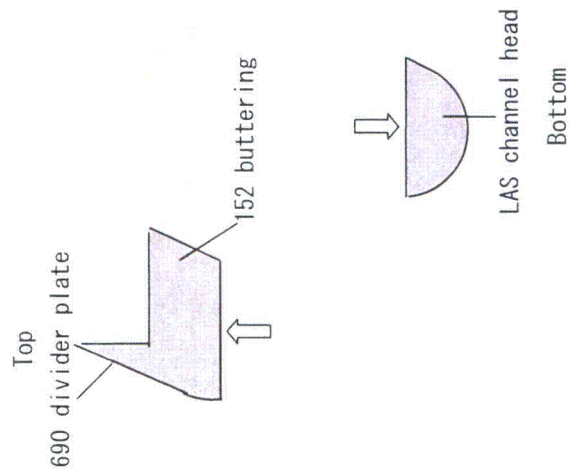


Fracture surface of sample B (152 buttering)



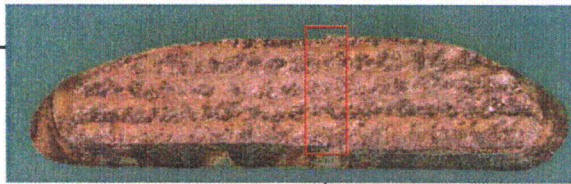
Fracture surface of sample B (Low Alloy Steel channel head)

Fig. A.19 Appearance of fracture surface





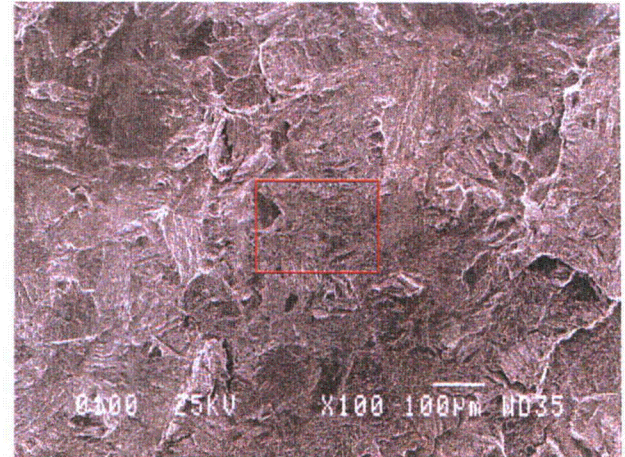
Fracture surface of sample B (152 buttering)



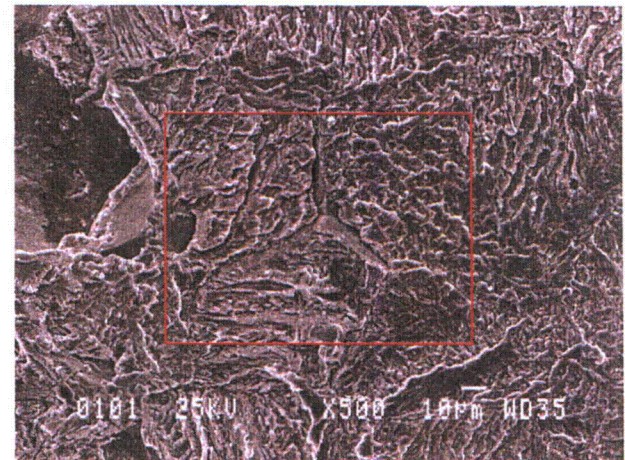
Enlarged



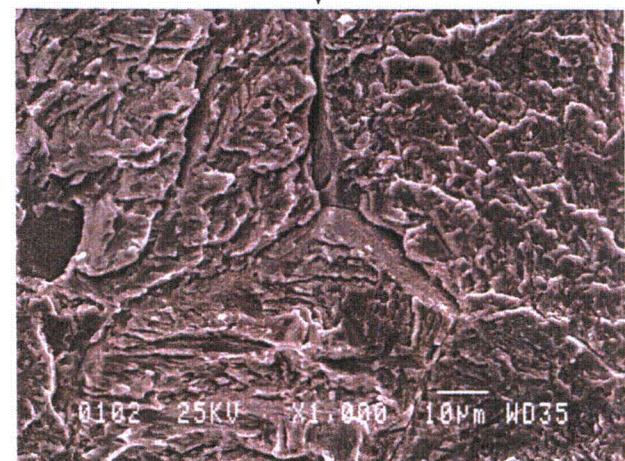
Detail observation of location A



Enlarged



Enlarged



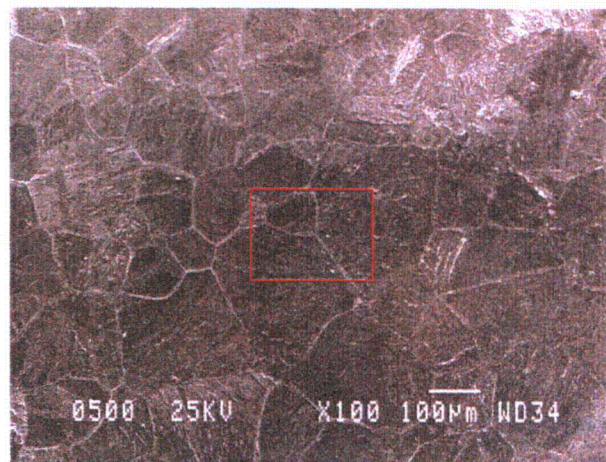
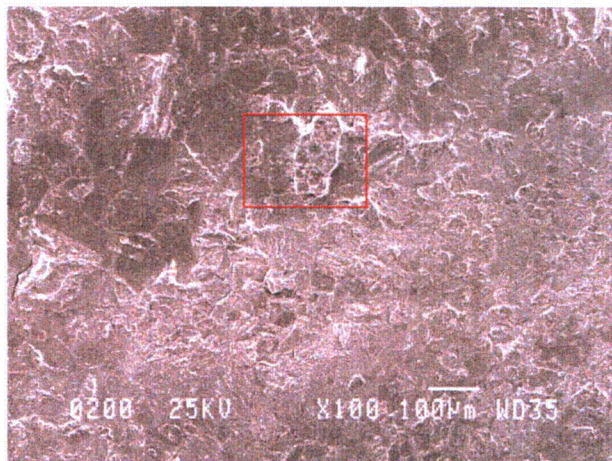
Quasi-cleavage fracture surface

Fig. A. 20(1) SEM observation of fracture surface of sample B (152 buttering)



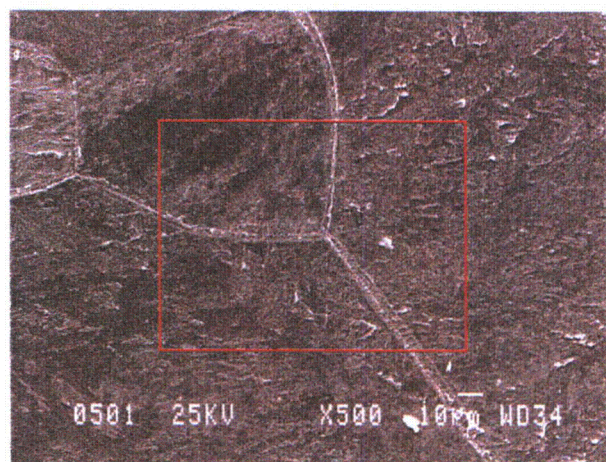
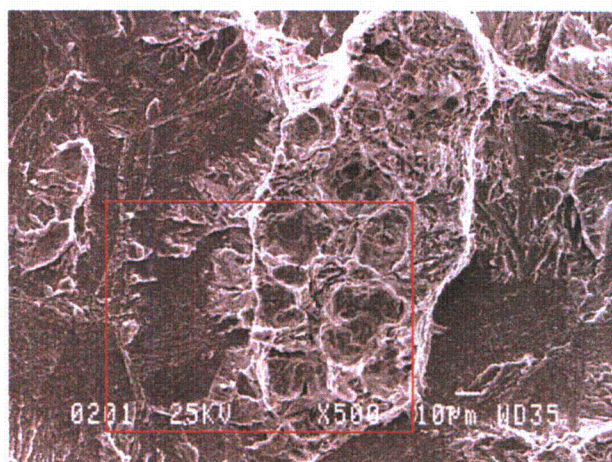
Detail observation of location B

Detail observation of location C



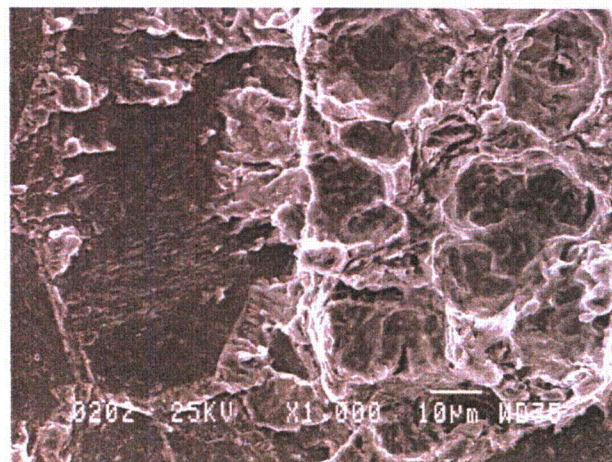
↓ Enlarged

↓ Enlarged



↓ Enlarged

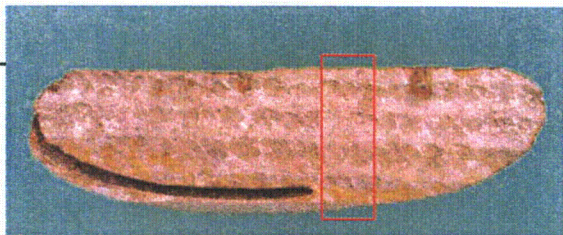
↓ Enlarged



Ductile fractured surface

Dendrite-boundary-like pattern

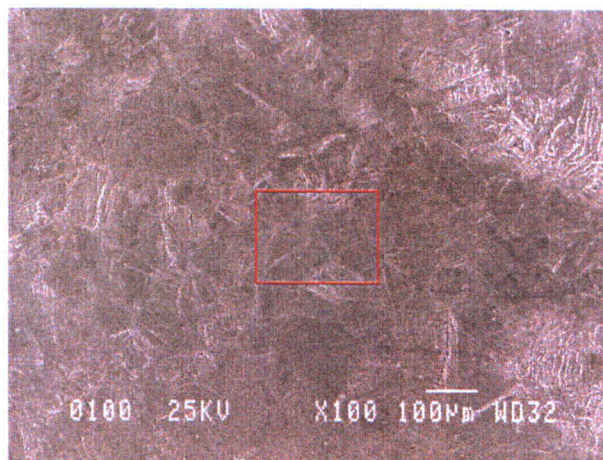
Fig. A. 20(2) SEM observation of fracture surface of sample B (152 buttering) (continued)



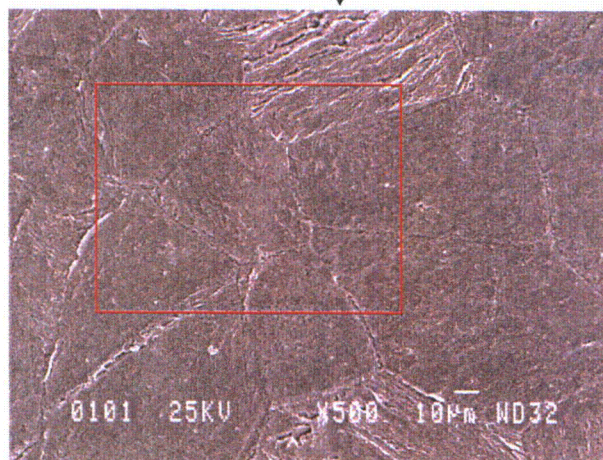
Fracture surface of sample B (Low alloy steel channel head)

Enlarged

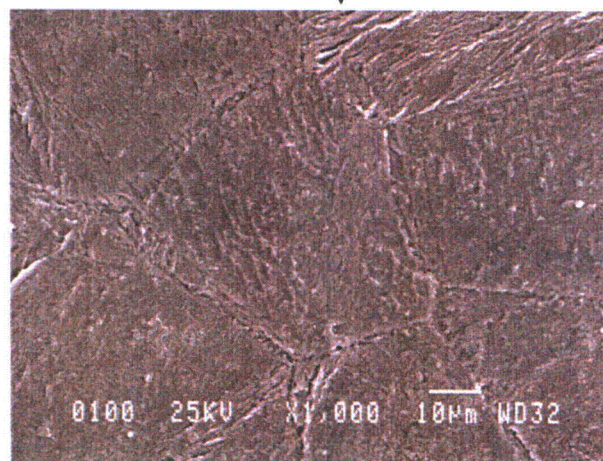
Detail observation of location A



Enlarged



Enlarged

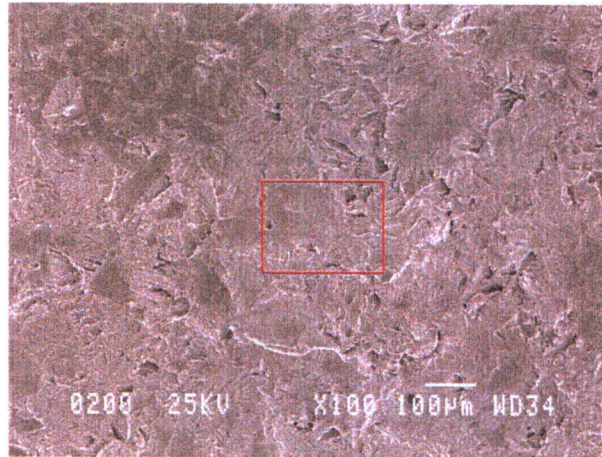


Grain-boundary-like pattern

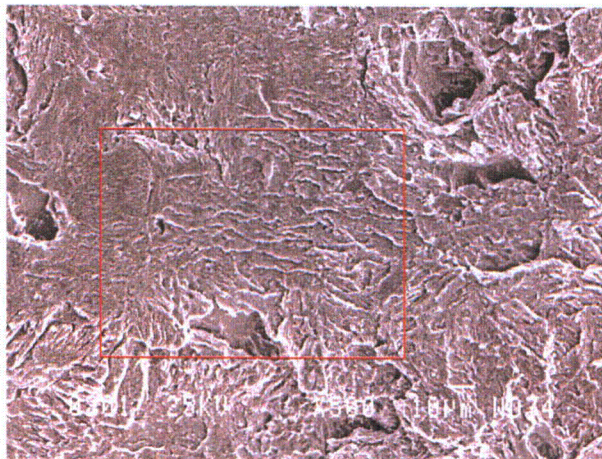
Fig. A. 21(1) SEM observation of fracture surface of sample B (Low alloy steel channel head)



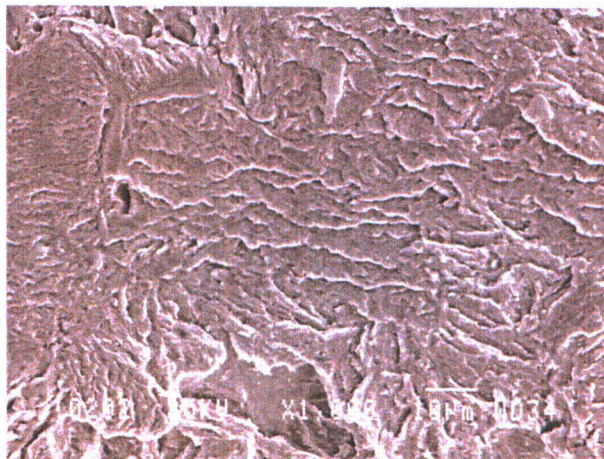
Detail observation of location B



↓ Enlarged



↓ Enlarged

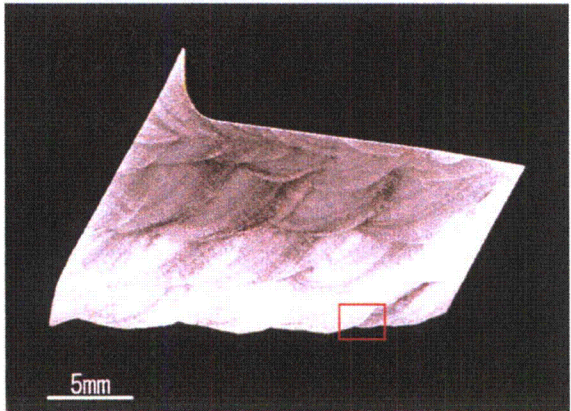
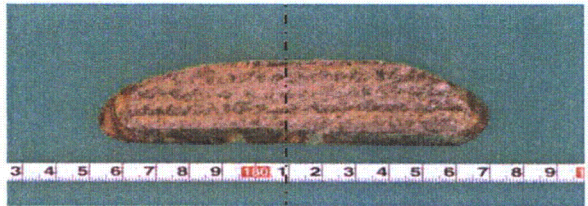


Quasi-cleavage fracture surface

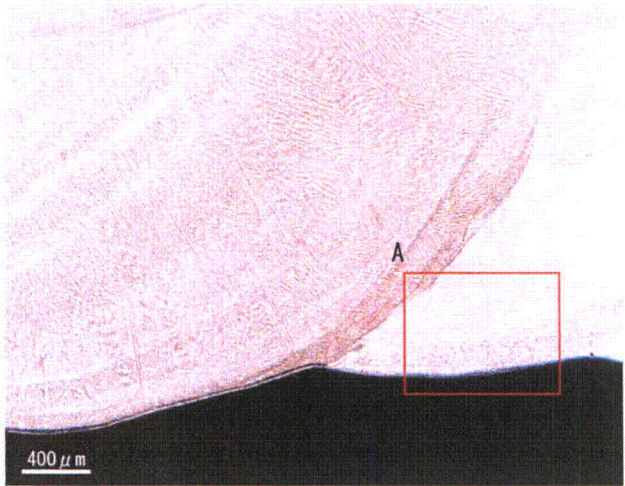
Fig. A. 21 (2) SEM observation of fracture surface of sample B (Low alloy steel channel head) (continued)



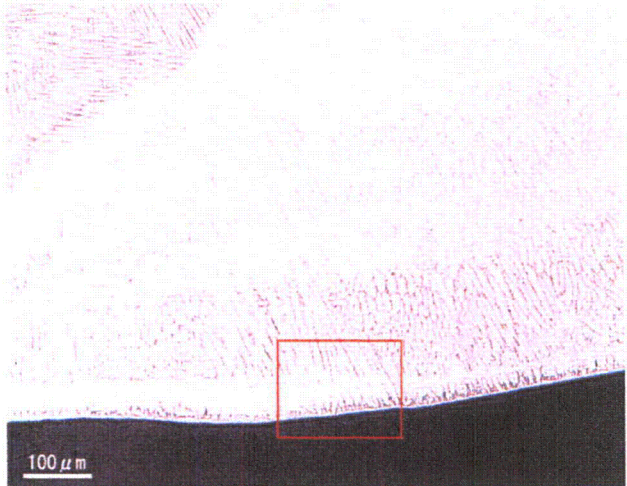
Cross section for observation



Enlarged



Enlarged



Enlarged

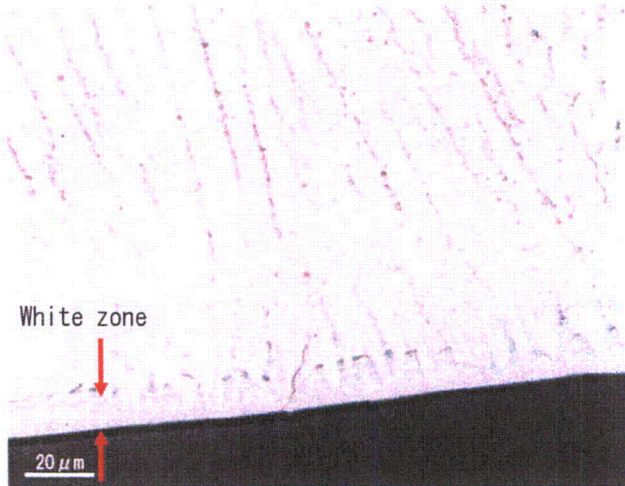
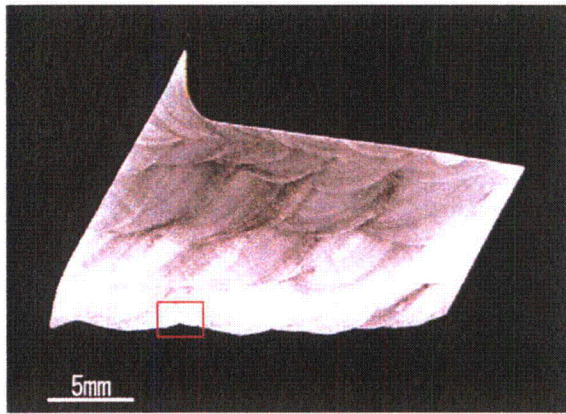
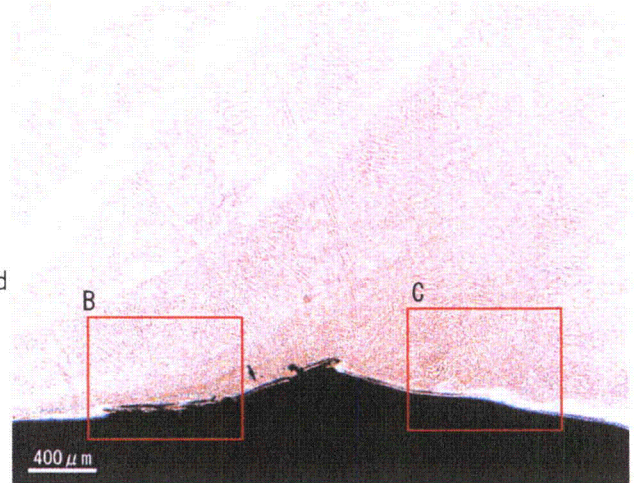


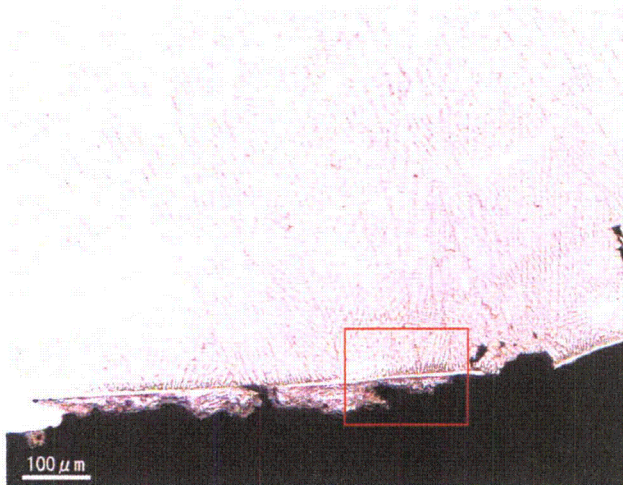
Fig. A. 22(1) Micro-structure observation of cross section of sample B (152 buttering)



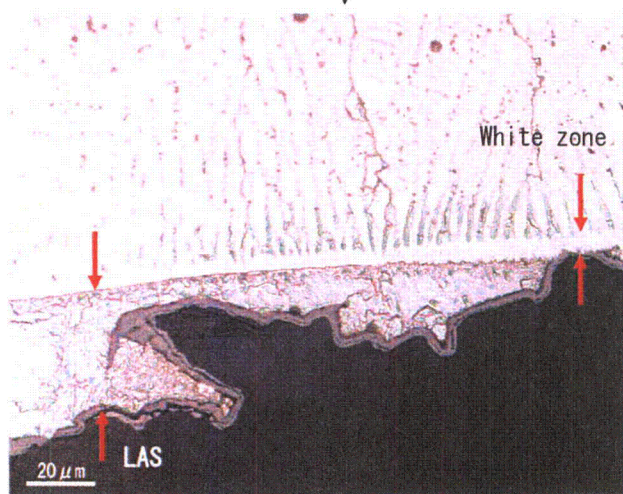
Enlarged



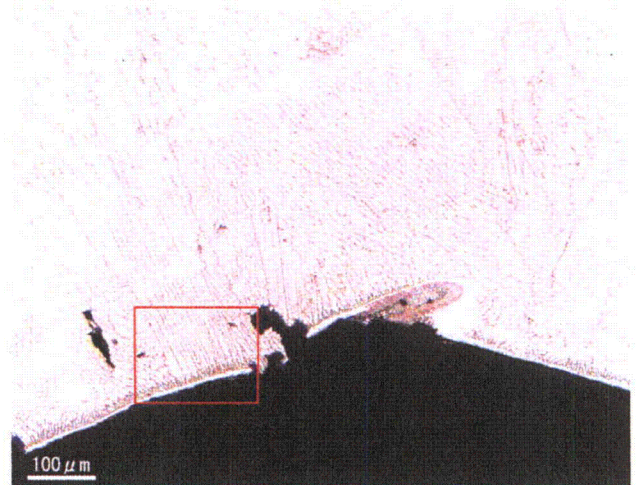
Detail observation of location B



Enlarged



Detail observation of location C



Enlarged

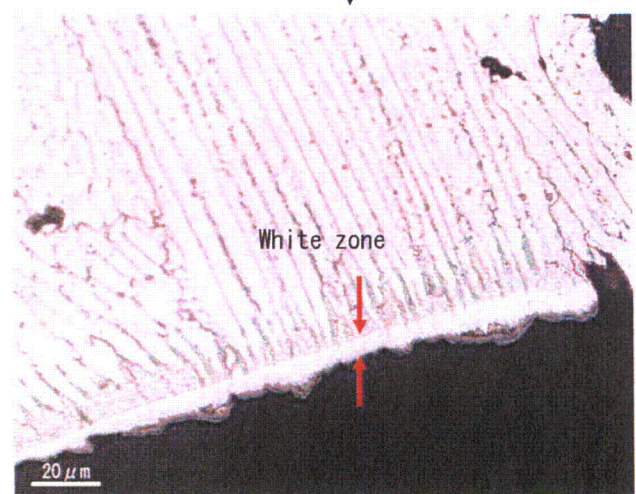
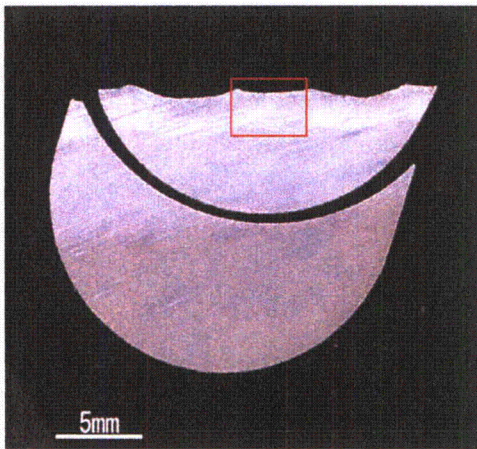
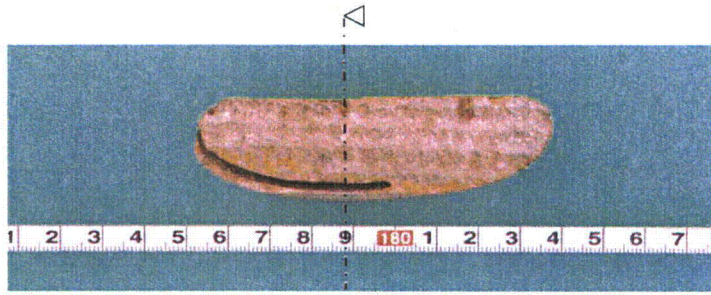


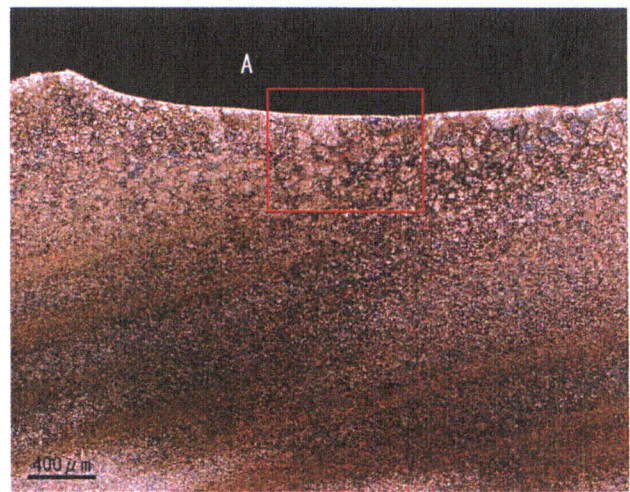
Fig. A.22(2) Micro-structure observation of cross section of sample B (152 buttering) (continued)



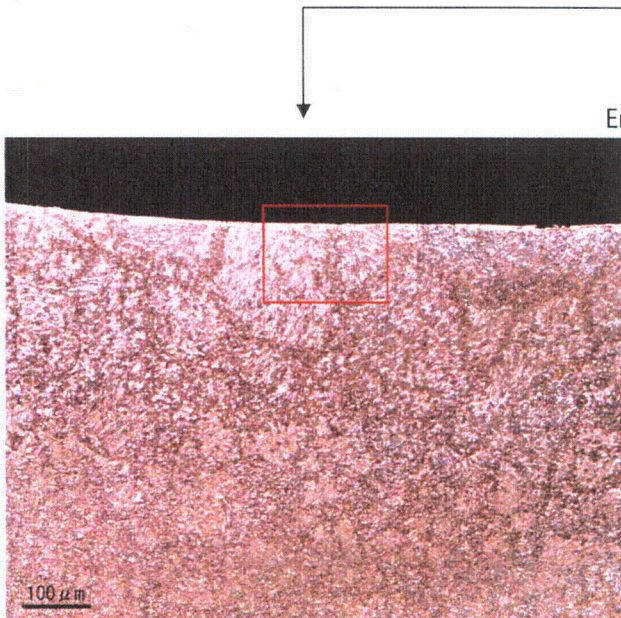
Cross section for observation



Enlarged



Enlarged



Enlarged

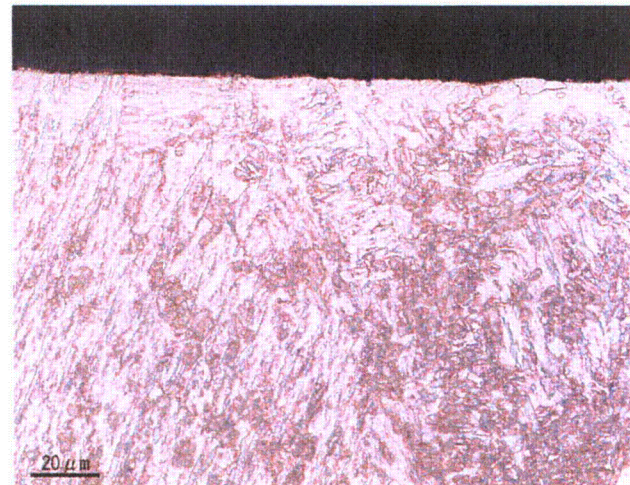
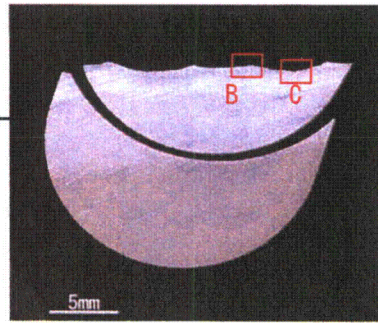
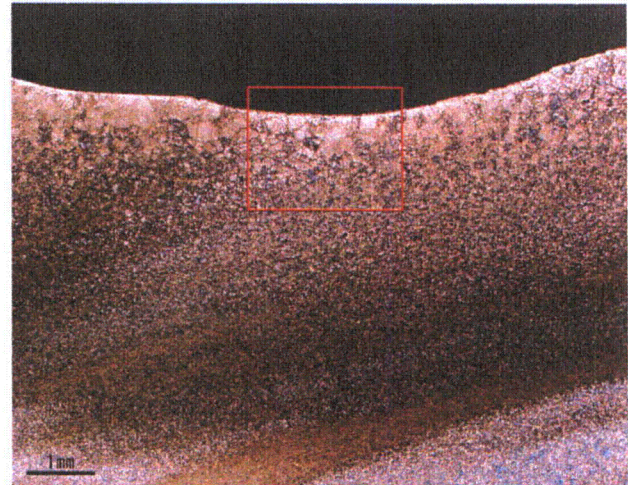
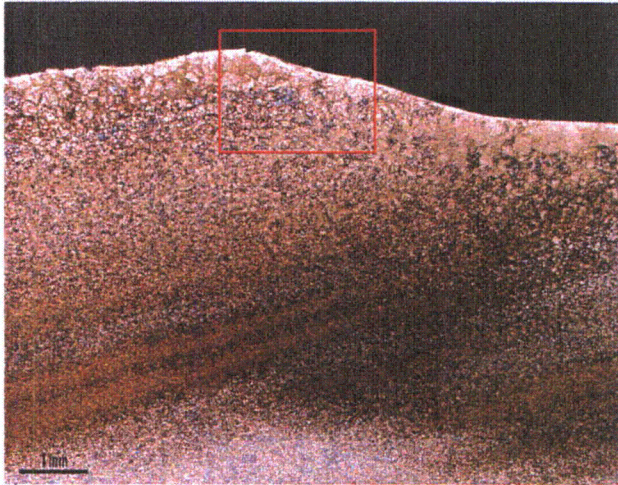


Fig. A. 23(1) Micro-structure observation of cross section of sample B (Low alloy steel channel head)



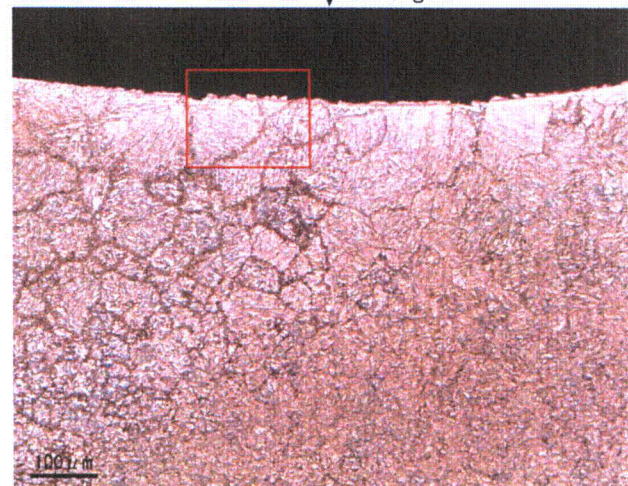
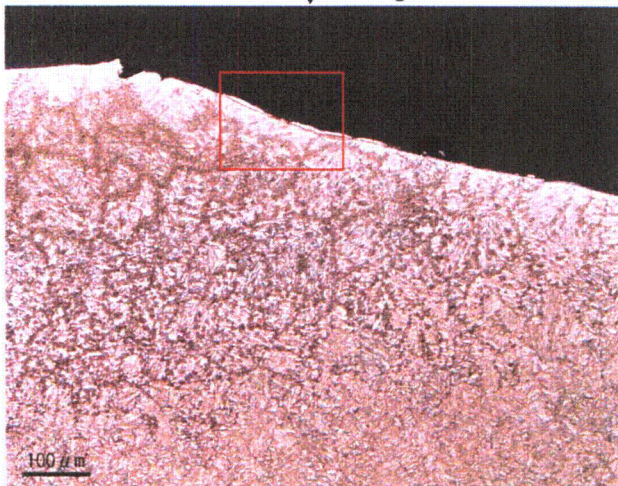
Detail observation of location B

Detail observation of location C



↓ Enlarged

↓ Enlarged



↓ Enlarged

↓ Enlarged

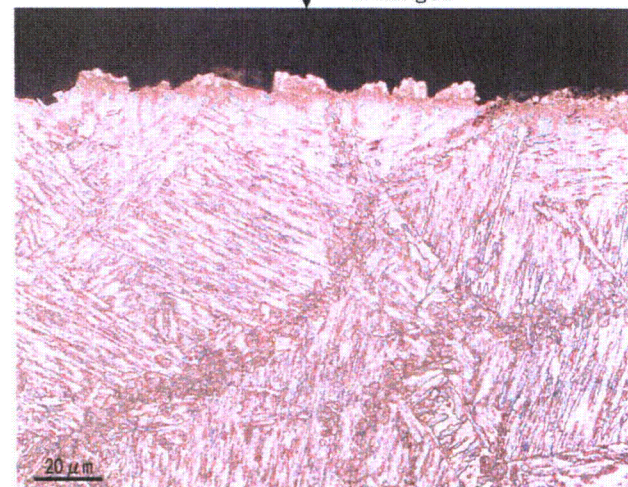
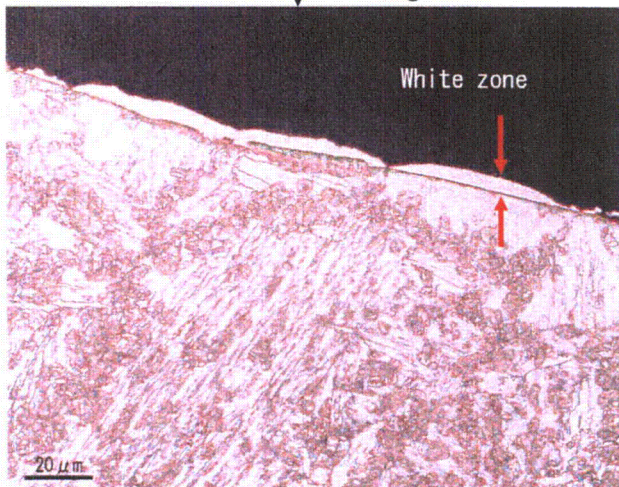


Fig. A. 23 (2) Micro-structure observation of cross section of sample B (Low alloy steel channel head) (continued)